Determination of antioxidants using chemiluminescence detection

by

Geoffrey Paul McDermott
B.FSc. (Hons)

Submitted in fulfilment of the requirements for the degree of

Doctor of Philosophy

Deakin University

February, 2011

DEAKIN UNIVERSITY

CANDIDATE DECLARATION

I certify that the thesis entitled:

'Determination of antioxidants using chemiluminescence detection'

submitted for the degree of Doctor of Philosophy is the result of my own work and that where reference is made to the work of others, due acknowledgment is given.

I also certify that any material in the thesis which has been accepted for a degree or diploma by any university or institution is identified in the text.

'I certify that I am the student named below and that the information provided in the form is correct'

Full Name..... GEOFFREY PAUL McDERMOTT .....

(Please Print)

Signature Redacted by Library

Signed.....

Date..... 13 / 2 / 2012 .....

DEAKIN UNIVERSITY

ACCESS TO THESIS – A

I am the author of the thesis entitled

'Determination of antioxidants using chemiluminescence detection'

submitted for the degree of Doctor of Philosophy

This thesis may be made available for consultation, loan and limited copying in accordance with the Copyright Act 1968.

'I certify that I am the student named below and that the information provided in the form is correct'

Full Name.....GEOFFREY PAUL McDERMOTT.....

(Please Print)

Signature Redacted by Library

Signed.....

Date.....13 /2 /2012.....

"Study hard what interests you the most in the most undisciplined, irreverent and original manner possible."

Richard P. Feynman

Table of Contents

AKNOWELDGEMENTS

I arrived at Deakin University on my first day not knowing anybody and now I am leaving with so many friends that I will have for life. Throughout the course of my degree I have been privileged to receive the support from these people, to whom I am deeply grateful.

First and foremost I would like to thank my family, Mum, Dad, Kate and David. Without the love and support you have all offered me throughout my studies I would not have been able to follow my dreams and make it this far.

An enormous thankyou belongs to my primary supervisor and good mate, Neil Barnett. You have been an inspiration to me, whether it is in the laboratory or down at the pub your continual guidance, advice and sharing of knowledge has gotten me through my PhD. Another massive acknowledgment belongs to Xavier Conlan and Paul Francis. You have both taught me so much more than just chemistry during my time at Deakin University and I feel privileged to have had you not only as supervisors but more importantly as good friends. Oh and Xavier one day the mighty Dees will make the top 8!

I also wish to express my gratitude to the following people: Nicole Stupka and Sheree Martin for providing me with cellular samples and for all of your ideas and assistance; Phil Jones for sharing your time and expertise in the laboratory (particularly when helping prepare a stable $[Ru(bipy)_3]^{3+}$ reagent). I have thoroughly enjoyed your visits and the many science conversations we have had around a BBQ; Greg Van Egmond for the intravenous collection of blood samples; Fred Pfeffer and Luke Henderson for sharing their extensive knowledge with me on all things organic chemistry; finally to all the PhD and honours students who I have had the benefit of

spending time with in the lab and at the pub. You always made coming to university fun and I feel fortunate to have shared such great times together.

I would like to a make a particular mention of the students Jessica Terry, Kayla Holt, Laura Noonan, Kristen Scott and Mariam Mnatsakanyan. Not only was it a pleasure to spend time with you all in the laboratory but without your invaluable skills I would not have had the breakthroughs that made much of the work presented in this thesis possible.

Anna you were my rock over the last four years. Your support, friendship and love have kept me going even when it felt like there was no light at the end of tunnel, I am forever grateful.

Finally I would like to acknowledge the financial support of the Australian Government who awarded me a scholarship.

PUBLICATIONS

Listed below are the references to publications that have resulted from the work presented in this thesis.

1. Xavier A. Conlan, Nicole Stupka, **Geoffrey P. McDermott**, Paul S. Francis and Neil W. Barnett, Rapid determination of intracellular glutathione using monolithic column high performance liquid chromatography after derivatisation with monobromobimane, *Biomedical Chromatography*, 24 (5) 455-457 (2010).

2. Xavier A. Conlan, Nicole Stupka, **Geoffrey P. McDermott**, Neil W. Barnett and Paul S. Francis, Correlation between permanganate chemiluminescence and *in-vitro* cell culture assay: physiologically-meaningful antioxidant activity of molecules, *Analytical Methods*, 2 171-173 (2010)

3. Mariam Mnatsakanyan, Tiffany A. Goodie, Xavier A. Conlan, Paul S. Francis, **Geoffrey P. McDermott**, Neil W. Barnett, David Shock, Fabrice Gritti, George Guiochon and R. Andrew Shalliker, High performance liquid chromatography with two simultaneous on-line antioxidant assays: evaluation and comparison of espresso coffees, *Talanta*, 81 (3) 837-842 (2010)

4. **Geoffrey P. McDermott**, Laura K. Noonan, Mariam Mnatsakanyan, R. Andrew Shalliker, Xavier A. Conlan, Neil W. Barnett and Paul S. Francis, High performance liquid chromatography with post-column 2,2-diphenyl-1-picrylhydrazyl radical scavenging assay: methodological considerations and application to complex samples, *Analytica Chimica Acta*, 675 76-82 (2010)

5. Mariam Mnatsakanyan, Paul G. Stevenson, Xavier A. Conlan, Paul S. Francis, Tiffany A. Goodie, **Geoffrey P. McDermott**, Neil W. Barnett and R. Andrew Shalliker, The analysis of cafe espresso using two-dimensional reversed phase-reversed phase high performance liquid chromatography with UV-absorbance and chemiluminescence detection, *Talanta*, 82 1358-1363 (2010)

6. **Geoffrey P. McDermott**, Xavier A. Conlan, Laura K. Noonan, Jason W. Costin, Mariam Mnatsakanyan, R. Andrew Shalliker, Neil W. Barnett and Paul S. Francis, Screening for antioxidants in complex matrices using high performance liquid chromatography with acidic potassium permanganate chemiluminescence detection, *Analytica Chimica Acta*, 684 134-141 (2010)

7. **Geoffrey P. McDermott**, Paul S. Francis, Kayla J. Holt, Kristen L. Scott, Sheree D. Martin, Nicole Stupka, Neil W. Barnett and Xavier A. Conlan, Determination of intracellular glutathione and glutathione disulfide using high performance liquid chromatography with acidic potassium permanganate chemiluminescence detection, *Analyst*, 136 2578-2585 (2011). (Selected for the front cover of the issue, see pg. ix)

8. **Geoffrey P McDermott**, Philip Jones, Neil W. Barnett, David N. Donaldson and Paul S. Francis, Stable tris(2,2′-bipyridine)ruthenium(III) for chemiluminescence detection, *Analytical Chemistry*, 83 5453-5457 (2011)

9. **Geoffrey P. McDermott**, Jessica M. Terry, Xavier A. Conlan, Neil W. Barnett and Paul S. Francis, Direct detection of biologically significant thiols and disulfides with manganese(IV) chemiluminescence, *Analytical Chemistry*, 83 6121-6430 (2011). (Selected for the front cover of the issue, see pg. x)

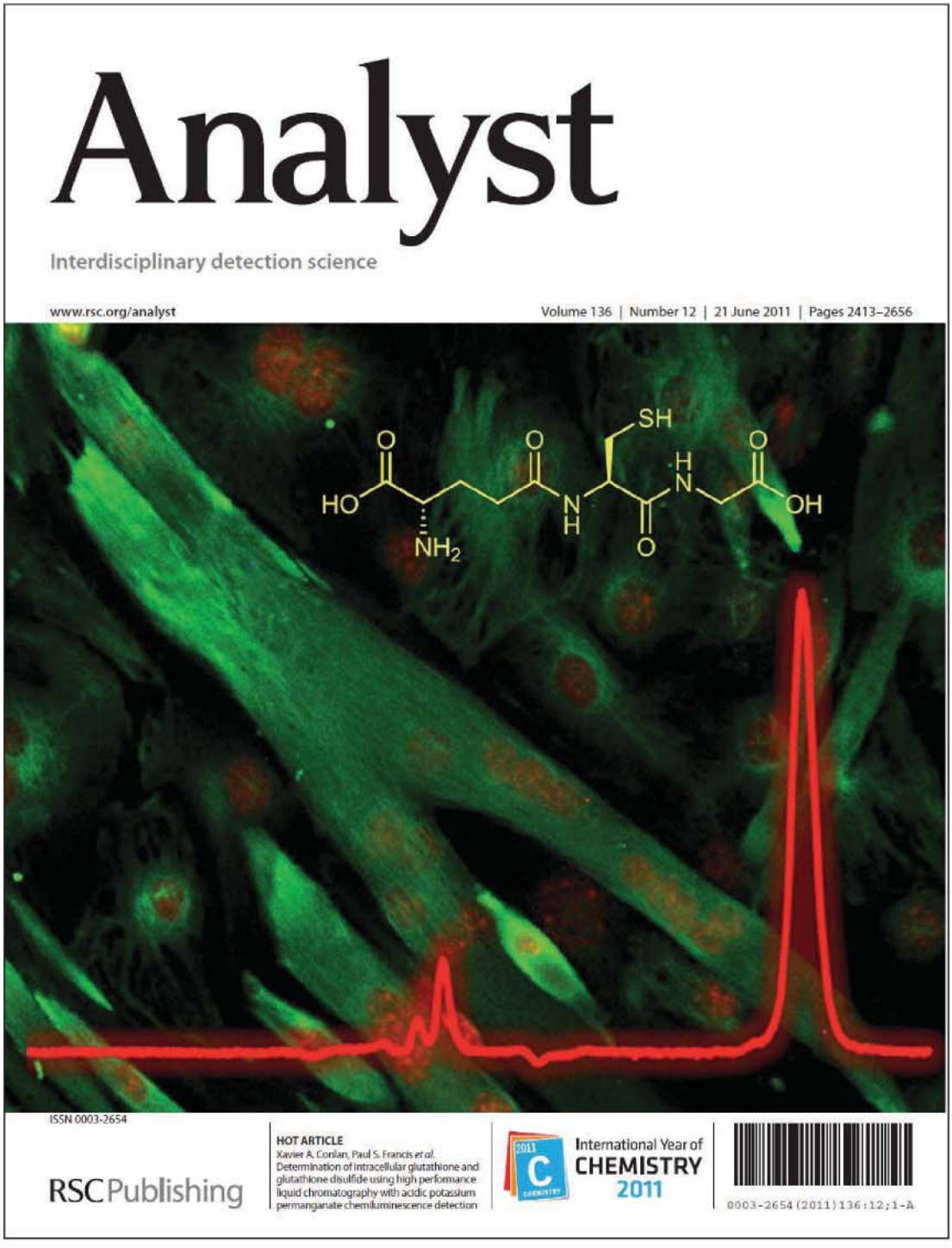
Analyst
Interdisciplinary detection science
www.rsc.org/analyst
Volume 136 | Number 12 | 21 June 2011 | Pages 2413–2656
SH
HO
O
O
N
H
H
N
O
OH
NH2
ISSN 0003-2654
RSC Publishing
HOT ARTICLE
Xavier A. Conlan, Paul S. Francis et al.
Determination of intracellular glutathione and glutathione disulfide using high performance liquid chromatography with acidic potassium permanganate chemiluminescence detection
International Year of CHEMISTRY 2011
0003-2654(2011)136:12;1-A

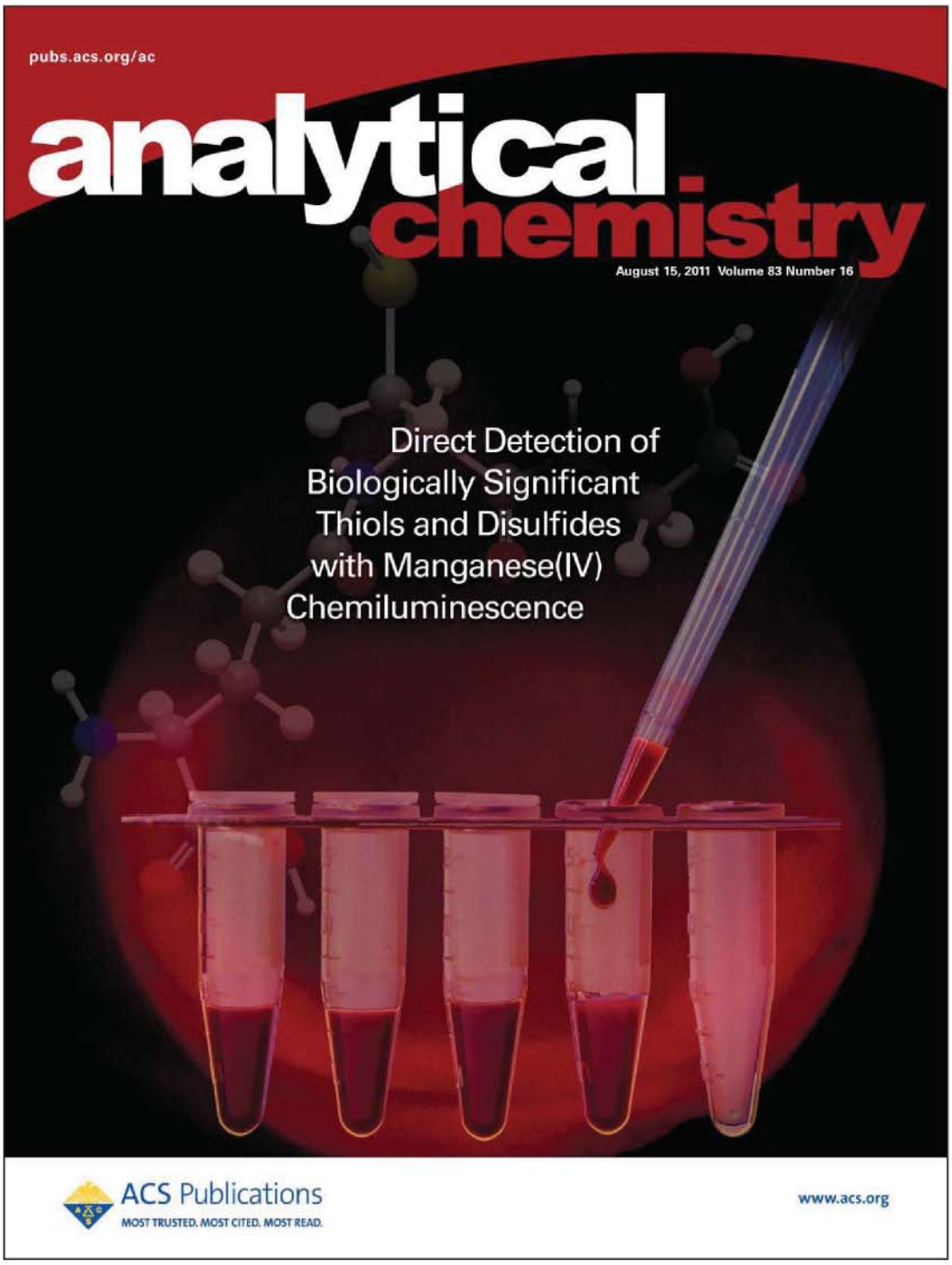
pubs.acs.org/ac
analytical chemistry
August 15, 2011 Volume 83 Number 16
Direct Detection of Biologically Significant Thiols and Disulfides with Manganese(IV) Chemiluminescence
ACS Publications
MOST TRUSTED. MOST CITED. MOST READ.
www.acs.org

Antioxidants are either synthesised within the human body (endogenous) or obtained from dietary sources (exogenous). The main role of antioxidants is to counter the detrimental effects of free radicals, but they are also essential for numerous metabolic processes. However, it is challenging to screen and identify antioxidants from complex samples using the high performance liquid chromatography (HPLC) based techniques available to-date. Herein, the development of post-column detectors (primarily based on chemiluminescence) for the determination of antioxidants in plant based matrices and physiological fluids is reported.

An improved post-column 2,2-diphenyl-1-picrylhydrazyl radical ($DPPH^{\bullet}$) scavenging assay for the screening of exogenous antioxidants was developed. Experimental parameters believed to be influential to $DPPH^{\bullet}$ response were studied in a univariate approach. The analytical utility of the optimised protocol was assessed by screening for antioxidants in extracts of thyme and green tea, in comparison with two commonly employed $DPPH^{\bullet}$ methodologies.

The use of HPLC with acidic potassium permanganate chemiluminescence detection to detect exogenous antioxidants in plant-derived samples was evaluated in comparison with two conventional post-column radical scavenging assays (2,2′-azinobis-(3-ethylbenzothiazoline-6-sulfonic acid) ($ABTS^{\bullet+}$) and $DPPH^{\bullet}$). Using flow injection analysis (FIA), experimental parameters that afforded the most suitable permanganate chemiluminescence signal for a range of known antioxidants were studied in a univariate approach. Acidic potassium permanganate chemiluminescence signal intensity was shown to accurately predict the ability of several antioxidants to positively act on cellular redox state and attenuate oxidative

stress in cultured skeletal muscle cells. Further investigations with antioxidant standards showed some differences in selectivity between HPLC and the optimised post-column permanganate chemiluminescence detection plus $DPPH^{\bullet}$ and $ABTS^{\bullet+}$. However, permanganate chemiluminescence detection was more sensitive. Screening for antioxidants in green tea, cranberry juice and thyme using potassium permanganate chemiluminescence offered several advantages over the traditional $DPPH^{\bullet}$ and $ABTS^{\bullet+}$ assays, including faster reagent preparation, superior stability, simpler post-column reaction manifold and greater compatibility with fast chromatographic separations using monolithic columns.

Measurement of the endogenous antioxidant glutathione (GSH) and its disulfide (GSSG) is a crucial tool to assess cellular redox state. A direct approach to determine intracellular GSH based on a rapid chromatographic separation coupled with acidic potassium permanganate chemiluminescence detection was extended to GSSG by incorporating thiol blocking and disulfide bond reduction. Importantly, this simple procedure avoided derivatisation of GSH (thus minimising auto-oxidation) and overcame problems encountered when deriving the concentration of GSSG from 'total GSH'. These analytes were determined in cultured muscle cells treated for 24 h with glucose oxidase (0, 15, 30, 100, 250 and 500 mU mL^{-1}), which exposed the cells to a continuous source of reactive oxygen species.

Two exceedingly stable tris(2,2′-bipyridine)ruthenium(III) ($[Ru(bipy)_3]^{3+}$) reagents were prepared by dissolving either $[Ru(bipy)_3](ClO_4)_2$ in acetonitrile (containing 0.05 M $HClO_4$) or $[Ru(bipy)_3]Cl_2.6H_2O$ in 95:5 glacial acetic acid:acetic anhydride (containing 0.05 M H_2SO_4), followed by oxidation with PbO_2. These conveniently prepared solutions provided highly reproducible chemiluminescence detection over long periods of analysis, avoiding the need for re-calibration or preparation of fresh

reagent solutions, and without the complications associated with on-line chemical or electrochemical oxidations. The reagent prepared in acetonitrile produced much greater signal intensities with a range of analytes and was deemed most suitable for HPLC with post-column chemiluminescence detection. Therefore, this reagent was explored for the direct detection of both GSH and GSSG. Preliminary FIA based experiments revealed that alkaline reaction conditions were necessary to evoke an analytically useful response with these analytes. However, this translated to insufficient limits of detection for GSH and GSSG when using post-column chemiluminescence detection.

HPLC with post-column manganese(IV) chemiluminescence provided a simple and rapid approach for the direct detection of biologically significant thiol and disulfide compounds related to the human endogenous antioxidant network, including cysteine, cystine, homocysteine, homocystine, GSH, GSSG and *N*-acetylcysteine. Detection limits for these analytes ranged from 5×10^{-8} M to 1×10^{-7} M. This approach was employed to determine two key biomarkers of oxidative stress, GSH and GSSG, in whole blood taken from twelve healthy volunteers. Samples were deproteinised, centrifuged and diluted prior to analysis, using a simple procedure that was shown to avoid significant artificial oxidation of GSH.

CHAPTER ONE

Introduction

- **Free radicals, antioxidants and oxidative stress**
- **Endogenous antioxidants**
- **Exogenous antioxidants**
- **Chemiluminescence**
- **Project aims**

1. Free radicals, antioxidants and oxidative stress

The evolution of normal metabolic processes such as respiration and photosynthesis unavoidably leads to the production of free radicals [1-4]. These species are defined as atoms, compounds, or ions that contain an unpaired electron in their atomic or molecular orbital [1-3]. Free radicals are well recognised for having both detrimental and beneficial effects on living systems (Figure 1) [2, 5-12]. Oxygen free radicals, commonly referred to as reactive oxygen species (ROS), in addition to reactive nitrogen species (RNS) generated at low/moderate concentrations are important in numerous physiological functions including: regulation of vascular tone, sensing of oxygen tension, enhancement of signal transduction from various membranes, and oxidative stress responses that ensure the maintenance of redox homeostasis [2, 6, 9, 10]. In contrast, an overproduction of ROS can cause damage to cellular lipids, proteins, or DNA, inhibiting their normal function [2, 5-8]. However, organisms have evolved a complex array of defences comprising of both endogenous (enzymatic and non-enzymatic) and exogenous antioxidants to control cellular levels of free radicals [1-3, 6, 7, 13-17]. These species have been recognised to protect cells by 'scavenging' free radicals from the body (causing a breakdown of radical chain reactions), suppressing free radical formation or by reducing oxidised cellular components [1-3, 6, 7, 13-17]. Consequently, the harmful effects of free radicals occur in biological systems when there is an overproduction of ROS/RNS along with a deficiency of antioxidants [1-3, 5-8, 13-17]. This is termed oxidative stress or nitrosative stress and has been implicated in numerous human diseases, including: cancer, atherosclerosis, Alzheimer's disease, inflammation, asthma, rheumatoid arthritis and is also linked to the process of ageing [2, 3, 18-23]. Due to the growing scientific consensus that acknowledges the general importance of

antioxidants in counteracting the effects of oxidative stress, these compounds and their (bio)chemistry are currently the subject of intensive research [2, 3, 5-12, 18-23].

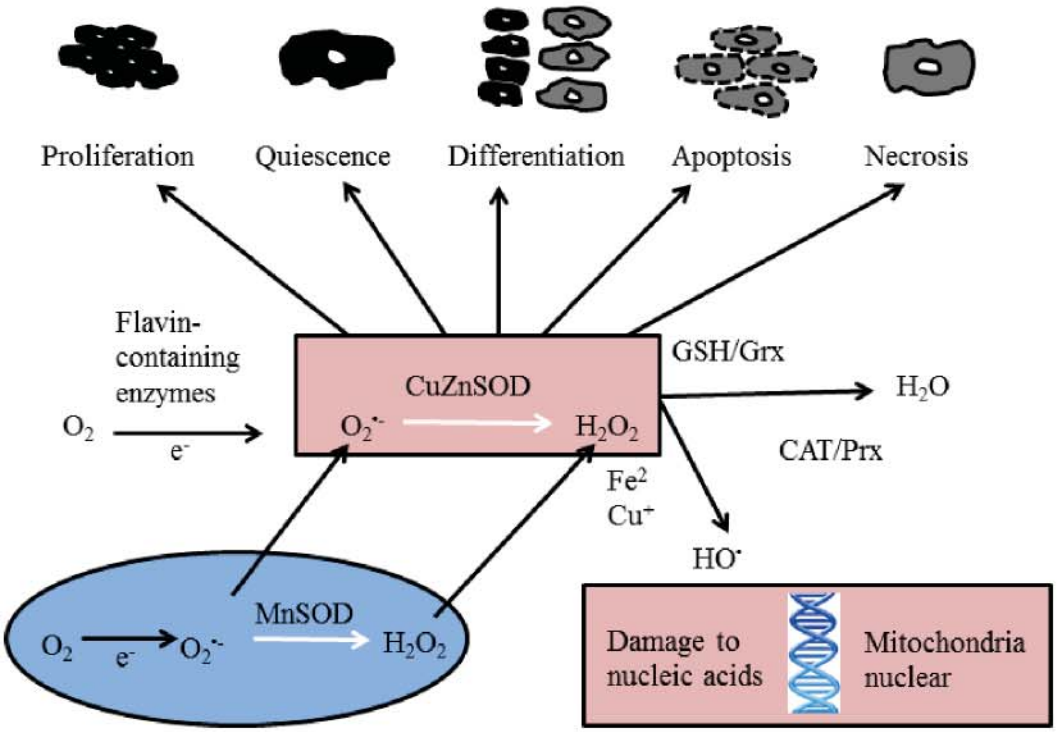

Figure 1. Reactive oxygen species signalling and cellular processes. ROS (e.g., $O_2^{\bullet-}$ and H_2O_2) are produced intracellularly by the mitochondrial electron-transport chain and flavin-containing enzymes. Superoxide dismutase (MnSOD and CuZnSOD) converts $O_2^{\bullet-}$ to H_2O_2; catalase, peroxiredoxin and glutathione /glutathione peroxide neutralise H_2O_2 to water. H_2O_2 in the presence of metals can generate hydroxyl radical ($HO^\bullet$) which damages cellular macromolecules. ROS can serve as secondary messengers influencing multiple signalling pathways which regulate proliferation, quiescence, differentiation and cell death [8].

2. Endogenous antioxidants

Endogenous antioxidants are produced by the human body and can be classified as either being low-molecular mass (non-enzymatic) or enzymatic [2, 3, 8, 24-30]. Superoxide dismutases, catalase and glutathione peroxidase are three major categories of enzymatic antioxidants [24-29]. Superoxide dismutases catalyse the conversion of two superoxide anions to hydrogen peroxide and oxygen (Figure 1) [28, 29]. Although hydrogen peroxide is a major contributor to oxidative damage, it is significantly less toxic than superoxide [3, 31]. Catalase then breaks down

hydrogen peroxide to water and oxygen, finishing the detoxification process started by superoxide dismutases (Figure 1) [25, 27]. Glutathione peroxidase is a group of enzymes that like catalase decomposes hydrogen peroxide and also reduces organic peroxides to alcohols, providing another route for eliminating toxic oxidants (Figure 1) [24-26]. Low-molecular mass antioxidants include uric acid, lipoic acid, albumin, bilirubin and various amino acids (such as glutathione (GSH), methionine, *N*-acetylcysteine) [3, 30]. However, of these compounds, the ubiquitous compound GSH functions as the principal antioxidant involved in cellular defence's mechanisms against free radicals [14, 32-36].

2.1 Glutathione and other low-molecular mass thiols

Glutathione (L-γ-glutamyl-L-cysteinyl-glycine) is the main non-protein thiol found in cells and is synthesised in two adenosine triphosphate-dependent steps as depicted in Figure 2 [37-40]. First, γ-glutamylcysteine is assembled from L-glutamate and cysteine by the enzyme γ-glutamylcysteine synthetase [37-40]. Next, glycine is added to the C-terminal of γ-glutamylcysteine by glutathione synthetase to form GSH [37-40], which contains two characteristic structural features (a γ-glutamyl linkage and a thiol moiety) which facilitate its participation in a number of physiological functions. These include: antioxidant defence, detoxification of electrophilic xenobiotics, modulation of redox-regulated signal transduction, storage and transport of cysteine, regulation of cell proliferation, synthesis of deoxyribonucleotides, regulation of immune responses, and regulation of leukotriene and prostaglandin metabolism [14, 32-36].

When functioning as an antioxidant, glutathione can donate a reducing equivalent to harmful free radical species, which results in the formation of the corresponding disulfide (GSSG) [14, 32-36]. To complete this intracellular redox cycle, GSH is

regenerated by the enzyme glutathione reductase in a nicotinamide adenine dinucleotide phosphate (NADPH) dependant reaction (Figure 2) [14, 32-36]. The molar ratio of GSH/GSSG in a cell is typically between 10:1 and 1000:1; however, under oxidative stress, this ratio decreases [14, 32-36]. Since oxidative stress has been implicated in a growing number of pathological and physiological conditions [14, 32-36], assessing the GSH/GSSG redox pair is an invaluable tool for researchers [14, 32-35, 41-48].

As can be seen in Figure 2, many other low-molecular mass thiols including homocysteine, cysteine, cysteinylglycine, γ-glutamylcysteine and methionine, play a central and co-operative role in the antioxidant defence network [16, 37-40]. Additionally, there is increasing evidence suggesting that thiol moieties located within these compounds act as redox sensitive switches thereby providing a common trigger for a variety of ROS mediated signalling events [43, 49-51].

In the metabolic pathways shown in Figure 2, cysteine is the rate-limiting precursor to GSH synthesis [37-40]. Cysteine is derived from the hydrolysis of extracellular GSH by γ-glutamyltranspeptidase (GGT) or from a process known as trans-sulfuration (Figure 2) [37-40, 52]. In the GGT-catalysed reaction, the γ-glutamyl moiety of GSH is transferred to an acceptor molecule such as water, certain L-amino acids, or peptides [37-40, 52]. This results in a cysteinylglycine fragment which is subsequently cleaved by membrane-bound dipeptidases to form cysteine and glycine (Figure 2) [37-40, 52]. Alternatively, in the trans-sulfuration metabolic pathway, the essential amino acid methionine is first converted to homocysteine by demethylation [38, 53, 54]. This thiol can then be used to either regenerate methionine, or to form cysteine through the intermediate cystathionine (Figure 2) [38, 53, 54]. Since these aforementioned thiols and their corresponding

disulfides have numerous roles in cellular metabolism and homeostasis, their accurate and interference-free measurement in physiological fluids and tissues is of great biological, clinical and pharmacological importance [14, 32-35, 55-58].

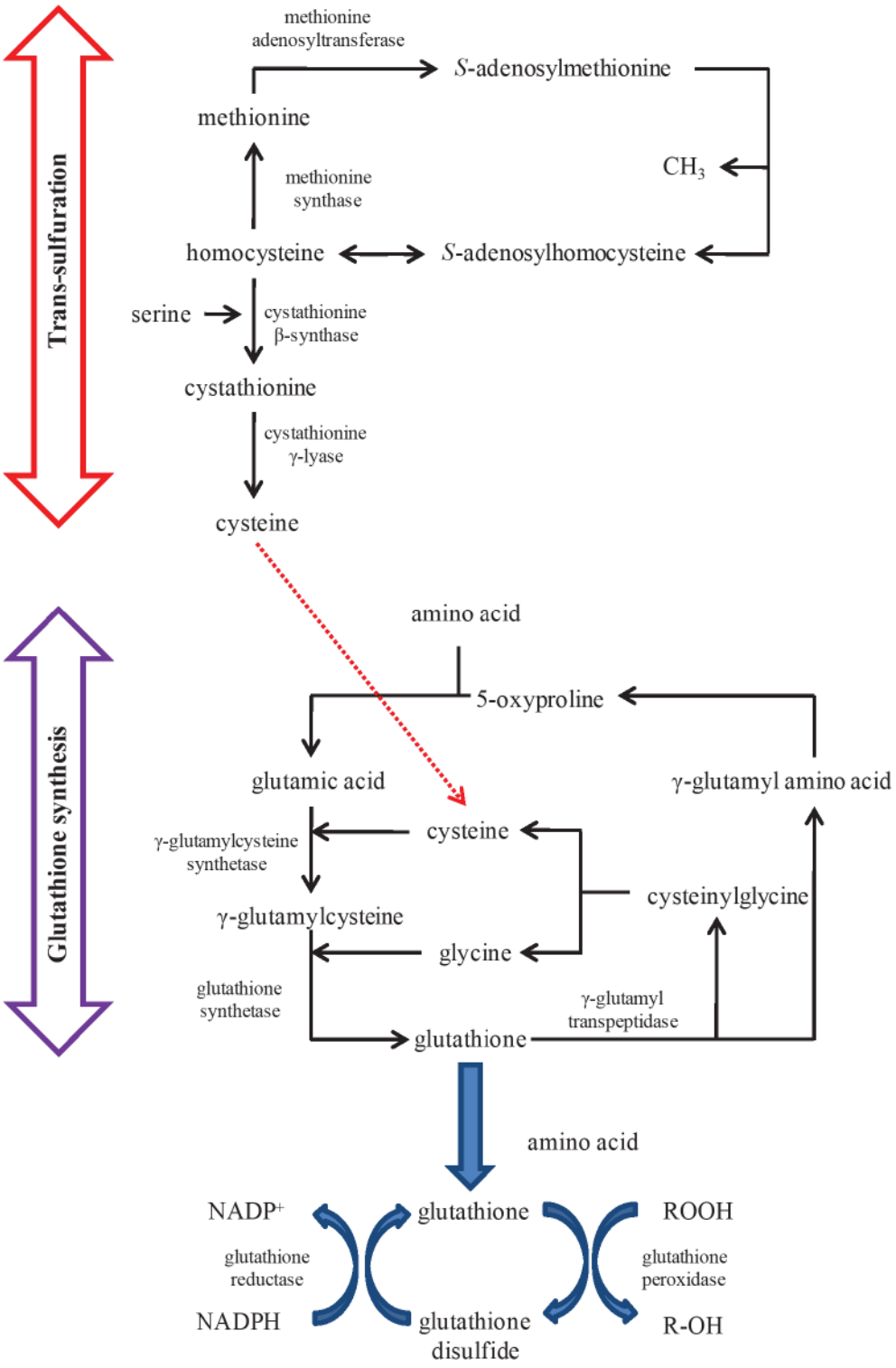

Figure 2. Schematic representation of the trans-sulfuration and glutathione biosynthetic and metabolic pathways [38, 46, 59].

2.1 Detection of biologically important thiols and disulfides

Numerous analytical methodologies exist for the quantification of low-molecular mass thiols and disulfides because of their importance in diagnosing and monitoring the presence of human diseases and metabolic disorders related to oxidative stress [14, 32-35, 55-58]. However, as identified in the key research papers and reviews, there are several major analytical challenges associated with their accurate measurement [33, 41-45, 47, 48, 56, 57, 60]. Firstly, thiols and disulfides do not possess chromophores or fluorophores and consequently derivatisation is an indispensable step in the majority of methods [33, 41-45, 47, 48, 56, 57, 60]. Yet this process can be time consuming and may add a significant source of error due to irreproducible derivatisation or undesirable side reactions [33, 41-45, 47, 48, 56, 57, 60]. Nevertheless, the most commonly reported approach comprises of the following two-step procedure: (i) derivatisation of free thiols followed by separation using either high performance liquid chromatography (HPLC) or capillary electrophoresis (CE) in conjunction, with UV-absorbance or fluorescence detection; (ii) reduction of disulfides to their respective thiols before subjecting the sample to the same aforementioned derivatisation, separation and detection process. The disulfide concentration can therefore be determined through the difference between the measurements obtained in steps 1 and 2 [33, 41-45, 47, 48, 56, 57, 60]. Secondly, intracellular thiols occur at concentrations several orders of magnitude higher than their disulfides, whereas extracellular thiol levels are significantly lower [33, 41-45, 47, 48, 56, 57, 60]. Therefore, lysis of cells such as erythrocytes or incomplete removal of the extracellular *milieu* prior to analysis leads to the inaccurate assessment of thiol concentrations. Thirdly, thiols are easily oxidised during sample pre-treatment, particularly under the alkaline conditions employed for most derivatisation approaches and disulfide bond reductions [33, 41-45, 47, 48, 56, 57,

60]. Since disulfides often occur at concentrations several orders of magnitude lower than thiols, auto-oxidation leads to considerable disulfide overestimation. Finally, some thiols and their disulfides occur at nM to low μM concentrations in particular matrices (e.g., GSH and GSSG in urine or in plasma, homocysteine and homocystine in blood, cysteine and cystine in tissues). This makes their determination difficult in these sample types as analyte levels are close to the limit of detection for most methodologies available to-date. These challenges have given rise to large discrepancies in reported thiol and disulfide concentrations as results from one approach are often not in agreement with those obtained from other methods [33, 41-45, 47, 48, 56, 57, 60].

Therefore, the most attractive methodologies for measuring biologically significant thiols and disulfides are those that employ minimal sample handling combined with direct detection of all target analytes in one chromatographic run. Three such approaches have been developed to-date, in which separation steps have been coupled with electrochemical, mass spectrometry or fluorescence quenching detection [42, 43, 46, 48, 56, 57, 60, 61]. Whilst these modes of detection offer advantages over the more popular derivatisation-based techniques in terms of procedural simplicity, their applications are limited by equipment complexity, cost, electrode stability and/or analysis time [42, 44, 60, 61]. These issues point to a clear need for a methodology that can directly detect multiple biologically important thiols and disulfides within one chromatographic run by employing simple instrumentation whilst also minimising artefacts related to sample preparation.

3. Exogenous antioxidants

Exogenous antioxidants are those obtained from dietary sources including fruits, vegetables and grains [62-65]. This term applies to compounds such as: Vitamins (A, C, E, K); trace elements (zinc and selenium); carotenoids (β-carotene, lycopene, lutein, zeaxanthin); phenolic acids (chlorogenic acids, gallic acid, caffeic acid, etc.); flavonols (quercetin, kaempferol, myricetin); flavanols (proanthocyanidins and catechins); anthocyanidins (cyanidin and pelagonidin); isoflavones (genistein, daidzein and glycitein); flavanones (naringenin, eriodictyol and hesperetin) and flavones (luteolin and apigenin) [62-65]. Human endogenous antioxidant defence systems are incomplete without these exogenous compounds playing an essential role in many metabolic pathways [1-3, 15, 66]. For example, the biologically significant form of Vitamin E (α-tocopherol) protects membranes from oxidation by lipid radicals produced in the lipid peroxidation chain reaction [67-69]. Whilst, the water-soluble redox catalyst, Vitamin C (ascorbic acid) can reduce and thereby neutralise free radicals from a variety of sources [68, 70, 71]. Both of the aforementioned exogenous vitamins can then be reduced back to their active form in the body by the endogenous antioxidant GSH [67-71].

Epidemiological studies have repeatedly shown that the intake of foods rich in naturally-occurring antioxidants, including nutrients (e.g., Vitamins) and phytochemicals (e.g., polyphenols) are associated with a lower incidence of cardiovascular disease, cancer, diabetes, osteoporosis and brain disorders [15, 62, 66, 72, 73]. Moreover, there is evidence that the observed associated health advantageous of plant food consumption may not be attributable to a specific compound, but rather to the whole fruit and vegetable, following additive or synergist actions of complex mixtures of phytochemicals and nutrients [74, 75].

Another well documented application of naturally occurring exogenous antioxidants is their use in foodstuffs to replace possibly toxic synthetic radical scavengers such as butylated hydroxytoluene (BHT) and tert-butyl hydroquinone (TBHQ); added to products to prolong their shelf life through prevention of lipid peroxidation [76-78]. Consequently, the detection, discovery and assessment of exogenous antioxidants in naturally occurring complex matrices is of the upmost importance to researchers in a diverse range of fields, such as nutrition, medicine, food and agricultural sciences, and drug discovery [2, 13, 17, 72, 76-79].

3.1 Detection and assessment of exogenous antioxidants

Traditionally, researchers have focused on developing methods to evaluate the antioxidant capacity of whole plants and foods [80-83]. These are often referred to as off-line or batch style approaches as they are generally performed in spectroscopic cuvettes [80-83]. Two of the more commonly used off-line techniques are based on measuring the ability of exogenous antioxidants to reduce a stable radical (representative of *in vivo* free radicals) [80-83]. The first approach involves the purple chromophore radical, 2,2-diphenyl-1-picrylhydrazyl ($DPPH^{\bullet}$) which is reduced by an antioxidant(s) to its corresponding pale yellow hydrazine (Figure 3) [80-84]. This can be spectrophotometrically monitored as a decrease in absorbance at 517 nm. After a period of time, the degree of decolourisation and decrease in absorbance is proportional to the number of electrons captured, and therefore to the concentration and antioxidant activity of the species itself [80-84]. The results of this technique are generally reported as the EC_{50}, defined as the amount of antioxidant necessary to decrease the initial $DPPH^{\bullet}$ concentration by 50% [80-83, 85].

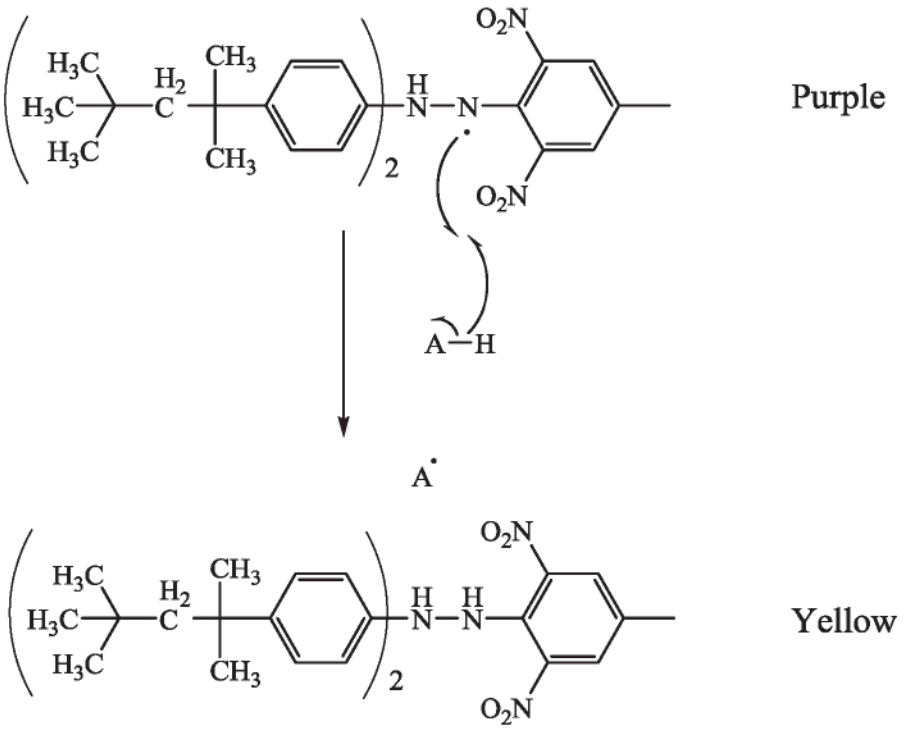

Figure 3. Reaction of an antioxidant (A—H) with DPPH$^{\bullet}$.

The second type of batch method is known as the TEAC (Trolox Equivalent Antioxidant Capacity) assay [80-83, 86]. Initially, the blue/green radical 2,2′-azinobis-(3-ethylbenzothiazoline-6-sulfonic acid) ($ABTS^{\bullet+}$) is generated by reaction of ABTS and potassium persulfate [80-83, 87, 88]. Although this radical absorbs at multiple wavelengths (415 nm, 645 nm, 734 nm and 815 nm), measuring the absorption at 734 nm eliminates colour interferences and is therefore a suitable assay for plant based samples [80-83, 87, 88]. Following the addition of a sample containing exogenous antioxidants, $ABTS^{\bullet+}$ is reduced back to ABTS (Figure 4). The degree to which this occurs is dependent on the duration of the reaction and most importantly the activity and concentration of the antioxidants [80-83, 87, 88]. Consequently, the extent of decolourisation as percentage inhibition of the $ABTS^{\bullet+}$ radical cation is determined as a function of concentration and time, and normally calculated relative to the reactivity of Trolox (an analogue of Vitamin E) under the same conditions [80-83, 87, 88].

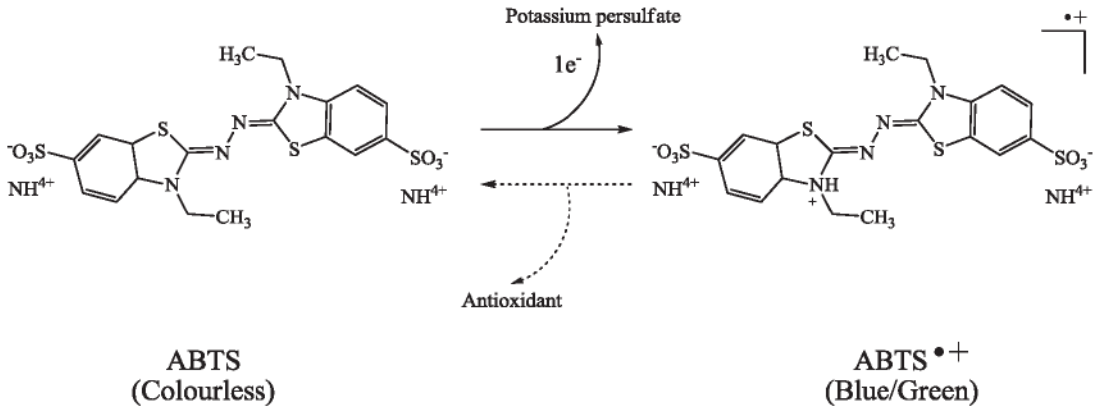

Figure 4. Reaction of $ABTS^{\bullet+}$.

Although off-line methods are sufficient to evaluate the antioxidant capacity of whole plants and foods, they are extremely time consuming and owing to sample complexity provide little information on the contribution of individual compounds to the overall response [80-83, 89, 90]. Instead, the discovery and assessment of individual antioxidants from within samples has conventionally been achieved using bioassay-guided fractionation which includes the following steps: (i) screening to determine whether the sample possess the desired biological activity using a batch style method; (ii) extractions with different solvents followed by activity assessment; (iii) fractionation and isolation of active components using chromatographic techniques followed by a repeat of the original batch analysis until the separated compounds are pure enough to identify unequivocally the active compound(s) [91, 92]. However, this is an expensive, labour-intensive and time-consuming process which sometimes leads to the loss of a compound's activity during isolation [89, 90, 92-94].

As an alternative approach, researchers have recently modified several off-line or batch style techniques, developing continuous-flow antioxidant detectors that can be coupled with HPLC [89, 90]. As described in the reviews by Niederländer *et al.* [89] and Shi *et al.* [90], these methodologies afford the determination of numerous

exogenous antioxidants on-line without prior isolation from the sample matrix. A schematic lay-out of the hardware required for exogenous antioxidant screening by HPLC is presented in Figure 5. The majority of applications employ free radical decolouration reactions, based upon either $DPPH^{\bullet}$ or $ABTS^{\bullet+}$ [89, 90]. These approaches involve merging a solution of either the $DPPH^{\bullet}$ or $ABTS^{\bullet+}$ reagent with the post-column HPLC eluate at a T-piece (using a second HPLC pump for the reagent line). The resulting stream is then passed through a reaction coil of adequate length and internal diameter to provide sufficient time for the reagent to react with any radical scavenging (i.e. antioxidant) species present, before entering a spectrophotometric detector (Figure 5). Like in their off-line counterparts, the degree to which the $DPPH^{\bullet}$ or $ABTS^{\bullet+}$ reagent is reduced depends on the activity and concentration of the antioxidant species [80, 89, 90]. Thus, radical scavenging compounds are detected as negative peaks, the size of which can be used as an indicator of a compounds bioactivity [80, 89, 90].

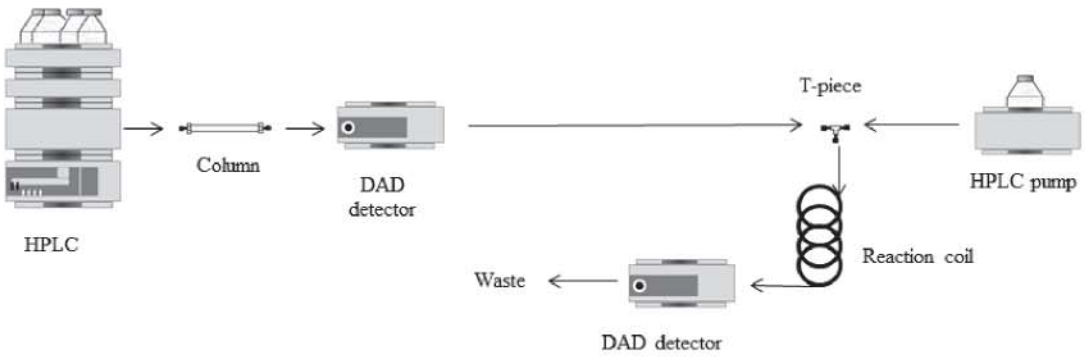

Figure 5. Instrument setup for HPLC with continuous-flow antioxidant detector.

Another less common type of on-line antioxidant assay employs indirect luminol chemiluminescence detection [89, 90, 95-97]. Here, syringe pumps are used to merge streams of luminol and an oxidant (typically hydrogen peroxide) at a T-piece, to generate chemiluminescence. This mixture is then combined with the HPLC eluate at a second T-piece and the resulting solution passed through a reaction coil to a

photo-detector, depicted in Figure 6. As with the aforementioned radical decolouration assays, antioxidants are detected as negative peaks, as they inhibit the reaction between luminol and oxidants causing quenching of the background chemiluminescence signal [89, 90, 95-97].

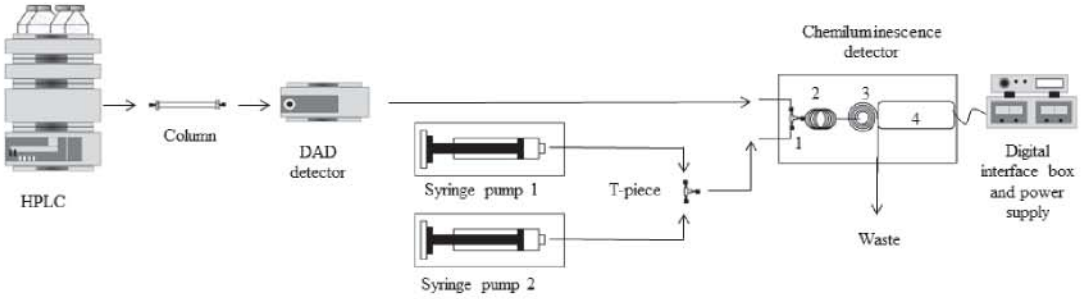

Figure 6. Instrument setup for HPLC with Luminol chemiluminescence detection. 1, T piece; 2, mixing coil; 3, reaction coil; 4, photomultiplier tube (PMT).

Although these on-line techniques have reportedly been employed for the determination of exogenous antioxidants in such samples as green tea, herb extracts, fruits and berries they suffer from significant shortcomings. The major constraint of the $DPPH^{\bullet}$ or $ABTS^{\bullet+}$ approaches is the time-scale required for sufficient reaction of these reagents and sample components in comparison with the chromatographic separation [89, 90, 98]. A long reaction coil (up to 15 m of 0.25 mm i.d. tubing) between the confluence point and detector is therefore required, but the solution transport through the coil also broadens each analyte zone, which has a detrimental effect on resolution [89, 90, 99-105]. Other issues associated with these techniques include the need for an additional HPLC pump and UV–vis detector, lengthy reagent preparation times and the irreproducibility associated with monitoring negative signals due to the inhibition of a high background [89, 90]. Although the combination of a chromatographic separation with post-column detection of antioxidants in natural matrices with simultaneous evaluation of their bioactivity

represents a powerful research tool, the aforementioned drawbacks have limited its use to only a small number of groups worldwide [89, 90].

4. Chemiluminescence

Chemiluminescence is defined as the production of light (ultraviolet, visible or near infrared) as the result of a chemical reaction [106]. This phenomenon is observed when a reaction produces an electronically excited species that either luminesces (direct chemiluminescence) or transfers its energy to a suitable compound, which then becomes the emitter (indirect or sensitised chemiluminescence) [106]. These light-producing reactions can be used for quantitative detection as the emission intensity is related to the concentrations of the chemical species involved [106]. Furthermore, chemiluminescence (particularly in the liquid phase) has become a well-established and widely applied analytical technique as it offers highly sensitive detection using relatively simple instrumentation [106-115].

An effective methodology for generating and measuring chemiluminescence emissions in a continuous stream is flow injection analysis (FIA) because it allows rapid and reproducible mixing of a sample and reagent(s) within close proximity to the detector [108, 112, 115, 116]. As described in the comprehensive review by Fletcher *et al.* [115], this approach has been used extensively to probe the fundamental chemistry of chemiluminescence reactions, optimise post-column reaction conditions for liquid chromatography and to quantify analytes in relatively simple matrices. When analysing more complex samples, FIA lacks the selectivity required to discriminate between the signal arising from the target analyte(s) and those of interfering compounds. However, selectivity can be introduced by means of a separation step and consequently, chemiluminescence detection is often coupled to

liquid chromatography or electrophoresis [107-111, 116]. The major problem encountered in these approaches is the compatibility between the conditions required for an efficient separation (most notably mobile phase composition and pH) and those needed for an optimal chemiluminescence emission [107-111]. Nevertheless, post-column chemiluminescence has been used to quantify numerous analytes in such matrices as physiological fluids along with plant, food, beverage and environmental samples [107-111].

4.1 Acidic potassium permanganate chemiluminescence

Acidic potassium permanganate chemiluminescence was first reported in 1917 by Harvey [117], but it was not employed analytically until 1975 by Stauff and Jaeschke [118] for the determination of sulfur dioxide. Since then hundreds of scientific papers have been published detailing its applications. As described in the comprehensive reviews by Hindson *et al.* [119] and Adcock *et al.* [113], the majority of these studies have employed permanganate chemiluminescence for the determination of organic compounds, which usually contain a phenolic and/or amine moiety. The characteristic red emission (λ_{max} = 689 ± 5 nm) has been shown to emanate from a manganese(II) species upon relaxation from an excited state ($^4T_1 \rightarrow {}^6A_1$ transition) [113, 120, 121]. Furthermore, in the presence of polyphosphates, a significant (~ 50 fold) increase in the intensity of this emission has been reported [113, 119]. However, it was not until recently that both a unified scheme for acidic potassium permanganate chemiluminescence and a mechanism for its enhancement were elucidated. Using spectroscopic and synthetic methods, Hindson *et al.* [122] demonstrated that a radical intermediate is generated from oxidation of the analyte by manganese(IV). This transient radical species was then shown to react with manganese(III) present in the solution to produce the previously

characterised manganese(II)* emission source as shown in Figure 7 [122]. Moreover, enhancement of emission intensity when the reaction was conducted in the presence of polyphosphates was found to proceed by two separate mechanisms that work in combination [122]. They report that in addition to preventing disproportionation of the manganese(III) intermediate, the polyphosphates formed 'cage like' structures around the manganese(II)*, limiting nonradiative pathways [122].

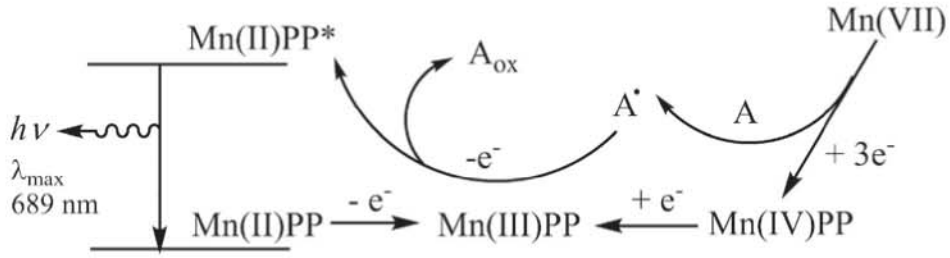

Figure 7. Postulated mechanism for permanganate chemiluminescence in the presence of polyphosphates (image from Hindson *et al.* [122]).

Although numerous analytes have been determined using permanganate chemiluminescence, phenols and polyphenols have received the most attention [113]. These compounds form one of the most important classes of exogenous antioxidants, and are widely distributed amongst many species of plants, being present in most edible fruits and vegetables [15, 123, 124]. Studies have primarily focused on the detection of individual phenols and polyphenols considered to be antioxidants using FIA based analytical techniques [113, 119, 125-127]. Of these reports, compounds including ascorbic acid, quercetin, catechin, melatonin, caffeic acid, quercetin, resveratrol and rosmarinic acid have been shown to result in a relatively intense emission, with limits of detection typically between 1 and 10 nM [113, 119, 125-127]. However, without a chromatographic separation step, these approaches are ineffective for the determination of multiple phenols in a complex sample. Costin *et al.* [126] used this to their advantage, employing FIA with permanganate chemiluminescence detection to monitor the total antioxidant capacity (reported as

total phenolic content) of six red and six white wine samples. A subsequent investigation by Francis and co-workers [98] extended this analytical methodology to measure the total antioxidant capacity of fruit juices and teas. The results obtained with permanganate chemiluminescence detection were directly compared to those of two conventional off-line approaches, the $DPPH^{\bullet}$ assay and a commercially available $ABTS^{\bullet+}$ test kit [98]. Good correlation was observed between the approaches and permanganate chemiluminescence was found to be far more rapid than the other two procedures which can take in excess of 30 min per sample [98]. This flow analysis methodology was coupled with HPLC to demonstrate the feasibility of permanganate chemiluminescence detection for the analysis of individual antioxidants from within complex samples [98]. Although this reagent has previously been used for quantitative post-column detection of various other biomolecules (such as neurotransmitters and their metabolites [128], opiate alkaloids [129], and adrenergic amines [130]), this was the first time it had been used to examine the reactivity of sample components. Preliminary screening of green and black tea was conducted, with several major antioxidants identified [98].

4.2 Tris(2,2′-bipyridine)ruthenium(III) chemiluminescence

Tris(2,2′-bipyridine)ruthenium(II) $[Ru(bipy)_3]^{2+}$ was originally synthesised in 1936 by Burstall [131] but it was not until three decades later that the first published account of chemiluminescence from this complex was reported by Hercules and Lytle [132]. Since that time, $[Ru(bipy)_3]^{2+}$ has attracted a large amount of attention as a sensitive and selective chemiluminescence reagent, with its analytical applications the subject of numerous reviews [109, 133-137]. Whilst a unified reaction scheme for $[Ru(bipy)_3]^{2+}$ chemiluminescence is yet to be elucidated, common to all analytical applications is the general detection chemistry (summarised in Scheme 1)

[109, 133-137]. It relies upon the initial oxidation of $[Ru(bipy)_3]^{2+}$ to produce the reagent, $[Ru(bipy)_3]^{3+}$ which in turn is reduced by a suitable analyte leaving the ruthenium(II) complex in an electronically excited state that subsequently returns to its ground state by emission of a photon [109, 133-137]. The methods of generating $Ru(bipy)_3^{3+}$ and its inherent instability in aqueous solution (due to its ability to oxidise water [138]) have proven to be significant impediments to the analytical utility of this chemiluminescence reagent [109, 133-137]. In the majority of applications reported to date the production of $[Ru(bipy)_3]^{3+}$ has been accomplished using electrochemical oxidation as the reagent can be produced immediately prior to reaction with the analyte, thus, overcoming issues with its instability [133, 136]. However, chemical oxidation using cerium(IV) sulfate or solid lead dioxide is steadily gaining in popularity [136].

$$[Ru(bipy)_3]^{2+} \xrightarrow{\text{Oxidation}} [Ru(bipy)_3]^{3+}$$

$$[Ru(bipy)_3]^{3+} \xrightarrow{\text{Reduction}} [Ru(bipy)_3]^{2+*}$$

$$[Ru(bipy)_3]^{2+*} \longrightarrow [Ru(bipy)_3]^{2+} + h\nu\ (620\ nm)$$

Scheme 1. Production of chemiluminescence from tris(2,2′-bipyridyl)ruthenium(II).

As described in numerous reviews [109, 133-137], $[Ru(bipy)_3]^{2+}$ chemiluminescence has primarily been employed for the detection of compounds containing an amine moiety including alkaloids, amino acids, organic acids pharmaceuticals, pesticides and proteins. Moreover, studies have shown that the signal intensity is normally greatest for tertiary amines, followed by secondary then primary amines [133, 136, 139, 140]. Perez-Ruiz *et al.* [141] investigated the use of $[Ru(bipy)_3]^{2+}$ chemiluminescence for detection of the amine containing amino acid, L-cysteine and its corresponding disulfide L-cystine. As previously described these

compounds form an important redox couple in the intracellular antioxidant defence network (Figure 2) [16, 37-40]. A complicated FIA manifold was employed where lines of L-cysteine and $[Ru(bipy)_3]^{2+}$ were merged with buffers before combining with a stream of peroxydisulphate and entering a UV reaction coil, in which $[Ru(bipy)_3]^{3+}$ was generated photochemically and reacted with L-cysteine to elicit a response [141]. Although L-cystine did not react with $[Ru(bipy)_3]^{3+}$ to yield chemiluminescence, a reductor column was fitted into the manifold in order to reduce cystine to cysteine prior to its determination [141]. Therefore, measurement of both amino acids was carried out by using a diverting valve so that the sample solution enters or bypasses the reductor column prior to filling the sample loop [141]. The proposed method was applied to the determination of L-cysteine and L-cystine in pharmaceutical formulations, but lacked the selectivity required for the quantification of these compounds in more complex matrices such as physiological fluids [141]. In a subsequent report, Nana *et al.* [142] describe the use of electrogenereated $[Ru(bipy)_3]^{2+}$ chemiluminescence for detection of the amine containing antioxidant GSH. Using a flow analysis technique, it was found that GSH enhanced the emission of $[Ru(bipy)_3]^{2+}$ at a hemim glassy carbon electrode [142]. However, the technique was not applied for the determination of GSH in any real samples [142].

4.3 Manganese(IV) chemiluminescence

As previously discussed, acidic potassium permanganate [manganese(VII)] has been extensively used as a chemiluminescence reagent for the detection of various organic compounds [113, 119]. However, researches have recently investigated other manganese-based oxidants for this purpose, including manganese(IV) [143]. The most commonly encountered form of this reagent is manganese dioxide, but its poor solubility in most solvents has limited its analytical applications [143]. Nevertheless,

under certain conditions potassium permanganate can be reduced to afford a suspension of manganese dioxide nano-particles which has been termed 'soluble' manganese(IV) [144-150]. In 1984 and again in 1993, Jáky *et al.* [146, 147] reported dissolving freshly precipitated manganese dioxide (produced by reduction of potassium permanganate with sodium formate) in 3 M aqueous orthophosphoric acid followed by agitating for 30 min then filtration to furnish, what they claim to be a non-colloidal brown solution of manganese(IV). However, researchers from within my laboratory found that an analogous reagent could be prepared without the filtration step, but required between 1 and 3 days for dissolution at room temperature [144]. Subsequent studies have revealed that the time taken to complete this step can be significantly reduced by subjecting the solution to ultrasonication for 30 minutes followed by heating at 80° C for 1h [145].

The light emitted from reactions with manganese(IV) has an emission maxima centred between 725 nm and 740 nm, characteristic of a many reactions with manganese based oxidants (i.e. permanganate) suggesting that it emanates from a manganese(II)* species [113, 121, 143-145, 151]. Furthermore, like permanganate, this emission can be greatly enhanced when conducted in the presence of certain species such as formaldehyde [125, 143-145, 152-154]. No apparent trend with respect to molecular structure and intensity has emerged, but it is clear that manganese(IV) offers markedly different selectivity than permanganate [143].

To-date, only a small number of compounds have been detected with manganese(IV) as detailed in the review of its analytical applications by Brown *et al.* [143]. The first investigation of chemiluminescence reactions with manganese(IV) was reported in 2001 by Hindson *et al.* [144], where analytical useful signals were recorded for twenty five organic and inorganic analytes. Since these initial

experiments, fifteen other manuscripts have emerged describing the use of manganese(IV) chemiluminescence for the detection of compounds such as ascorbic acid, opiate alkaloids and indoles [143, 155]. With the exception of one investigation [145], these applications have exclusively been based on FIA methodology [143, 155]. As a demonstration of post-column chemiluminescence detection with manganese(IV) Brown *et al.* [145] separated and determined six opiate alkaloid standards. However, this technique has not yet been applied to the detection of compounds in real samples such as biological fluids.

5. Project aims

Owing to the many key cellular roles that both endogenous and exogenous antioxidants play within metabolic processes, their detection and quantification is of significant importance to researchers from numerous disciplines. However, as antioxidants are often encountered in complex sample types (i.e. physiological fluids), it is challenging to screen and identify these species using the various HPLC based techniques previously outlined in this chapter. Therefore, this thesis primarily focuses on the coupling of HPLC separations with sensitive and selective post-column chemiluminescence detection for the determination and assessment of exogenous and endogenous antioxidants within biological based matrices.

CHAPTER TWO

High-performance liquid chromatography with post-column 2,2-diphenyl-1-picrylhydrazyl radical scavenging assay

- **Introduction**
- **Experimental**
- **Results and discussion**
- **Conclusion**

1. Introduction

As detailed in chapter 1, numerous batch-type assays have been developed to measure the total antioxidant capacity of various foods and biological matrices [80-83]. Whilst proving practical for determining total antioxidant capacity, batch assays provide little information on the contribution of individual compounds to the overall antioxidant effect of a sample [89, 90]. To address this issue, post-separation on-line assays for gas chromatography (GC) and HPLC to assess the potency of individual antioxidants from complex matrices have been developed [89, 90].

One of the most popular on-line (post-column) HPLC based antioxidant assays involves decolouration of $DPPH^{\bullet}$ [89, 90]. The original off-line version was introduced in 1958 by Blois [156] and subsequently converted to its post-column form by van Beek and co-workers [101] in 2000. Since then over twenty papers have emerged exploiting the post-column assay for detection of antioxidants in such samples as fruit, wood and herb extracts [99-103, 105, 157-173]. Typically, the assay involves merging a methanolic or buffered stream of the long lived $DPPH^{\bullet}$ radical with the post-column eluate at a T-piece. The resulting stream is then passed through a reaction coil of adequate length and diameter to provide sufficient time for $DPPH^{\bullet}$ to react with any radical scavenging species present (i.e. antioxidants), before entering a spectrophotometric detector and finally to waste. Thus, antioxidants are detected as negative peaks by monitoring the decrease in absorbance of the purple $DPPH^{\bullet}$ (517 nm) as it is reduced to the corresponding pale yellow hydrazine derivative [80].

Although the post-column $DPPH^{\bullet}$ assay is relatively simple in design, the response is dependent on experimental variables such as reagent concentration, pH, dissolved oxygen content, reaction coil dimensions and mobile phase composition [89, 90]. In

their original procedure, van Beek and co-workers [101] optimised several aspects, based on the response from model antioxidant compounds. In a subsequent publication [100], these authors modified reagent conditions (including adding an aqueous buffer solution to the methanolic DPPH$^{\bullet}$ reagent) to compensate for the presence of acid in the HPLC mobile phase, which improved separation, but had a deleterious effect on sensitivity. Other researchers have examined reaction coil internal diameter [164] and length [105, 167], buffer type [162, 167], and reagent flow rate [164]. As shown in Table 1, differences have arisen between the methodologies used by various research groups.

This chapter describes the systematic investigation of the relationships between experimental parameters and DPPH$^{\bullet}$ signal to develop a superior post-column radical scavenging assay, which was demonstrated by screening for antioxidants within green tea and thyme extracts, in comparison with contemporary methodology.

Table 1. Summary of post-column DPPH$^{\bullet}$ radical scavenging assay conditions used by various research groups.

	References		References
DPPH$^{\bullet}$ concentration		**DPPH$^{\bullet}$ buffer**	
0.13 M*	[161-163]	5 mM citric acid–disodium hydrogen phosphate buffer (pH 7.6) containing 75% Methanol	[99, 100, 104, 172]
1.3×10^{-4} M	[157-160, 167, 170, 172]	12.5 mM citric acid-sodium citrate buffer (pH 7.6) containing 75% methanol	[161-163]
1×10^{-4} M	[104, 165, 169, 173]	5 mM ammonium acetate in 100% methanol	[165, 166]
4×10^{-5} M	[166]	100mM 2-(N morpholino)ethanesulfonic acid buffer (pH 6.0) containing 50% methanol	[102]
3×10^{-5} M	[168]	10 mM ammonium citrate buffer (pH 7.4) containing 55% methanol	[167]
2×10^{-5} M	[105]	None (100% hexane)	[105]
1×10^{-5} M	[99-103]	None (100% methanol)	[101, 103, 157-160, 168-170, 172, 173]
DPPH$^{\bullet}$ sparging gas		**Reaction coil**	
Helium	[99, 100, 104]	15 m × 0.25 mm i.d PEEK tubing	[99-105]
Nitrogen	[161-163]	14 m × 0.25 mm i.d PEEK tubing	[166]
No sparging	[101-103, 105, 157-160, 164-173]	13 m × 0.25 mm i.d PEEK tubing	[161-163]
Assay temperature		5 m × 0.25 mm i.d PTFE tubing	[168]
Room temperature	[99-101, 103-105, 157-159, 161-168, 170-173]	4.4 m × 0.25 mm i.d PEEK tubing	[165]
60° C	[102, 169]	4 m × 0.18 mm i.d knitted PEEK tubing	[173]
		2.15 m × 0.77 mm capillary	[157]
		1.17 m × 0.33 mm i.d. knitted PTFE tubing	[164]
		0.2, 3.5 or 7m × 0.25 mm i.d. fused silica tubing	[167]

*Most likely a typographical error in the original papers.

2. Experimental

2.1 Chemicals and reagents

Deionised water (Continental Water Systems, Victoria, Australia) and analytical grade reagents were used unless otherwise stated. Chemicals were obtained from the following sources: 2,2-Diphenyl-1-picrylhydrazyl, caffeic acid, ethoxyquin, ferulic acid, gallic acid, quercetin, rosmarinic acid and rutin from Sigma-Aldrich (New South Wales, Australia); L-ascorbic acid, HPLC grade methanol and sodium citrate from BDH Chemicals (Poole, England) and citric acid and glacial acetic acid from Univar (New South Wales, Australia).

Antioxidant stock solutions (1×10^{-3} M) were prepared in 100 % analytical grade methanol and appropriately diluted into 100 % analytical grade methanol.

The DPPH$^{\bullet}$ stock solution was prepared in methanol at the beginning of each day of analysis at a concentration of 1×10^{-3} M. This solution was appropriately diluted and mixed with a 40 mM citric acid-sodium citrate buffer (pH 6) at a ratio of 75:25. The resulting DPPH$^{\bullet}$ reagent was degassed with nitrogen and kept protected from light by wrapping in aluminium foil before use.

2.2 Sample preparation

2 g of Twinings of London, Pure Green Tea (AB Food & Beverages Australia, Victoria, Australia) was weighed out from tea bags and transferred to a 250 mL beaker containing 200 mL of boiling deionised water. The tea was left stirring on the hot plate for 2 minutes, then allowed to cool to room temperature, filtered (0.45 μm, Millipore Millex-HN Nylon) and analysed.

Dried thyme (0.5 g) was extracted according to the procedure of Koleva and co-workers [174], using 100 mL acetonitrile-acetic acid-water (70:1:29 by volume) followed by sonication for 15 min. A 1 mL aliquot was diluted with 3 mL of water, filtered (0.45 μm, Millipore Millex-HN Nylon) and analysed.

2.3 High performance liquid chromatography with post-column DPPH$^{\bullet}$ antioxidant assay

Chromatographic analysis was carried out on an Agilent Technologies 1200 series liquid chromatography system, equipped with a quaternary pump, solvent degasser system, autosampler and diode array detector (Agilent Technologies, Victoria, Australia). Figure 5 shows the on-line DPPH$^{\bullet}$ assay manifold, which consisted of an isocratic HPLC pump (Agilent Technologies), a polyaryletheretherketone (PEEK) reaction coil (Upchurch Scientific, Washington, USA), and a UV-vis absorbance detector (Agilent Technologies). The flow rate of the DPPH$^{\bullet}$ reagent was set to 0.75 mL min^{-1} (unless otherwise stated) and any induced reduction was detected as a negative peak. Hewlett-Packard Chemstation software (Agilent Technologies) was used to control the HPLC pumps and acquire data from the diode array and UV-vis absorbance detectors.

In optimisation experiments, analyte standards were injected (20 μL) onto a Chromolith SpeedROD RP-18 monolithic column (50 mm × 4.6 mm i.d.; Merck) and eluted with 100% methanol at a flow rate of 0.75 mL min^{-1}. Reagent conditions are described in corresponding figure captions. Thyme and green tea samples were separated using a reverse phase Alltech Alltima C18 analytical column (250 mm × 4.6 mm i.d., particle size 5 μm, Agilent Technologies) operating at room temperature with an injection volume of 20 μL and a flow rate of 1 mL min^{-1}. Gradient elution was performed using 0.05% v/v acetic acid (solvent A) and HPLC

grade methanol (solvent B) as outlined in Table 2. All solvents were filtered through a 0.45 μm nylon membrane. For comparison purposes, the time axis of the respective chromatograms were adjusted to account for the differences in volume between the column and detectors for each DPPH$^{\bullet}$ assay.

Table 2. Gradient elution profile.

Time (min)	Solvent A (%)	Solvent B (%)
0	80	20
2	80	20
22	30	70
26	30	70
26.01	80	20
30	80	20

3. Results and Discussion

3.1 Optimisation of the post-column DPPH• antioxidant assay

To establish conditions that afford the best response from the DPPH• reaction, various parameters believed to be influential, including reagent concentration, pH, dissolved oxygen content, tubing length and internal diameter and assay temperature were optimised in a univariate approach. In a preliminary examination of DPPH• reagent flow rates, 0.75 mL min^{-1} proved to be the most compatible for a wide range of mobile phase flow rates, and is similar to that used in previous studies [101, 161-163]. Eight antioxidants (Figure 8) commonly found in plant, food and beverage extracts were selected as model compounds that have previously been classified to represent three types of kinetic behaviour with respect to their reaction with the DPPH radical: rapid, intermediate or slow [84, 101, 157].

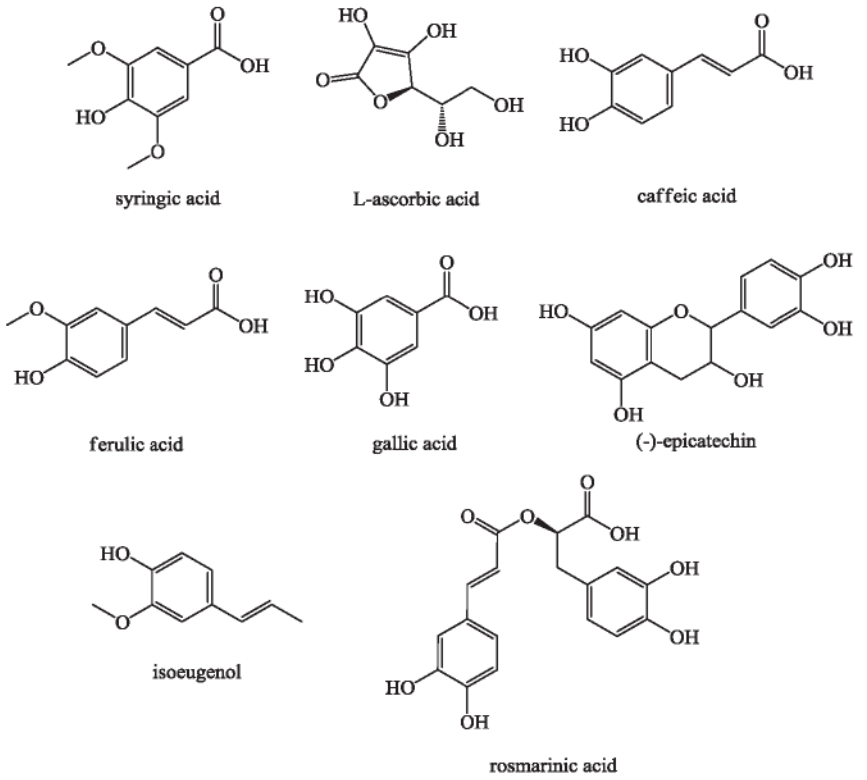

Figure 8. Model antioxidant compounds.

3.1.1 Reagent concentration

In their cornerstone paper, van Beek and co-workers [101] investigated the influence of DPPH$^{\bullet}$ reagent concentration, establishing 1×10^{-5} M to be optimum in terms of signal-to-noise ratio under their experimental conditions. In subsequent publications researchers have employed either the same, or considerably higher DPPH$^{\bullet}$ reagent concentrations (see Table 1) without experimental justification. One research group has reported using 50 mg mL^{-1} (0.13 M) [161-163]. Although this was most likely a typographical error, I attempted to prepare the reagent at this concentration. Even with sonication the DPPH$^{\bullet}$ did not completely dissolve in methanol.

I examined the influence of reagent concentration (between 1×10^{-6} M and 5×10^{-4} M) on the reaction of DPPH$^{\bullet}$ with the eight model antioxidant compounds at 1×10^{-5} M and 1×10^{-4} M. The results for caffeic acid (representative of all standards) are shown in Figure 9. In the parameter range studied, the response grew with increasing DPPH$^{\bullet}$ concentration for all analytes. However, an increase in noise was also observed, particularly at low analyte concentrations. I found that under our conditions, a DPPH$^{\bullet}$ concentration of 5×10^{-5} M generally provided the best overall signal-to-noise for low and high analyte concentrations, and was used through the remaining optimisation experiments.

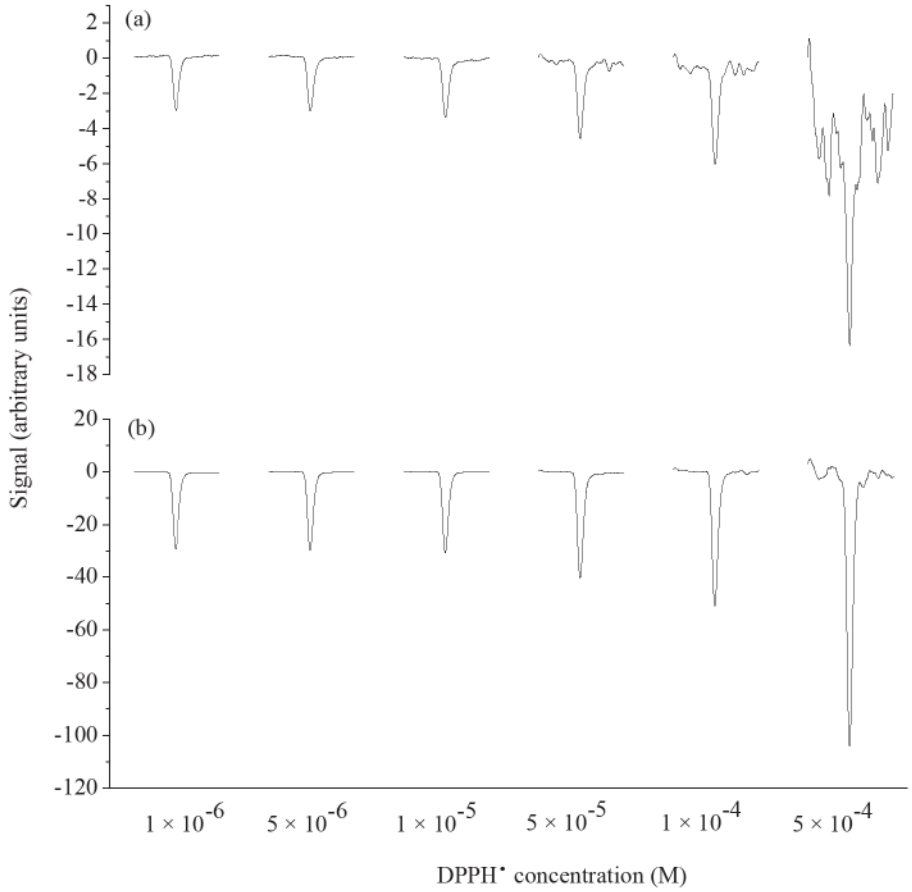

Figure 9. Influence of DPPH$^{\bullet}$ concentration on response for caffeic acid at (a) 1×10^{-5} M and (b) 1×10^{-4} M. HPLC conditions: Column, Chromolith SpeedROD RP-18 monolith; injection volume, 20 µL; mobile phase, 100% methanol; flow rate, 0.75 mL min^{-1}. DPPH$^{\bullet}$ assay conditions: Reaction coil, 15 m × 0.25 mm i.d. PEEK tubing; DPPH$^{\bullet}$ flow rate, 0.75 mL min^{-1}; Detection, 517 nm.

3.1.2 Reagent pH

Researchers who utilise off-line DPPH$^{\bullet}$ assays for measurement of total antioxidant capacity normally prepare the reagent in 100% methanol or ethanol [80, 81, 83]. As a result, this approach has been translated to many post-column DPPH$^{\bullet}$ procedures, with several groups preparing the reagent in 100% methanol [101, 103, 157-160, 164, 168, 170-173]. However, unlike its off-line counterpart, measurements made post-column cannot always be performed in a 100% alcoholic environment, as chromatographic separations often require the use of acids, water or other organic solvents, which can have a profound influence on the DPPH$^{\bullet}$ reaction

[89, 90]. Furthermore, since the post-column assay is predominantly applied to complex biological extracts that require highly efficient HPLC separations, then little compromise to the mobile phase composition and pH can be afforded.

In the initial post-column DPPH$^{\bullet}$ method developed by van Beek and co-workers [101], the reagent was dissolved in 100% methanol, but in a subsequent publication they recommended preparing the reagent in 75% methanol and 25% 20 mM citric acid-disodium hydrogen phosphate buffer (pH 7.6), to compensate for the presence of acid in the mobile phase [100]. Since then, several research groups have utilised buffered DPPH$^{\bullet}$ solutions for their post-column assays [99, 100, 104, 161-163]. Koşar *et al.* [162] noted that the optimum range for the DPPH$^{\bullet}$ reaction is pH 5.0 to 6.5 (as described by Blois [156]), but curiously, they used a DPPH$^{\bullet}$ solution buffered at pH 7.6 [161-163]. They also evaluated three different buffer systems and found that the reagent was most stable using a citric acid-sodium citrate buffer [162]. Oki *et al.* [102] buffered their DPPH$^{\bullet}$ reagent at pH 6.0 using 2-(N-morpholino)ethanesulfonic acid, but they offer no reasoning as to why this pH value was used. Bartasiute *et al.* [167] selected a more physiologically relevant pH of 7.4 in an attempt to obtain better in vivo predictability of their assay results. However, to the best of my knowledge, no attempt has been made at optimising buffer pH for maximum signal response.

To establish the influence of pH, the eight antioxidants at two different concentrations (1×10^{-5} M and 1×10^{-4} M) were screened with 5×10^{-5} M DPPH$^{\bullet}$ solutions in 75% methanol: 25% 40 mM citric acid-sodium citrate buffer of seven different pH values (8, 7.5, 7, 6.5, 6, 5.5 and 5). Since Ozcelik *et al.* [175] showed that the absorbance of DPPH$^{\bullet}$ can shift depending on pH and solvent, an appropriate wavelength to measure DPPH$^{\bullet}$ in the buffered solution had to first be established.

Using a spectrophotometer, the maximum absorbance across all pH values was located at 521 nm. Furthermore, monitoring of DPPH$^{\bullet}$ absorption over time revealed that the reagent was stable for at least 24 h. As can be seen in Figure 10, a buffered DPPH$^{\bullet}$ solution at pH 6 produced the largest response for all eight antioxidants.

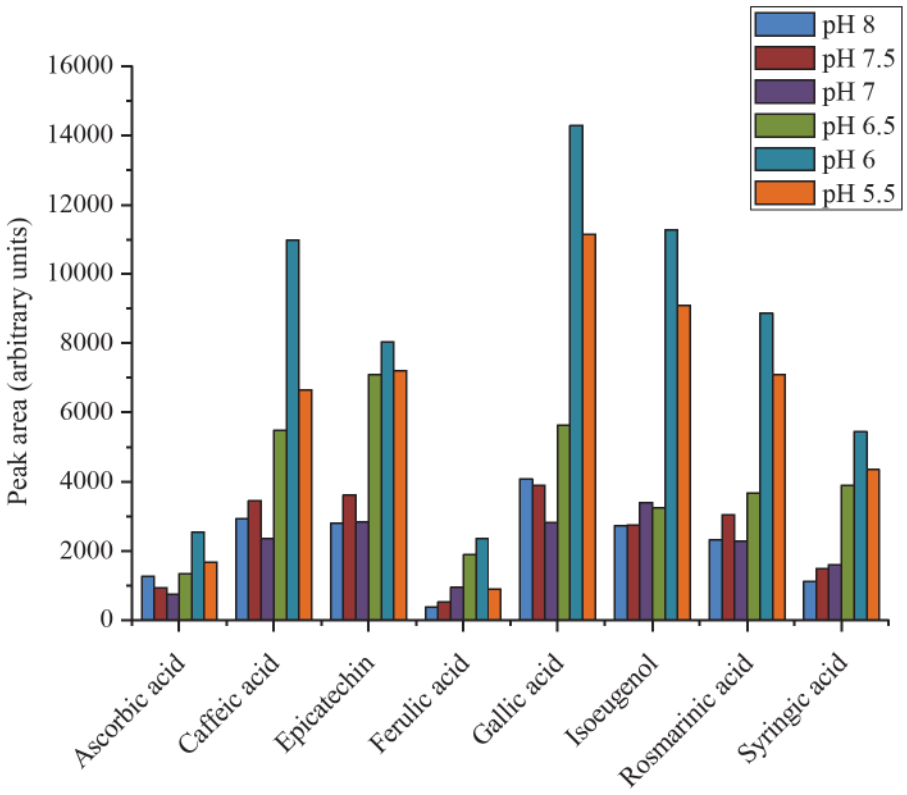

Figure 10. Influence of citric acid-sodium citrate buffered reagent solution pH. HPLC conditions same as Figure 9. DPPH$^{\bullet}$ assay conditions: Reaction coil, 15 m × 0.25 mm i.d. PEEK tubing; DPPH$^{\bullet}$ flow rate, 0.75 mL min^{-1}; Detection, 521 nm; DPPH• solution, 5 × 10^{-5} M in methanol: 40 mM citric acid-sodium citrate buffer (75:25). Analyte concentration: 1 × 10^{-4} M.

3.1.3 Reagent degassing

In addition to buffering their DPPH$^{\bullet}$ solution, van Beek and co-workers [100] further improved sensitivity by sparging their reagent with helium which reportedly led to an improvement in the minimum detectable amount of two model compounds, carvacrol and rosmarinic acid, along with reducing baseline drift, most likely due to the elimination of dissolved oxygen. Similarly, Koşar *et al.* [161-163] degassed a

citrate buffered (pH 7.6) DPPH$^{\bullet}$ solution with nitrogen after filtering it through a 0.45 μm membrane filter. However, in the most recent of these publications, Koşar *et al.* [162] suggest that degassing is not necessary when using a citric acid-sodium citrate buffered reagent, which was found to provide a stable baseline with minimum noise. Moreover, the majority of reported procedures for post-column DPPH$^{\bullet}$ radical scavenging assays do not incorporate reagent degassing (Table 1). Under the conditions of this investigation, degassing the reagent solution with either nitrogen or helium yielded a two- to six-fold increase in DPPH$^{\bullet}$ response for all antioxidants when tested at a concentration of 1×10^{-4} M (Figure 11). Although a citric acid-sodium citrate buffered DPPH$^{\bullet}$ reagent solution may provide a stable baseline with minimum noise [162], degassing should still be performed to achieve greater assay sensitivity. Since there was little difference in signal improvement (Figure 11), sparging with nitrogen was preferred as it is a more economical alternative to helium. As a result, remaining experiments were performed with a reagent solution of 5×10^{-5} M DPPH$^{\bullet}$ in 75% methanol and 25% 40 mM citric acid-sodium citrate buffer at pH 6, degassed with nitrogen.

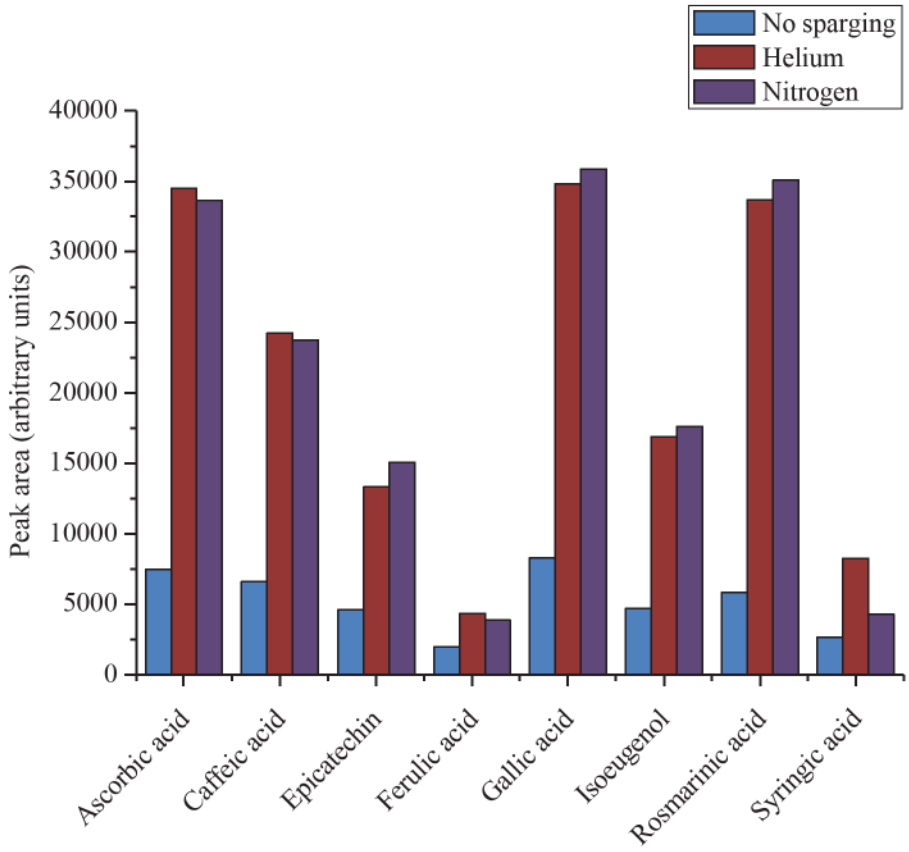

Figure 11. Influence of degassing the DPPH$^{\bullet}$ reagent. HPLC conditions same as Figure 9. DPPH$^{\bullet}$ assay conditions: Reaction coil, 15 m × 0.25 mm i.d. PEEK tubing; DPPH$^{\bullet}$ flow rate, 0.75 mL min^{-1}; Detection, 521 nm; DPPH$^{\bullet}$ solution, 5×10^{-5} M in methanol: 40 mM citric acid-sodium citrate buffer (75:25) pH 6. Analyte concentration: 1×10^{-4} M.

3.1.4 Reaction coil length (residence time)

As previously mentioned, the kinetic behaviour of antioxidants on reaction with DPPH$^{\bullet}$ within batch-type assays has been classified into three main types; rapid, intermediate, or slow, depending on the nature of the compound [84]. Off-line DPPH$^{\bullet}$ experiments often require reaction times of up to 30 minutes to allow the reduction of DPPH$^{\bullet}$ to reach a steady state [80, 81, 83]. However, such long reaction times are not feasible for the on-line, post-column DPPH$^{\bullet}$ assay.

In their initial publication, van Beek and co-workers [101] compared 9 s and 30 s reaction times on the DPPH$^{\bullet}$ signal-to-noise ratio for eugenol and isoeugenol, using

two different DPPH$^{\bullet}$ concentrations (5×10^{-6} M and 1×10^{-5} M). Along with concluding that the effect of DPPH$^{\bullet}$ concentration and reaction time are largely independent, they found that the 30 s reaction time, which required a 15 m × 0.25 mm i.d. reaction coil, provided the best response. Although the tubing was small in diameter, the solution transport through this 15 m coil broadens each reaction zone, which can lead to poor resolution in DPPH$^{\bullet}$ quenching chromatograms. Nevertheless, the aforementioned DPPH$^{\bullet}$ reaction coil dimensions have remained largely unchanged across the majority of post-column DPPH$^{\bullet}$ assay publications (Table 1). However, a recent publication by Bartasiute *et al.* [167] has suggested that when water is present in the reaction coil (i.e. when using a buffered DPPH$^{\bullet}$ solution and/or an aqueous HPLC mobile phase), the reaction is governed by thermodynamics rather than kinetics. This implies that shorter reaction coils may be incorporated, as the reaction between the antioxidant and DPPH$^{\bullet}$ is thought to rapidly achieve a steady-state [167]. Thus, the influence of reaction coil length (15, 10, 5, 4, 3, 2, 1 m; all 0.25 mm i.d.) on DPPH$^{\bullet}$ response was investigated. A reaction coil of 2 m (residence time of 4 s) gave similar peak areas to that of a 15 m coil (residence time of 30 s) (Figure 12). Furthermore, a 13 m decrease in reaction coil length resulted in significantly lower backpressure on the HPLC system. The influence of reagent concentration and pH, and the effect of degassing were re-examined using a reaction coil length of 2 m (using eight antioxidant standards at three different concentrations), and the optimum conditions were again found to be 5×10^{-5} M DPPH$^{\bullet}$ in 75% methanol and 25% 40 mM citric acid-sodium citrate buffer at pH 6, degassed with nitrogen.

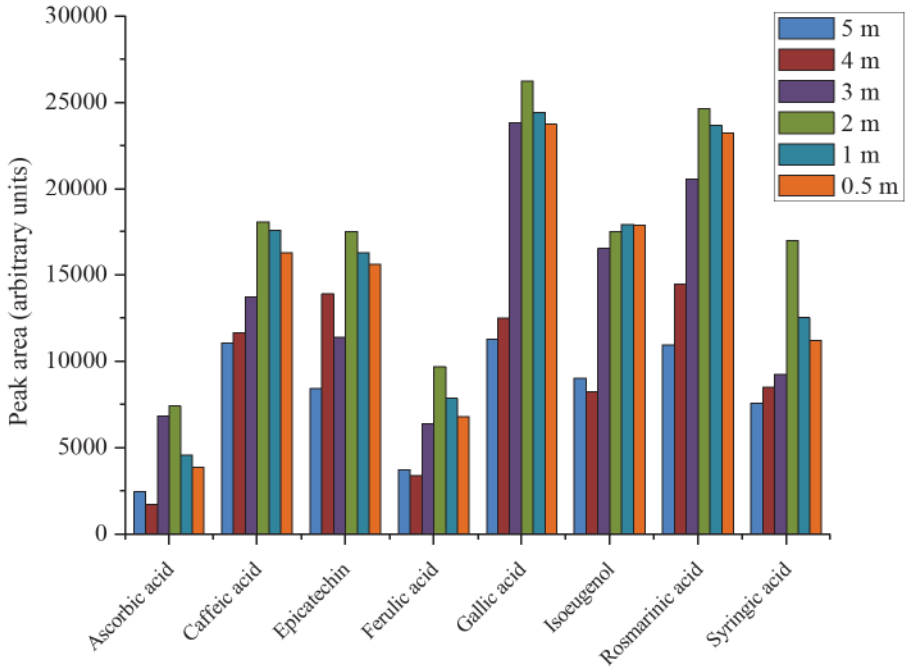

Figure 12. Influence of reaction coil length. HPLC conditions same as Figure 9. DPPH$^{\bullet}$ assay conditions: Reaction coil i.d., 0.25 mm i.d. PEEK tubing; DPPH$^{\bullet}$ flow rate, 0.75 mL min^{-1}; Detection, 521 nm; DPPH• solution, 5 × 10^{-5} M in methanol: 40 mM citric acid-sodium citrate buffer (75:25) pH 6, degassed with nitrogen. Analyte concentration: 1 × 10^{-4} M.

3.1.5 Reaction coil temperature

The final experimental parameter examined was reaction coil temperature. During their investigation into changes in radical-scavenging activity of mulberry fruit during maturation, Oki *et al.* [102] heated their post-column reaction coil to 60° C. Likewise, I have previously used a reaction coil heated to 60° C for the comparison of antioxidant profiles of espresso coffee brews [169]. To investigate the influence of temperature, the optimised DPPH$^{\bullet}$ reactor was coiled around a heating block, maintained at a constant temperature using a digital control. The reaction coil was heated from room temperature to 120° C by increments of 20° C.

The results in Figure 13 show that no advantage in overall response was gained by heating the reaction coil. Whilst signals for quercetin, rosmarinic acid and rutin improved slightly with increasing temperature, ascorbic acid, caffeic acid,

ethoxyquin and gallic acid signals decreased. Room temperature was therefore concluded to be sufficient for post-column measurements.

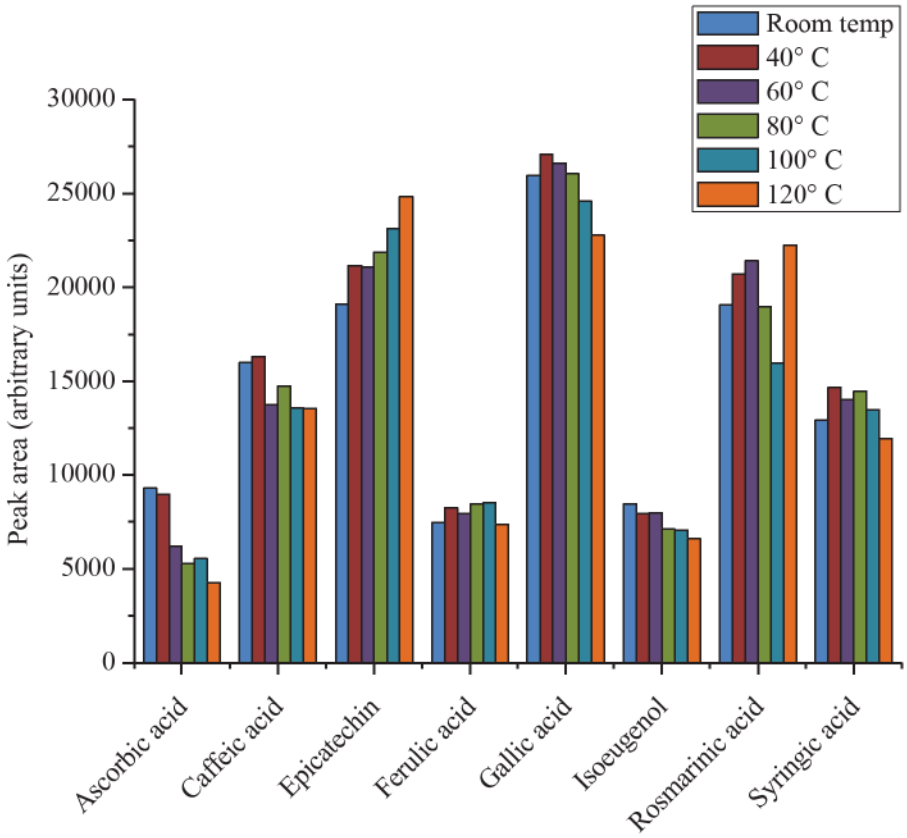

Figure 13. Influence of reaction coil temperature. HPLC conditions same as Figure 9. DPPH$^{\bullet}$ assay conditions: Reaction coil length, 15 m × 0.25 mm i.d. PEEK tubing; DPPH$^{\bullet}$ flow rate, 0.75 mL min^{-1}; Detection, 521 nm; DPPH$^{\bullet}$ solution, 5×10^{-5} M in methanol: 40 mM citric acid-sodium citrate buffer (75:25) pH 6, degassed with nitrogen. Analyte concentration: 1×10^{-4} M.

3.2 Evaluation of optimised post-column DPPH$^{\bullet}$ assay

To assess the analytical utility of the post-column assay protocol described herein, it was used to screen for radical scavenging compounds in thyme and green tea extracts, with results directly compared to those generated using the two commonly employed methodologies of van Beek and co-workers (Koleva *et al.* [101] and Dapkevicius *et al.* [100]). A comparison between the UV absorption and DPPH$^{\bullet}$ quenching chromatograms obtained using the different post-column reaction protocols (Table 3) for the screening of radical scavenging compounds in thyme is

presented in Figure 14. Firstly, comparing the conditions of Koleva *et al.* [101] and Dapkevicius *et al.* [100] (Figure 14, chromatograms b and c), many of the same peaks were detected, but the latter approach was more sensitive towards several compounds (peaks 7, 11, 12, 13 and 16), which can predominantly be attributed to buffering and degassing the reagent solution. Under our conditions (Figure 14d), the same compounds were again detected, but peaks 1, 3, 4, 7, 8 and 16 were significantly greater in intensity. Moreover, the shorter reaction coil resulted in greater chromatographic resolution, without loss of $DPPH^{\bullet}$ response.

Table 3. Post-column $DPPH^{\bullet}$ antioxidant assay conditions.

	This thesis	**Koleva *et al.* [101]**	**Dapkevicius *et al.* [100]**
$DPPH^{\bullet}$ flow rate (mL min^{-1})	0.75	0.7	0.5
$DPPH^{\bullet}$ concentration (M)	5×10^{-5}	1×10^{-5}	1×10^{-5}
$DPPH^{\bullet}$ buffer	25% 40 mM citric acid-sodium citrate buffer (pH 6), 75% methanol	None (100% methanol)	25% 20 mM citric acid-sodium citrate buffer (pH 7.6), 75% methanol
$DPPH^{\bullet}$ sparging	Nitrogen	None	Nitrogen
Reaction coil	2 m × 0.25 mm i.d. PEEK tubing	15 m × 0.25 mm i.d. PEEK tubing	15 m × 0.25 mm i.d. PEEK tubing

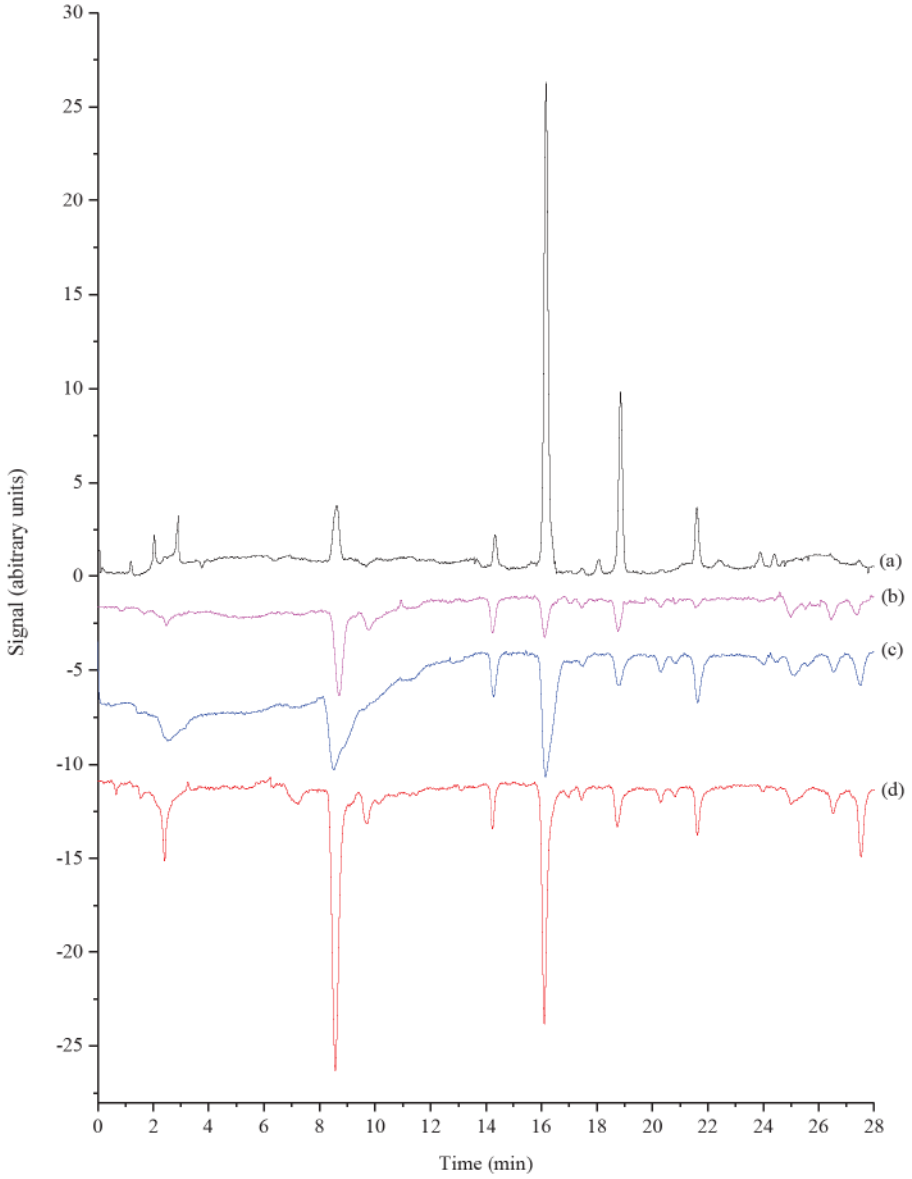

Figure 14. HPLC traces of a thyme extract with: (a) UV absorbance detection at 280 nm; (b) DPPH$^{\bullet}$ detection using the method of Koleva *et al.* [101]; (c) DPPH$^{\bullet}$ detection using the method of Dapkevicius *et al.* [100] and (d) DPPH$^{\bullet}$ detection using method described in this chapter.

A green tea extract that contained higher concentrations of antioxidant compounds than those in the diluted thyme extract was also examined using the three on-line DPPH$^{\bullet}$ assays described in Table 3. Our optimised conditions enabled the detection of a greater number of potential antioxidants, and in general produced larger signals (Figure 15, chromatogram d). Of particular interest is the region between 19.0 and 21.5 min, where two relatively small, broad peaks with shoulders were observed

using the conditions of Koleva *et al.* [101], two larger peaks with a smaller peak in between using the method described by Dapkevicius *et al.* [100]), and four distinct peaks using our conditions. Furthermore, peaks 6, 7 and 8 were much more prominent in chromatogram (d).

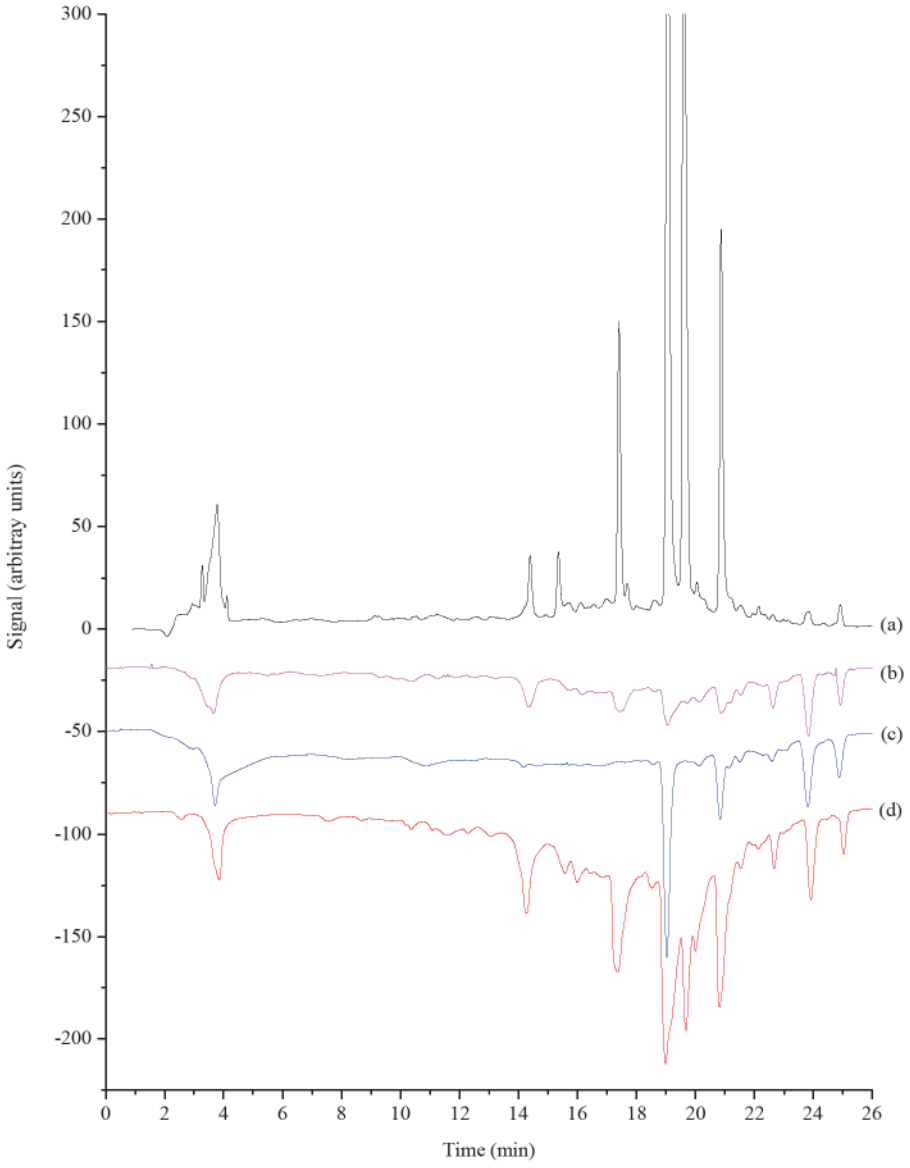

Figure 15. HPLC traces of a green tea extract with: (a) UV absorbance detection at 280 nm; (b) DPPH$^{\bullet}$ detection using the method of Koleva *et al.* [101]; (c) DPPH$^{\bullet}$ detection using the method of Dapkevicius *et al.* [100] and (d) DPPH$^{\bullet}$ detection using method described in this chapter.

An additional comparison between the three post-column DPPH$^{\bullet}$ assays (Table 3) was carried out by screening for radical scavenging compounds in red wine

(Figure 16). Here, the methodologies of Koleva *et al.* [101] and Dapkevicius *et al.* [100] both resulted in uncharacteristic DPPH$^{\bullet}$ chromatograms, comprising of positive absorbance peaks. It has been noted that for the off-line version of the DPPH$^{\bullet}$ reaction, spectrophotometric measurements can be affected by compounds that absorb at the wavelength of determination [82], so HPLC analysis of red wine was also carried out measuring absorbance at 517 nm. It can be seen in Figure 16 that the chromatogram collected generally matched the aforementioned DPPH$^{\bullet}$ quenching profiles. Owing to the complex nature of the sample, a broad peak, comprised of numerous compounds can be observed from 12 minutes to 24 minutes in the red wine UV chromatogram at 517 nm. This is most likely to be the result of co-eluting anthocyanins along with their respective glycosides, which are responsible for the red/purple colouring of red wine [176]. In contrast, it can be seen in Figure 16 that compounds absorbing at 517 nm in the sample matrix had no observable effect on the DPPH$^{\bullet}$ signal when employing the procedure described herein. This is almost certainly a consequence of the increase in reagent concentration in comparison to that used by Koleva *et al.* [101] and Dapkevicius *et al.* [100], resulting in a baseline absorbance significantly larger than that of any possible interfering compounds.

Further examination of the DPPH$^{\bullet}$ quenching chromatogram for red wine collected using the method described herein shows no baseline noise and sharp negative peaks. Once again, this highlights the importance of using a buffered and degassed reagent in addition to a relatively short reaction coil. Although numerous peaks are observable in the DPPH$^{\bullet}$ chromatogram, as previously mentioned, the complex nature of the sample matrix resulted in poor resolution between eluting compounds, making identification of individual peaks difficult.

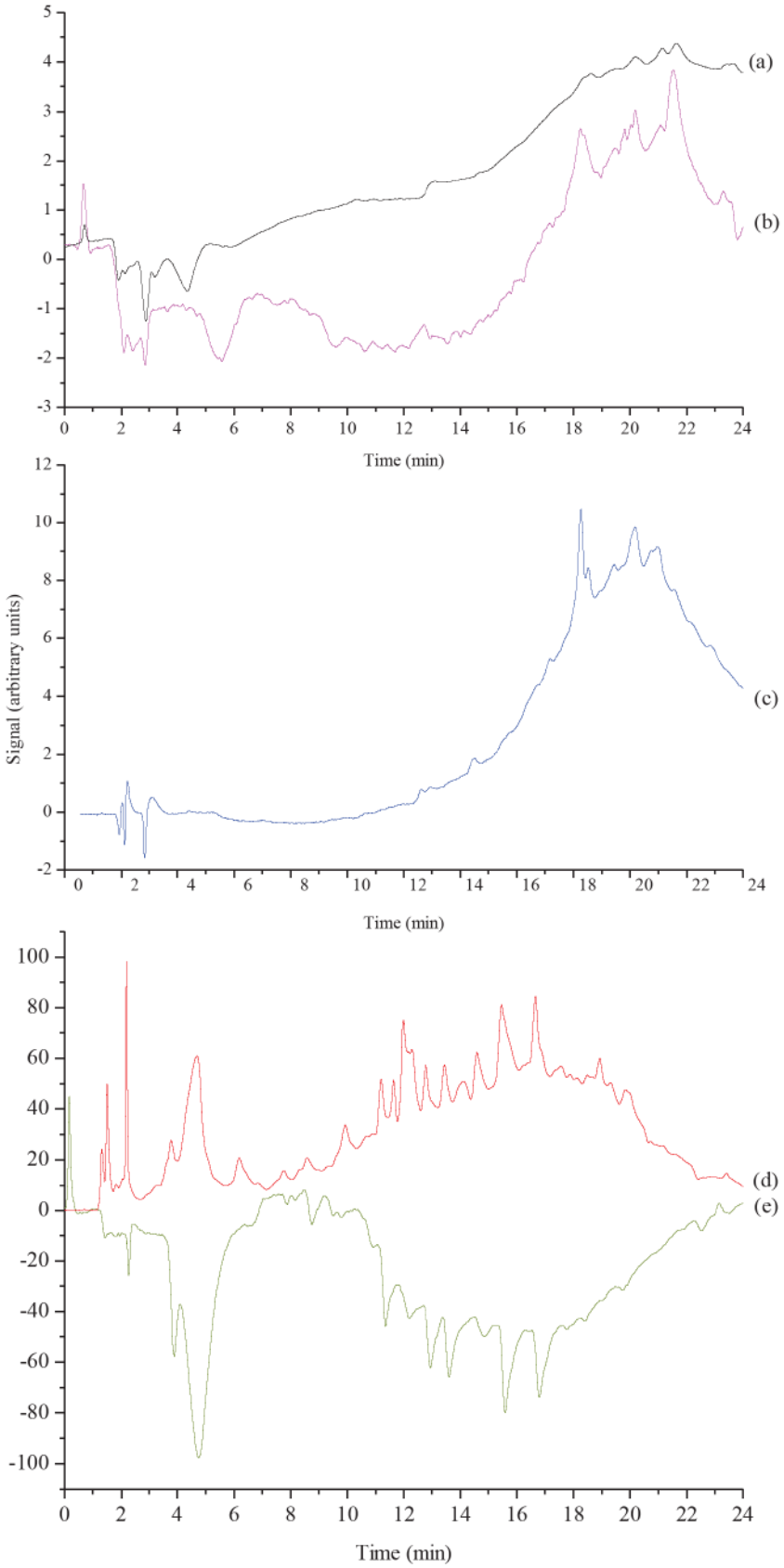

Figure 16. HPLC chromatographic profiles of red wine with: (a), DPPH$^{\bullet}$ detection using the method of Dapkevicius *et al.* [100]; (b), DPPH$^{\bullet}$ detection using the method of Koleva *et al.* [101]; (c) UV detection 517 nm; (d), UV detection 280 nm; (e) DPPH$^{\bullet}$ detection using method described in this chapter.

4. Conclusions

In this chapter a systematic optimisation of experimental parameters believed to be influential to $DPPH^{\bullet}$ response was undertaken in a univariate approach. Optimum conditions were found to be: 5×10^{-5} M $DPPH^{\bullet}$ reagent prepared in a 75% methanol: 25% 40mM citric acid–sodium citrate buffer (pH 6) solution, degassed with nitrogen; reaction coil of 2 m × 0.25 mm i.d. PEEK tubing; detection at 521 nm; analysis at room temperature. The analytical utility of this protocol was evaluated by screening for antioxidants in thyme and green tea, in comparison with two commonly employed methodologies, and resulted in a recent publication [177].

CHAPTER THREE

Screening for antioxidants in complex matrices using high performance liquid chromatography with acidic potassium permanganate chemiluminescence detection

- **Introduction**
- **Experimental**
- **Results and discussion**
- **Conclusion**

1. Introduction

The ability of exogenous antioxidants to protect against oxidative damage has been comprehensively studied from various perspectives [2, 13, 17, 72, 76-79]. The primary focus, however, has been on their potential to assist endogenous antioxidants in preventing free-radical induced oxidative stress within the human body, implicated in a growing number of pathophysiological conditions [2, 13, 17, 72, 79]. As described in chapter 1, many off-line, batch style methodologies have been developed for the determination of exogenous antioxidants [80-83]. These assays are routinely employed to measure the total antioxidant capacity of whole plant and food matrices, but owing to sample complexity they generally prove to be insufficient for the assessment of individual antioxidants [80-83]. As an alternative, researchers have recently modified several batch analysis techniques, developing continuous-flow antioxidant detectors that can be coupled to HPLC systems [89, 90]. Over the last decade, these post-column antioxidant activity-based detectors have appeared in over forty publications and are the subject of reviews by Niederländer *et al.* [89] and Shi *et al.* [90]. The majority of applications employ free radical decolouration reactions, based upon either the DPPH radical or the ABTS radical cation [89, 90].

High performance liquid chromatography with post-column acidic potassium permanganate chemiluminescence detection has been used for the determination of many oxidisable compounds [113, 119], and is an attractive option for the screening of potential antioxidants in complex matrices. In this protocol a peristaltic pump is employed to merge acidic potassium permanganate with the HPLC eluant at a T-piece directly connected to a coiled flow-cell that is mounted flush against a PMT. All equipment is housed inside a light tight box (Figure 17). Here, acidic potassium permanganate can react with potential antioxidants to produce light, which emanates

from an electronically excited manganese(II) species [120]. Unlike the other post-column antioxidant assays, compounds are detected as positive peaks from a stable background rather than negative signals from inhibition of a high background. The term 'antioxidant' in the context of this methodology is defined as a readily oxidisable compound, meaning not all reductants that produce light with this reagent [113, 119] may be considered as dietary or primary antioxidants as outlined by Halliwell *et al.* [178] and Huang *et al.* [80]. Nevertheless, many known antioxidants (e.g. Gallic acid, quercetin, resveratrol and rosmarinic acid [113, 119]) have been shown to result in a relatively intense emission.

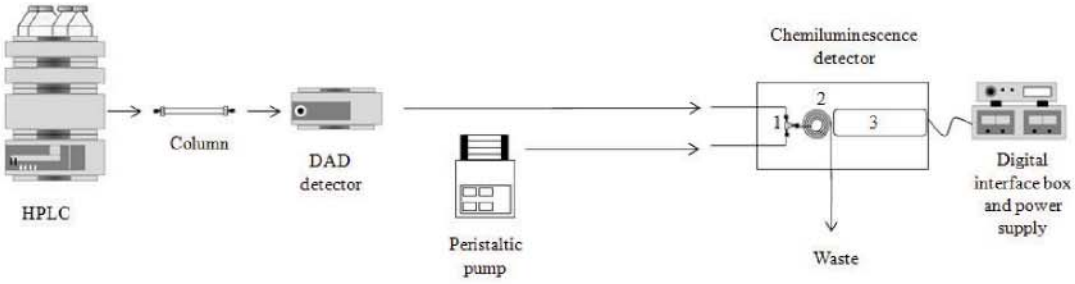

Figure 17. Instrument setup for HPLC with post-column acidic potassium permanganate chemiluminescence detection. 1, T-Piece; 2, reaction coil; 3, PMT.

Using FIA methodology, Francis *et al.* [98] recently developed a procedure to measure the total antioxidant capacities of numerous plant-derived beverages based on acidic potassium permanganate chemiluminescence, which showed good agreement with conventional $DPPH^{\bullet}$ and $ABTS^{\bullet+}$ batch assays. This study included a demonstration of HPLC with post-column permanganate chemiluminescence detection for screening of antioxidants in green and black tea samples, but it was not directly compared with on-line $DPPH^{\bullet}$ and $ABTS^{\bullet+}$ protocols [98].

In a subsequent investigation, permanganate chemiluminescence detection and the $DPPH^{\bullet}$ radical decolouration assay were simultaneously employed for the evaluation and comparison of antioxidants in espresso coffee samples, by dividing the post-

column HPLC eluate (50:50 ratio, controlled with a pressure regulator) [169]. The results from the two approaches were similar, but some differences in selectivity were observed. Chromatograms generated with the chemiluminescence detection contained more peaks, which was attributed to the greater sensitivity of the reagent towards minor, readily oxidisable sample components [169].

Although these studies provide some insight into the potential of acidic potassium permanganate chemiluminescence as an antioxidant screening tool, a more comprehensive study is required to assess the utility of this approach compared to more traditional techniques. Therefore, this chapter presents a systematic evaluation of this chemiluminescence procedure in direct comparison with the two most commonly employed post-column antioxidant assays ($DPPH^{\bullet}$ and $ABTS^{\bullet+}$).

2. Experimental

2.1 Chemicals, reagents and sample preparations

Deionised water (Continental Water Systems, Victoria, Australia) and analytical grade reagents were used unless otherwise stated. Chemicals were obtained from the following sources: 2,2′-Azinobis-(3-ethylbenzothiazoline-6-sulfonic acid), butylated hydroxyanisole, butylated hydroxytoluene, caffeic acid, catechin, o-coumaric acid, 2,2′-diphenyl-1-picrylhydrazyl, epicatechin, disodium hydrogen phosphate, ethoxyquin, ferulic acid, gallic acid, gentisic acid, 3,4-hydroxybenzoic acid, 4-hydroxycinnamic acid, isoeugenol, propyl gallate, quercetin, rosmarinic acid, rutin, sodium polyphosphates (+80 mesh), syringic acid, sodium hydroxide, trifluoroacetic acid, trolox and vanillin from Sigma–Aldrich (New South Wales, Australia); citric acid, glacial acetic acid and potassium persulfate from Univar (New South Wales, Australia); HPLC grade methanol, phosphoric acid, potassium dihydrogen phosphate and sodium citrate from BDH Chemicals (Poole, England); potassium permanganate and sodium chloride from Chem-Supply (South Australia, Australia); analytical grade methanol and sulfuric acid from Merck (Victoria, Australia); potassium chloride from Ajax (NSW, Australia) and acetonitrile from Burdick & Jackson (Michigan, USA).

Antioxidant stock solutions (1×10^{-3} M) were prepared in 100 % analytical grade methanol and appropriately diluted into 100 % analytical grade methanol.

The acidic potassium permanganate reagent (1×10^{-3} M) was prepared by dissolution of potassium permanganate in a 1% (m/v) sodium polyphosphate solution and adjusted to pH 2 with sulfuric acid.

The $DPPH^{\bullet}$ stock solution was prepared in methanol at the beginning of each day of analysis at a concentration of 1×10^{-3} M. This solution was appropriately diluted into methanol and mixed with a 100 mM citric acid-sodium citrate buffer (pH 6) at a ratio of 75:25. The resulting $DPPH^{\bullet}$ reagent (5×10^{-5} M) was degassed with nitrogen and kept protected from light by wrapping in aluminium foil before use.

The ABTS reagent (2×10^{-3} M) was dissolved in 8×10^{-3} M phosphate-buffered saline (PBS, consisting of 8.2 g NaCl, 0.27 g KH_2PO_4, 1.4 g Na_2HPO_4, and 0.15 g KCl per L) and adjusted to pH 7.4 with sodium hydroxide, and potassium persulfate solution in ultrapure water was added (3×10^{-4} M final concentration) to produce the $ABTS^{\bullet+}$ radical cation [174]. To obtain a maximum conversion of ABTS to $ABTS^{\bullet+}$ the mixture was stored in the dark at room temperature for 16-17 h then diluted into methanol and mixed with PBS at a ratio of 90:10 [174]. The resulting $ABTS^{\bullet+}$ reagent (2.5×10^{-6} M) was degassed with nitrogen and kept protected from light by wrapping in aluminium foil before use [174].

2.2 Sample preparation

2 g of Twinings of London, Pure Green Tea (AB Food & Beverages Australia, Victoria, Australia) was weighed out from tea bags and transferred to a 250 mL beaker containing 200 mL of boiling deionised water. The tea was left stirring on the hot plate for 2 minutes, then allowed to cool to room temperature, filtered (0.45 μm, Millipore Millex-HN Nylon) and analysed.

Dried thyme (0.5 g) was extracted according to the procedure of Koleva and co-workers [174], using 100 mL acetonitrile-acetic acid-water (70:1:29 by volume) followed by sonication for 15 min. A 1 mL aliquot was diluted with 3 mL of water, filtered (0.45 μm, Millipore Millex-HN Nylon) and analysed.

Cranberry juice (Ocean Spray International, Inc. Victoria, Australia) was simply filtered (0.45 μm, Millipore Millex-HN Nylon) and analysed.

2.3 Flow injection analysis

A conventional FIA manifold with chemiluminescence detector was constructed in our laboratory. A peristaltic pump (Gilson Minipuls 3, John Morris Scientific, Balwyn, Victoria, Australia) with bridged PVC tubing (DKSH, Caboolture, Queensland, Australia) was used to propel solutions through 0.8 mm id PTFE tubing (DKSH). Antioxidant standards (1×10^{-5} M) were injected (70 μL) with an automated six-port valve (Valco Instruments, Houston, Texas, USA) into a carrier stream (100% methanol unless otherwise stated), which merged with a solution of acidic potassium permanganate at a T-piece, and the light emitted from the reacting mixture was detected with a custom built flow-through chemiluminometer, which consisted of a coiled flow-cell comprising of 0.8 mm i.d. PTFE tubing (DKSH) mounted flush against the window of an Electron Tubes photomultiplier tube (model 9828SB, ETP, Ermington, New South Wales, Australia) set at a constant voltage of 900 V from a stable power supply (PM28BN, ETP) *via* a voltage divider (C611, ETP). The flow-cell, photomultiplier tube and voltage divider were encased in a padded light-tight housing, and the output from the photomultiplier was documented with a chart recorder (YEW type 3066, Yokogawa Hokushin Electric, Tokyo, Japan).

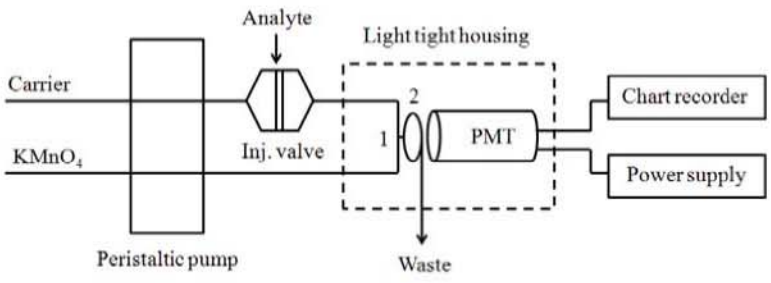

Figure 18. Schematic of FIA manifold. (1) T-piece; (2) transparent PTFE-PFA tubing reaction coil

2.4 High performance liquid chromatography

Chromatographic analysis was carried out on an Agilent Technologies 1200 series liquid chromatography system, equipped with a quaternary pump, solvent degasser system, autosampler and diode array detector (Agilent Technologies, Victoria, Australia). Hewlett-Packard Chemstation software (Agilent Technologies) was used to control the HPLC pump and acquire data from the diode array, UV-vis absorbance and chemiluminescence detectors. For comparison purposes, the time axes of the respective chromatograms were adjusted to account for differences in volume between the column and the various detectors. Acidic potassium permanganate, $DPPH^{\bullet}$ and $ABTS^{\bullet+}$ post-column reaction methodologies are described in the relevant sections below.

When obtaining comparative signals and analytical figures of merit, antioxidant standards were injected (20 μL) onto a Chromolith SpeedROD RP-18 monolithic column (50 mm × 4.6 mm i.d.; Merck) and eluted with 100% HPLC grade methanol at a flow rate of 0.75 mL min^{-1}. Green tea, cranberry juice and white wine samples were separated using a reverse phase Alltech Alltima C18 analytical column (250 mm × 4.6 mm i.d., particle size 5 μm, Agilent Technologies). Thyme extracts were separated using a Chromolith performance RP-18 monolithic column (100 mm × 4.6 mm i.d.; Merck). All analysis was carried out at room temperature with an injection volume of 20 μL, employing the gradients outlined in Table 4. Before use in the HPLC system, all sample solutions and solvents were filtered through a 0.45 μm nylon membrane.

Table 4. Gradient elution profiles. Solvent A was 0.05% (v/v) aqueous acetic acid and solvent B was HPLC grade methanol.

Time (min)	%A	%B	Flow rate (mL min^{-1})	Time (min)	%A	%B	Flow rate (mL min^{-1})
Green tea				**Thyme (Procedure 1)**			
0	80	20	1	0	97	3	1
2	80	20	1	6	97	3	1
22	30	70	1	36	70	30	1
26	30	70	1	66	20	80	1
26.01	80	20	1	69	97	3	1
30	80	20	1	69.01	97	3	1
Cranberry juice				**Thyme (Procedure 2)**			
0	97	3	1	0	97	3	3
2	97	3	1	2	97	3	3
12	70	70	1	12	70	30	3
22	30	70	1	22	20	80	3
23	20	80	1	23	97	3	3
23.01	97	3	1	23.01	97	3	3
25	97	3	1	25	97	3	3

2.5 Post-column $DPPH^{\bullet}$ and $ABTS^{\bullet+}$ radical scavenging

Post-column $DPPH^{\bullet}$ or $ABTS^{\bullet+}$ radical scavenging was achieved using the protocols outlined in chapter 2 and Koleva *et al.* [174], respectively (manifold shown in Figure 5). A quaternary HPLC pump (Agilent Technologies) was used to propel either the $DPPH^{\bullet}$ (0.75 mL min^{-1}) or $ABTS^{\bullet+}$ (0.5 mL min^{-1}) reagent, which merged with the HPLC eluant at a T-piece before entering a polyaryletheretherketone (PEEK, Upchurch Scientific, Washington, USA) reaction coil ($DPPH^{\bullet}$: 2 m × 0.25 mm i.d (100 µL), $ABTS^{\bullet+}$: 15 m × 0.25 mm i.d, (740 µL)), and through to a UV-vis absorbance detector (Agilent Technologies). Any induced reduction was detected as a negative peak at 521 nm and 734 nm for the $DPPH^{\bullet}$ and $ABTS^{\bullet+}$ reagents, respectively.

2.6 Post-column acidic potassium permanganate chemiluminescence

Post-column acidic potassium permanganate chemiluminescence was generated using the manifold outlined in Figure 17. The reagent, propelled at a flow rate of 2.5 mL min^{-1} using a Gilson Minipuls 3 peristaltic pump (John Morris Scientific, Victoria, Australia) with bridged PVC tubing (DKSH), merged with the HPLC eluant at a T-piece, and the light emitted from the reacting mixture was detected with a custom built flow-through chemiluminometer, which consisted of a coiled flow-cell comprising of 0.8 mm i.d. PTFE tubing (DKSH), mounted flush against the window of Electron Tubes photomultiplier tube (model 9878SB, ETP) set at a constant voltage of 900 V from a stable power supply (PM20D, ETP) *via* a voltage divider (C611, ETP). The flow-cell, photomultiplier tube and voltage divider were encased in a padded light-tight housing, and a Hewlett-Packard analogue to digital interface box (Agilent Technologies) was used to convert the signal from the chemiluminescence detector.

2.7 Primary skeletal muscle cell culture

Primary skeletal muscles cells (myoblasts) were isolated by enzymatic digestion of vastus lateralis muscle biopsies from healthy elderly donors undergoing elective hip replacement surgery. Myoblasts were expanded in growth media on extracellular matrix (ECM)-coated culture flasks (#E1270, Sigma-Aldrich; ECM diluted 1:75 in skeletal muscle growth medium (SkGM)) in 5% O_2 and 5% CO_2 at 37° C until passage 3 and experiments were carried out at passage 4. Myoblasts were cultured in 5% oxygen representing physiological oxygen levels. Low oxygen culture conditions provide a reducing redox environment compared to standard 20% oxygen culture conditions.

2.8 Detection of reactive oxygen species in muscle cells

Fresh stock solutions (50 mM) of resveratrol, rosmarinic acid, gallic acid, o-coumaric acid, cinnamic acid and flavone (Sigma Aldrich) were prepared in deionised water. Myoblasts were seeded into 96-black well, clear bottom plates in 5% CO_2, and either 5% or 20% O_2, at 37° C and proliferated until 80% confluent in growth media. To stimulate the formation of multinucleated muscle fibres (myotubes), cells were cultured in differentiation media for 5 days. For the chronic phenol treatment experiments, phenol stocks were diluted in differentiation media and myotubes were treated for 2 days. For the acute phenol treatment experiments, myotubes were cultured in differentiation media for a further 2 days. At 7 days differentiation, myotubes were loaded with 10 μM 2′,7′-dichlorofluorescin diacetate (DCFDA, #C6827, Molecular Probes) in PBS for 30 min. Then for the acute treatment experiments, antioxidant stocks were diluted in Dulbecco's modified Eagle's medium DMEM (minus phenol red) and then control and phenol-treated myotubes were exposed to 50 μM H_2O_2 or vehicle to assess the acute effects on phenols on ROS levels in the basal state or in response to oxidative stress. For the chronic treatment experiments, to determine whether the phenols may accumulate within myotubes and minimise the potentially confounding effects of phenols neutralising H_2O_2 in the cell culture media rather than intracellularly, all myotubes were treated only with DMEM (minus phenol red) with or without 50 μM H_2O_2. Oxidation of DCFDA was measured using a FlexStationII384 scanning Fluorometer (Molecular Devices) at 488 nm (excitation) and 518 nm (emission) at 37° C for 20 min with a reading every 30 sec. For each treatment the average fluorescence between 4 wells was determined and subtracted from the background auto-fluorescence; then the area under the curve was calculated. Data are presented as mean ± SEM and ROS levels are expressed relative to control.

3. Results and Discussion

3.1 Preliminary chemiluminescence investigations

It is well established that acidic potassium permanganate chemiluminescence emission can be influenced by the reaction environment [113, 119]. Therefore, using FIA and twenty antioxidant compounds commonly encountered in natural and synthetic matrices (butylated hydroxyanisole (BHA), BHT, caffeic acid, catechin, o-coumaric acid, epicatechin, ethoxyquin, ferulic acid, gallic acid, gentisic acid, 3,4-hydroxybenzoic acid, 4-hydroxycinnamic acid, isoeugenol, propyl gallate, quercetin, rosmarinic acid, rutin, syringic acid, trolox and vanillin), a series of univariate searches was performed on sodium polyphosphate and potassium permanganate concentration, flow rate and pH to determine reaction parameters that would afford the best chemiluminescence signal with representative results of six compounds shown in Figure 19. Based upon these experiments, a 1×10^{-3} M potassium permanganate solution containing 1 % (w/v) sodium polyphosphates adjusted to pH 2 with sulphuric acid, delivered at a flow rate of 2.5 mL min^{-1} per line, was considered most suitable for the range of compounds examined and was therefore utilised in all further experiments.

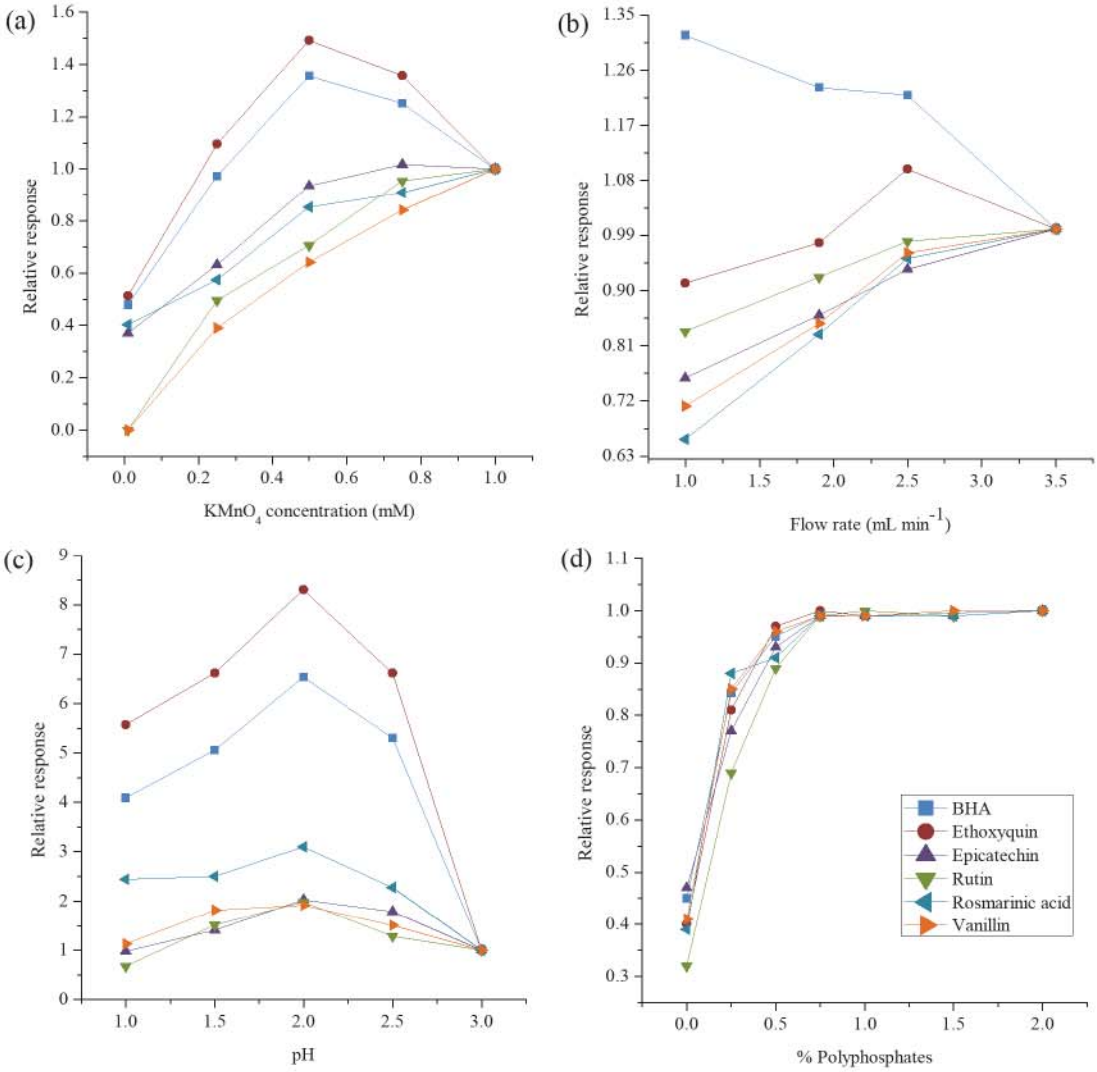

Figure 19. Effect of (a) potassium permanganate concentration (b) flow rate through FIA manifold (c) reagent pH and (d) percentage sodium polyphosphates added to reagent on the chemiluminescence signal of six model antioxidant analytes.

Since acidic potassium permanganate chemiluminescence detection was to be employed post-column, the influence of the mobile phase on emission was considered. Firstly, the separation of complex matrices often requires acidification of the HPLC eluant to improve separation efficiency. However, traditional post-column reactions involving $DPPH^{\bullet}$, $ABTS^{\bullet+}$ or luminol usually employ reagent buffering to ensure neutral or alkaline conditions after merging with the HPLC eluant [89, 90]. Using FIA and the same twenty antioxidant standards (1×10^{-5} M) employed in reagent optimisation, the effect of acidifying the aqueous carrier stream

(0.1% v/v; representing the HPLC mobile phase) on signal intensity was examined. Acidification with three different acids (phosphoric, acetic or trifluoroacetic) had a negligible effect on the chemiluminescence response, and therefore unlike post-column reactions with $DPPH^{\bullet}$, $ABTS^{\bullet+}$ or luminol, buffering of the reagent was not required.

Secondly, highly efficient HPLC separations that employ organic modifiers such as methanol or acetonitrile in the mobile phase are often required for complex biological extracts. Consequently, using FIA and the model antioxidants catechin and gallic acid, the effect of adding methanol or acetonitrile to an aqueous carrier stream (representing HPLC mobile phase) on signal intensity was examined. As can be seen in Figure 20, the organic modifier had a critical effect on permanganate chemiluminescence intensity. In concordance with previous observations [113], acetonitrile quenched the chemiluminescence signals, whilst methanol only produced minor differences in their response. Therefore HPLC mobile phases containing acetonitrile as the organic modifier are not recommended for use with acidic potassium permanganate.

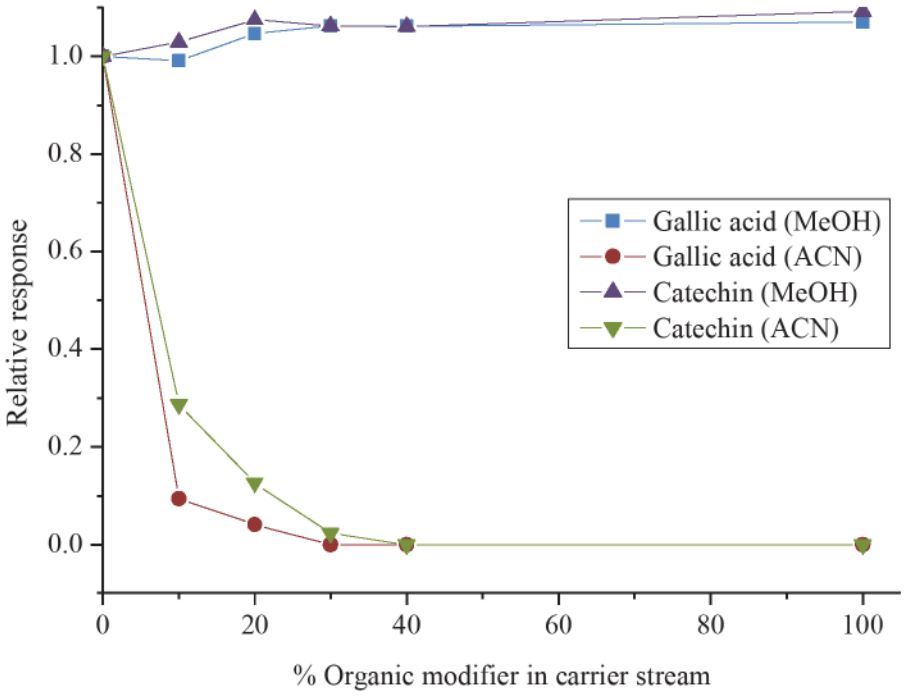

Figure 20. Effect of percentage organic modifier on the acidic potassium chemiluminescence response of catechin and gallic acid (1×10^{-5} M).

3.2 Correlation between acidic potassium permanganate chemiluminescence and *in vitro* cell culture assay

Although, acidic potassium permanganate chemiluminescence emission intensity is known to result from a combination of the concentration and/or reactivity of a particular compound [113, 119], the relationship between the response for an individual analyte and its activity in biological systems had not previously been explored. Therefore the relative chemiluminescence signal intensity for several key bioactives (including simple organic acids (gallic acid, cinnamic acid and o-coumaric acid), some more complex polyphenols (resveratrol and rosmarinic acid) and structurally related compound: flavone) was compared with their antioxidant activity in human primary skeletal muscle cell cultures.

Firstly, FIA methodology was used to generate the relative signals produced by these analytes (1×10^{-5} M) by injecting them into a flowing stream of water

(2.5 mL min^{-1}) which merged with the acidic potassium permanganate reagent (1×10^{-3} M containing 1 % (w/v) sodium polyphosphates adjusted to pH 2 with sulphuric acid; 2.5 mL min^{-1}) at a T-piece inside the flow-through chemiluminometer immediately prior to entering the detection cell. As can be seen in Figure 21, strong intensities were observed for gallic acid, resveratrol and rosmarinic acid. o-Coumaric acid afforded a more moderate response, whilst cinnamic acid and flavones elicited a relatively small emission intensity. Similar observations were made using other analyte concentrations, from 1×10^{-3} M to 1×10^{-5} M.

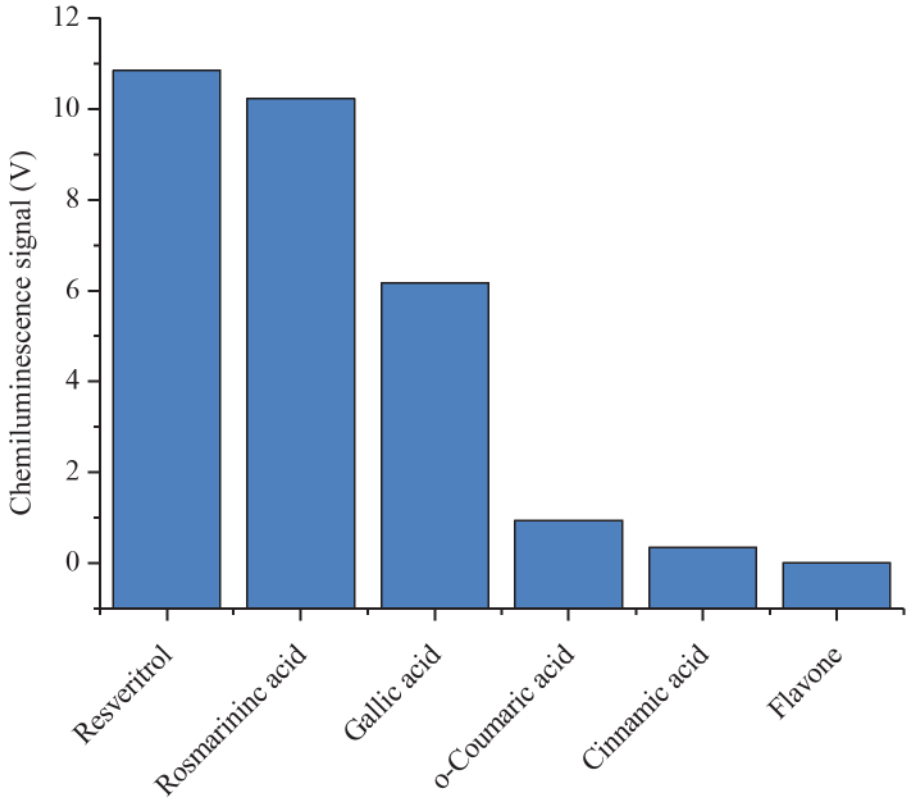

Figure 21. Chemiluminescence response (1×10^{-5} M standards).

To assess the relationship between chemiluminescence intensity and in vitro cell culture antioxidant assays, ROS levels were measured in human primary skeletal muscle cell (myotube) cultures. Skeletal muscle is a highly metabolically active tissue constituting ~40% of body weight and are quite responsive to cell stress [179].

The concentration at which individual phenols were tested was selected from preliminary studies of a wider concentration range where cytotoxicity and antioxidant efficacy were evaluated. At the concentrations used here none of the phenols had unwanted toxic effects, determined by a commercially available CytoTox 96 Assay (Promega) which quantifies the levels of lactate dehydrogenase (a stable cytosolic enzyme that is released upon cell lysis).

In initial experiments, myotubes were treated acutely with a given antioxidant and cell ROS levels were assessed in the basal state or in response to oxidative stress (50 mM H_2O_2) by monitoring the intracellular oxidation of the probe DCFDA using a fluorescent plate reader (Figure 22a). Oxidation of DCFDA is a commonly used assay of generalised oxidative stress, rather than assaying specific free radical species [178, 180]. In subsequent experiments to determine whether the selected compounds can accumulate in the cell and modulate redox state, myotubes were pre-treated with a given antioxidant for 2 days prior to a brief washout period. Once again, ROS levels were then assessed in the basal state or in response to oxidative stress (50 mM H_2O_2) using the probe, DCFDA (Figure 22b). From these experiments, the *in vitro* antioxidant potential was assessed and information about cellular uptake was also obtained. To summarise, resveratrol, gallic acid and rosmarinic acid reduced oxidative stress in the basal state and in response to H_2O_2 treatment, and data from the 2 days phenol treatment experiments suggest that these compounds accumulate within myotubes. o-Coumaric acid did not accumulate in the cell, but in the acute phenol treatment experiments it was able to quench H_2O_2 in the cell culture media and thus reduce intracellular stress. Following acute and 2 day treatment, flavone and cinnamic acid did not attenuate ROS levels within myotubes nor in the cell culture media in response to H_2O_2. Based on these *in vitro* cell culture assays, at the concentrations used, resveratrol, gallic acid and rosmarinic acid were

the most potent antioxidants, with o-coumaric acid having modest antioxidant effects, and flavone and cinnamic acid had no antioxidant activity. These observations demonstrated a clear correlation between the acidic potassium permanganate chemiluminescence intensity and cellular antioxidant activity. However, it should be borne in mind that, as for all *in vitro* antioxidant assays, further biological testing of candidate compounds would be required to confirm the activity predicted by this post-column reaction.

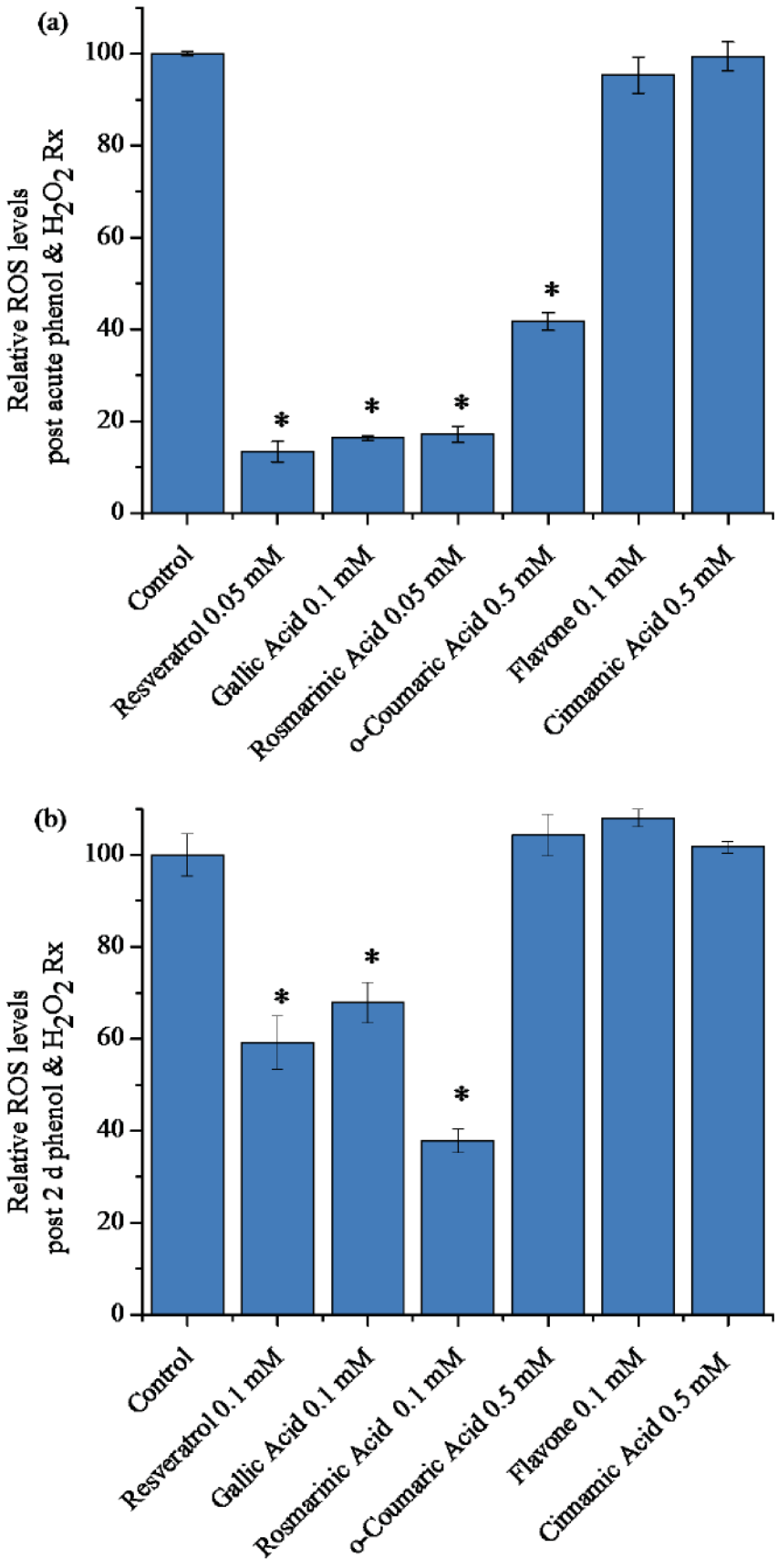

Figure 22. Effect of (a) acute and (b) 2 day antioxidant treatment on ROS levels in myotubes following H_2O_2 treatment. Symbols show significant differences at $p < 0.05$ (one-way ANOVA).

3.2 Selectivity and sensitivity of post-column reactions

To establish the relative selectivity of the methodologies, responses for twenty antioxidant standards (the same used in preliminary FIA experiments) were obtained using HPLC with post-column acidic potassium permanganate chemiluminescence detection and then with the on-line $DPPH^{\bullet}$ and $ABTS^{\bullet+}$ radical scavenging assays (Figure 23). It should be noted that lower analyte concentrations were required for chemiluminescence detection due to the inherent sensitivity of the method (i.e. 1×10^{-5} M compared to 1×10^{-4} M).

As shown in Figure 23a, strong correlation was observed between the post-column $DPPH^{\bullet}$ and $ABTS^{\bullet+}$ radical scavenging assays ($R^2 = 0.907$), due to the similarity in their reaction mechanisms. Both reagents function by abstracting an electron from the antioxidant, causing a characteristic colour change that results in a decrease in absorbance [80]. Dudonné *et al.* [181] reported a similar correlation coefficient ($R^2 = 0.906$) when comparing the total antioxidant capacity of thirty plant extracts using batch-style $DPPH^{\bullet}$ and $ABTS^{\bullet+}$ methodologies.

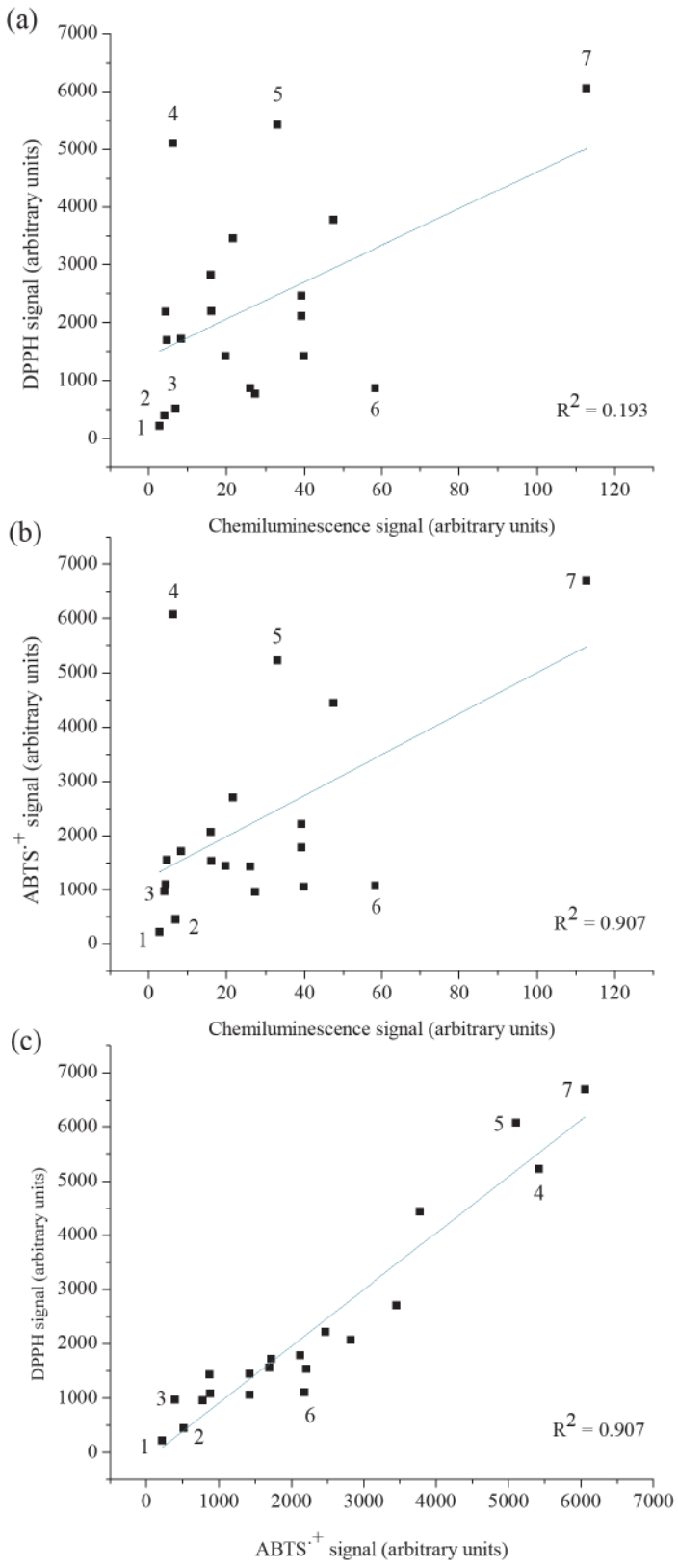

Figure 23. Correlation between signals of antioxidant standards obtained using HPLC with permanganate chemiluminescence and DPPH$^{\bullet}$ or ABTS$^{\bullet+}$ radical scavenging post-column detection. (1) Vanillin; (2) 3,4-dihydroxybenzoic acid; (3) 4-hydroxycinnamic acid; (4) rutin; (5), syringic acid; (6), rosmarinic acid; (7) quercetin.

Francis *et al.* [98] have previously reported that the total antioxidant capacity of a wide range of beverages established with permanganate chemiluminescence using FIA methodology, described in the experimental section, was in good agreement with results obtained using batch-style $DPPH^{\bullet}$ and $ABTS^{\bullet+}$ protocols. However, on-line screening of individual antioxidant compounds using HPLC revealed poor correlation between post-column permanganate chemiluminescence and $DPPH^{\bullet}$ or $ABTS^{\bullet+}$ radical scavenging assays ($R^2 = 0.193$ and $R^2 = 0.228$ respectively), which was attributed to differences in oxidant strength, reaction pathway [80, 122], and conditions such as pH. Of the compounds tested, vanillin, 3,4-dihydroxybenzoic acid and 4-hydroxycinnamic acid produced the poorest signals and quercetin produced the greatest signal with all three methods (Figure 23). However, rutin and rosmarinic acid produced a large signal with both radical decolourisation assays, but a relatively poor response with permanganate chemiluminescence. Conversely, syringic acid displayed a poor signal with $DPPH^{\bullet}$ and $ABTS^{\bullet+}$ assays, but gave a reasonably large chemiluminescence response. In off-line batch-type methodologies, the signal is the combined response of many antioxidants. This appears (to certain extent) to cancel out differences in selectivity towards individual compounds, which accounts for the previously observed agreement between permanganate chemiluminescence and the radical decolourisation assays [98].

The antioxidant signals arise from a combination of the chemical nature of the compound and its concentration. The sensitivity of the three on-line approaches was compared by preparing calibration curves for six antioxidants (using 20 standard solutions between 1×10^{-9} M and 1×10^{-4} M for each antioxidant, and the HPLC conditions described the Experimental section). As can be seen in Table 5, permanganate chemiluminescence was more sensitive than $DPPH^{\bullet}$ or $ABTS^{\bullet+}$ detection for all antioxidants. This enhanced detection sensitivity is attributable not

only to the inherently higher sensitivity of chemiluminescence [182], but also the generation of positive peaks on a stable background. Of further note were the improvements in linearity (correlation coefficients, R^2) and precision gained by using permanganate chemiluminescence over DPPH$^{\bullet}$ or ABTS$^{\bullet+}$.

Table 5. Analytical figures of merit for antioxidant standards using HPLC with either post-column permanganate chemiluminescence, DPPH$^{\bullet}$ or ABTS$^{\bullet+}$ radical scavenging detection.

	Chemiluminescence			DPPH$^{\bullet}$			ABTS$^{\bullet+}$		
	R^2	LOD[a] (µM)	RSD (%)[b,c]	R^2	LOD[a] (µM)	% RSD[b, d]	R^2	LOD[a] (µM)	RSD (%)[b, d]
Epicatechin	0.998	0.05	2.10	0.997	3	3.89	0.999	1	3.47
Rosmarinic acid	0.998	0.075	1.20	0.998	0.5	4.69	0.997	0.3	3.88
Quercetin	0.999	0.1	1.02	0.996	3	3.34	0.998	1	4.15
Caffeic acid	0.999	0.5	1.64	0.994	5	3.16	0.998	1	3.23
Gallic acid	0.999	0.4	0.19	0.998	5	3.12	0.996	2.5	3.89
Rutin	0.998	0.5	0.59	0.998	1	3.66	0.998	1	3.31

[a] Limit of detection (3σ)

[b] n = 6

[c] Relative standard deviation (1×10^{-5} M)

[d] Relative standard deviation (1×10^{-4} M)

3.3 Application to real samples

As a final assessment, a variety of extracts known to be rich in antioxidants were screened using HPLC with post-column permanganate chemiluminescence detection and the results were directly compared to those generated using HPLC with DPPH$^{\bullet}$ or ABTS$^{\bullet+}$ assays. Several major advantages of the methodology outlined herein were noted during instrument set-up and reagent preparation. Firstly, since the post-column chemiluminescence detection requires only a peristaltic pump and flow-through chemiluminometer, it was much simpler than the manifolds required for the DPPH$^{\bullet}$ and ABTS$^{\bullet+}$ assays, which require an additional HPLC pump and UV-Vis absorbance detector. Secondly, the reagent preparation time was significantly

reduced, because the permanganate solution could be used immediately. In contrast, the $ABTS^{\bullet+}$ reagent must be left in the dark for a period of 16-17 h (to ensure maximum conversion of ABTS to $ABTS^{\bullet+}$) and then degassed prior to use. Likewise, the $DPPH^{\bullet}$ reagent required degassing. Furthermore, although stock solutions of $DPPH^{\bullet}$ and $ABTS^{\bullet+}$ may be stored for a period of days with minimal reagent degradation [162, 174, 183], their corresponding working solutions need to be prepared on an almost daily basis. Alternatively, a permanganate working solution could be continuously used and stored for an extended period of time.

Samples selected for comparison were green tea, cranberry juice and thyme. In the case of green tea (Figure 24a), almost all of the major UV-absorbance peaks (retention times of 3.1, 13.6, 14.5, 16.7, 18.3, 18.8, 20.1 and 23 min) were also observed in the traces for permanganate chemiluminescence and $DPPH^{\bullet}$ assay, indicating that each of these compounds may possess significant antioxidant activity. Most were also observed in the $ABTS^{\bullet+}$ quenching chromatogram, with the exception of those at 13.6, 14.5 and 16.7 min. In general, the chemiluminescence peaks appeared sharper that those for the radical decolourisation assays, which was attributed to differences in the required reaction coil length and the contribution of this parameter to post-column band broadening. For cranberry juice (Figure 24b), several of the major UV-absorbance peaks (retention times of 2.1, 3.7, 6.3, 13.6, 14.5, 15.7 and 17.3 min) were also observed in the traces for chemiluminescence, $DPPH^{\bullet}$ and $ABTS^{\bullet+}$ assays, although the peak heights were far lower than those in the chromatograms for green tea. Highlighting the complementary differences in selectivity, the compound eluting at 6.3 min produced a large peak in the $ABTS^{\bullet+}$ trace, but only minor responses in the $DPPH^{\bullet}$ and chemiluminescence traces. In contrast, peaks at 18, 21.1 and 23 min were much larger in the chemiluminescence trace.

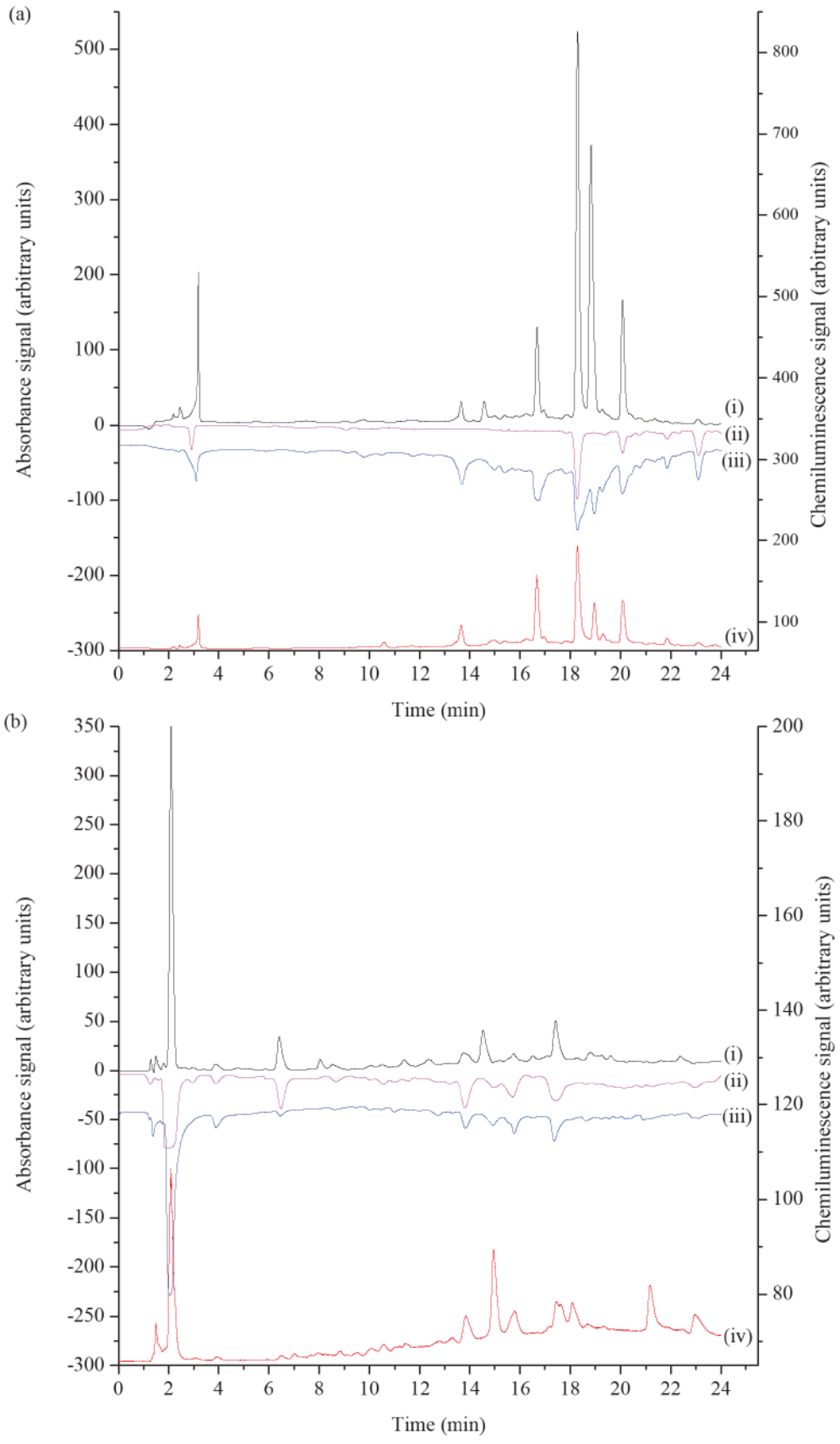

Figure 24. Combined plots of the (i) UV absorbance, (ii) $DPPH^{\bullet}$ (iii) $ABTS^{\bullet+}$ and (iv) permanganate chemiluminescence chromatograms of (a) green tea and (b) cranberry juice. Detailed chromatographic conditions for both samples are described in the experimental section.

Analysis of the thyme extract (Figure 25a) revealed three major peaks in the UV absorbance trace (with retention times of 34.4, 41.1 and 42 min). The first of these peaks corresponded to large responses in chemiluminescence, $DPPH^{\bullet}$ and $ABTS^{\bullet+}$ traces. The other two were also seen in the chromatograms for all three post-column reactions, but were far less prominent in the chemiluminescence trace. In addition, many other constituents produced minor peaks in the UV absorbance chromatogram, but strong responses with the post-column reactions, indicative of compounds at low concentration with high antioxidant activity. Although many of these compounds were detected in all three approaches to screen for antioxidants, significant differences in selectivity were observed, particularly in the region between 36 to 55 min.

In previous studies in which $DPPH^{\bullet}$ or $ABTS^{\bullet+}$ post-column radical scavenging reactions were employed, the chromatographic separations were performed using particle packed columns containing a C18 stationary phase [89, 90]. Due to the limiting backpressure from these columns, and the times thought to be needed for sufficient reaction with the radical scavenging agents, the flow rate of the mobile phase has been restricted to 0.8 mL min^{-1} or lower. Consequently, long chromatographic separation times of up to 70 min have been reported [183]. However, recent investigations involving these post-column reactions have shown that much shorter reaction times can be used without a significant loss of sensitivity [99, 101, 102, 104, 167, 184-186]. Moreover, the introduction of monolithic columns has enabled separation at much higher flow rates (up to 10 mL min^{-1}), whilst maintaining separation efficiency [187]. Therefore, the use of monolithic column HPLC coupled with the post-column reactions was explored to reduce chromatographic run times for faster antioxidant screening.

After a preliminary separation of a thyme extract using a commercially available monolithic column (Figure 25a), the mobile phase flow rate was increased from 1 to 3 mL min^{-1} (Figure 25b), and the solvent gradient was adjusted accordingly (Table 4). As shown in Figure 25b, the general features of the chromatogram were conserved for each mode of detection. However, noting the scale of Figure 25a and 19b, the $ABTS^{\bullet+}$ assay was less sensitive at the higher mobile phase flow rate. Furthermore, some losses in resolution were observed (see for example the peak at 19.3 min in Figure 25b) and the 15 m of tubing (0.25 mm i.d.) employed in this method [174] resulted in a very a high backpressure. The sensitivity of the $DPPH^{\bullet}$ assay was not significantly affected by the increase in flow rate. Although 15 m of tubing (upwards of 500 μL to as much as 750 μL) is also commonly used for the post-column $DPPH^{\bullet}$ assay [99-104, 167], I employed the optimised procedure reported in chapter 2, in which 2 m of tubing (0.25 mm i.d., 100 μL) was used, and therefore the problems associated with high backpressures were avoided. Higher flow rates were more compatible with permanganate chemiluminescence reactions due to the more rapid combination and propulsion of the post-column reaction mixture into the flow-cell, which allowed a greater proportion of the transient emission to be detected [128, 129]. This was reflected in the greater sensitivity shown in the chemiluminescence trace in Figure 25a to that of Figure 25b.

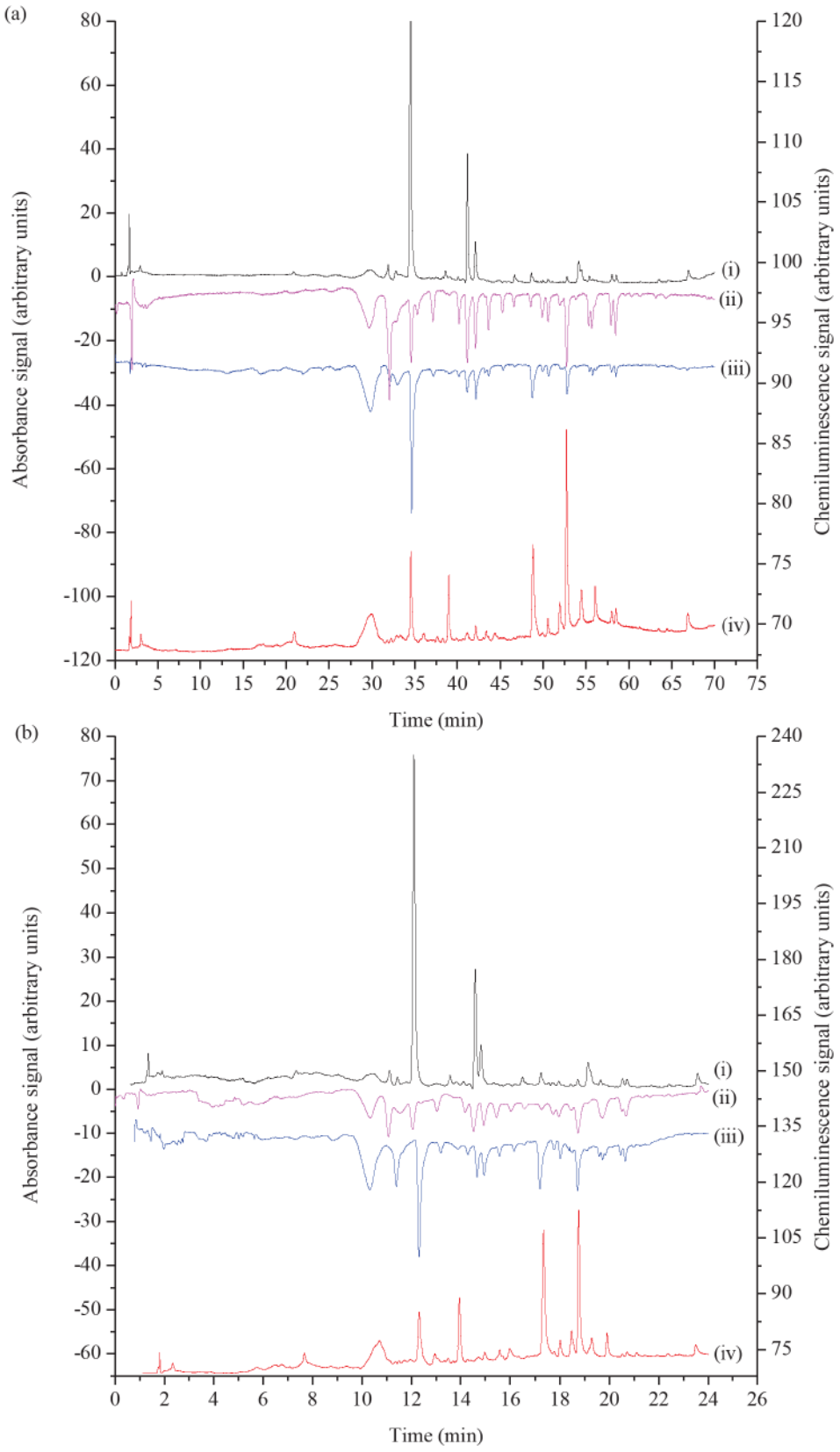

Figure 25. Combined plots of the (i) UV absorbance, (ii) $DPPH^{\bullet}$ (iii) $ABTS^{\bullet+}$ and (iv) permanganate chemiluminescence chromatograms of thyme extract using a RP-18 monolithic column and gradient elution programs outlined in Table 4 at (a) 1 mL min^{-1} (procedure 1) and (b) 3 mL min^{-1} (procedure 2). Further chromatographic conditions are described in the experimental section.

4. Conclusions

High performance liquid chromatography with post-column acidic potassium permanganate chemiluminescence detection was shown to be a viable alternative to traditional radical decolourisation assays for the screening of potential antioxidants in complex matrices. Using FIA, experimental parameters that afforded the most suitable permanganate chemiluminescence signal for a range of known antioxidants were studied in a univariate approach. Optimum conditions were found to be: 1×10^{-3} M potassium permanganate solution containing 1% (w/v) sodium polyphosphates adjusted to pH 2 with sulphuric acid, delivered at a flow rate of 2.5 mL min^{-1} per line. Employing these conditions, acidic potassium permanganate chemiluminescence signal intensity was shown to predict the ability of several antioxidant standards to positively act on cellular redox state and attenuate oxidative stress in cultured skeletal muscle cells. Although many of the same sample components responded with each of the three post-column reactions, differences in selectivity were observed, due to the disparity between their respective reaction pathways and conditions. However, screening for antioxidants in green tea, cranberry juice and thyme using potassium permanganate chemiluminescence offered advantages such as greater sensitivity, faster reagent preparation and superior stability, simpler post-column reaction manifold, and greater compatibility with fast chromatographic separations using monolithic columns. This work has resulted in the following publications [169, 188-190].

CHAPTER FOUR

Determination of intracellular glutathione and glutathione disulfide using high performance liquid chromatography with acidic potassium permanganate chemiluminescence

- **Introduction**
- **Experimental**
- **Results and discussion**
- **Conclusion**

1. Introduction

Beginning with the early observations of Hopkins in the 1920s, [191-193] glutathione (GSH, Figure 26) has been extensively studied by researchers from a diverse range of disciplines [14, 32-35, 194, 195]. Investigations have primarily focused on the many biochemical properties of GSH as it is the major low-molecular weight antioxidant species present in eukaryotic cells, and a regulator of protein and cell functionality [14, 32-36]. As discussed in chapter 1, GSH has the potential to reduce free radicals and reactive oxygen species (ROS), which results in the formation of the corresponding disulfide, GSSG (Figure 26) [14, 32-36]. Therefore, the molar ratio of GSH/GSSG can be used as a biomarker for oxidative stress [14, 32-35, 41-48].

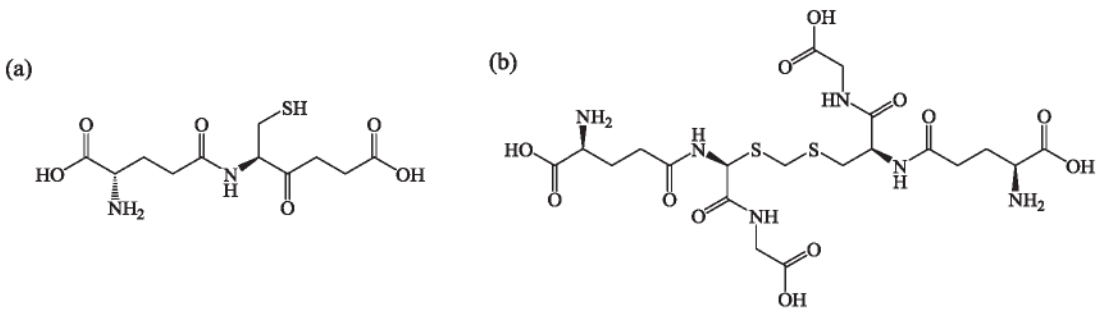

Figure 26. Structures of (a) glutathione and (b) glutathione disulfide.

The importance of GSH and GSSG measurement for the assessment of intracellular redox state is reflected by the plethora of analytical methodologies, including liquid chromatography, gas chromatography or capillary electrophoresis separation with fluorescence, electrochemical, mass spectrometry or UV absorbance detection, which are the subject of numerous reviews [33, 41-48]. As identified in these articles and described in chapter 1, there are several major analytical challenges associated with the accurate measurement of GSH and GSSG [33, 41, 42, 44-48, 196-211]. Methodologies that employ direct detection and minimal sample handling

are therefore more desirable. Electron spin resonance, nuclear magnetic resonance, electrochemical, UV absorbance, fluorescence quenching or mass spectroscopy have been utilised to determine GSH (and in some cases GSSG) without derivatisation, and these approaches have been described in the following references [33, 41-43, 46, 48, 212-214]. However, they suffer from limitations in terms of performance, equipment costs, complexity, sensitivity and/or analysis time. An often overlooked alternative for the direct measurement of GSH is chemiluminescence [215-222], which offers highly sensitive detection using relatively simple instrumentation [106, 109, 113-115]. Beginning in 1984, Hinze *et al.* [218] reported the detection of GSH and several other biologically significant reductants based on the chemiluminescence reaction with lucigenin, but they primarily focused on the effect of micellar systems upon the emission. Several subsequent publications have described the determination of GSH using batch or flow-injection analysis with chemiluminescence detection, based on (i) enhancement of the emission from the oxidation of luminol [215, 216, 223], (ii) quinine sensitised emission from the oxidation of the analyte [220, 221], or (iii) reaction with permanganate and tris(1,10-phenanthroline)ruthenium(II) [217]. Preliminary applications to several blood samples showed reasonable agreement with a spectrophotometric assay [216, 223], but without chromatographic or electrophoretic separation, these methods lack the selectivity required to accurately measure GSH in complex biological matrices. Two attempts have been made to address this issue to-date. Firstly, by Li *et al.* [219] who utilised HPLC with post-column Rhodamine B sensitised cerium(IV) chemiluminescence for the detection of GSH and cysteine. However, poor chromatographic resolution between these analytes was reported and the analytical methodology was not applied to biological samples [220]. Secondly, Zhao *et al.* [222], determined GSH and other intracellular thiols by microchip

electrophoresis with luminol chemiluminescence. The method was applied to single red blood cells from healthy subjects and cancer patients, but the sensitivity was not sufficient to quantify GSH in some samples. Furthermore, none of the chemiluminescence-based procedures reported to date have included strategies for GSSG detection, which is essential to establish cellular redox state.

This chapter describes the determination of intracellular GSH and GSSG based on a rapid chromatographic separation coupled with post-column acidic potassium permanganate chemiluminescence detection. For direct GSH measurement, samples were simply diluted into an acidic solution prior to injection onto the column. In a separate analysis step, GSSG was quantified by masking endogenous thiols, disulfide bond reduction, and detection of the newly formed GSH. Furthermore, this approach was utilised to assess the redox state of cultured muscle cells (C2C12 myotubes) treated with various concentrations of glucose oxidase, which causes oxidative stress through the continuous production of hydrogen peroxide.

2. Experimental

2.1 Chemicals and reagents

Deionised water (Continental Water Systems, Victoria, Australia) and analytical grade reagents were used unless otherwise stated. Chemicals were obtained from the following sources: *N*-Ethylmaleimide, glucose oxidase, L-glutathione, L-glutathione disulfide, 2-mercaptoethanol, tris(2-carboxyethylphosphine), sodium polyphosphate (+80 mesh) and thiazolyl blue tetrazolium bromide from Sigma–Aldrich (New South Wales, Australia); Dulbecco's modified Eagle's medium, fetal bovine serum, Hank's Buffered Salt Solution and horse serum from Invitrogen (Victoria, Australia); potassium permanganate and sodium chloride from Chem-Supply (South Australia, Australia); analytical grade methanol, sulfuric acid (98% w/v) and tris(hydroxymethyl)methylamine from Merck (Victoria, Australia); hydrochloric acid (32% w/v) from Ajax Finechem (New South Wales, Australia) and formic acid from Hopkin and Williams (Essex, England).

Stock solutions (1×10^{-3} M) of GSH and GSSG were prepared and diluted in aqueous formic acid (pH 2.8).

The acidic potassium permanganate reagent (1×10^{-3} M) was prepared by dissolution of potassium permanganate in a 1% (m/v) sodium polyphosphate solution and adjusted to pH 3 with sulfuric acid.

2.2 Flow injection analysis

A conventional FIA manifold with a chemiluminescence detector was constructed in our laboratory. A peristaltic pump (Gilson Minipuls 3, John Morris Scientific, Balwyn, Victoria, Australia) with bridged PVC tubing (DKSH, Caboolture, Queensland, Australia) was used to propel solutions through 0.8 mm i.d. PTFE

tubing (DKSH, Caboolture, Queensland, Australia). Standards (1×10^{-5} M) were injected (70 µL) with an automated six-port valve (Valco Instruments, Houston, Texas, USA) into a carrier stream (100% methanol unless otherwise stated), which merged with a solution of acidic potassium permanganate at a T-piece, and the light emitted from the reacting mixture was detected with a custom built flow-through chemiluminometer, as described in chapter 3, section 2.3. The output from the photomultiplier was documented with a chart recorder (YEW type 3066, Yokogawa Hokushin Electric, Tokyo, Japan).

2.3 High performance liquid chromatography

Chromatographic analysis was carried out on an Agilent Technologies 1200 series liquid chromatography system, equipped with a quaternary pump, solvent degasser system and autosampler (Agilent Technologies, Forest Hill, Victoria, Australia). Hewlett-Packard Chemstation software (Agilent Technologies) was used to control the HPLC pump and acquire data from the chemiluminescence detector. Before use in the HPLC system, all sample solutions and solvents were filtered through a 0.45 µm nylon membrane.

Table 6. Optimised separation conditions for the determination of GSH.

Injection volume	20 µL
Mobile phase	97% aqueous formic acid (pH 2.8), 3% methanol
Flow rate	1 mL min^{-1}
Column	Alltech Alltima C18 (250 mm × 4.6 mm 1.d., 5µm)

Post-column acidic potassium permanganate chemiluminescence was generated using the manifold outlined in Figure 17. The reagent, propelled at a flow rate of 2.5 mL min^{-1} using a Gilson Minipuls 3 peristaltic pump (John Morris Scientific, Balwyn, Victoria, Australia) with bridged PVC tubing (DKSH, Caboolture,

Queensland, Australia), merged with the HPLC eluant at a T-piece and the light emitted from the reacting mixture was detected with a custom built flow-through chemiluminometer, as described in chapter 3, section 2.6.

2.4 Cell culture and glucose oxidase treatment

Mouse C2C12 myoblasts were maintained in DMEM, (5.5 mM glucose), supplemented with 10% fetal bovine serum (FBS) at 37°C and 5% CO_2. To stimulate myotube formation, myoblasts were grown to confluence and then transferred to DMEM supplemented with 2% horse serum (HS). For determination of GSH and GSSG content, cells were grown in 6-well tissue culture plates, and for the oxidative stress and viability assays cells were grown in 96-black well, clear bottom tissue culture plates. To induce oxidative stress, C2C12 myotubes at 4 d post-differentiation were treated with 0, 30, 100, 250 or 500 mU mL^{-1} glucose oxidase in 50 mM sodium acetate buffer (pH 5.1) for 24 h. Glucose oxidase increases ROS levels in the cell culture medium by catalysing the oxidation of glucose to produce D-glucono-δ-lactone and H_2O_2 [224, 225]. This exposed the myotubes to a continuous, more biologically relevant source of ROS (that can cross the cell membrane to alter intracellular redox state) than a single concentrated, rapidly metabolised dose [224, 225].

2.5 Sample collection and analysis

For determination of GSH and GSSG content, C2C12 myotubes were harvested by trypsinisation and resuspended in 200 µL of deionised water. A 35 µL aliquot was solubilised in 10% sodium dodecyl sulfate (SDS) to a final concentration of 0.2% SDS (v/v) for protein determination using the bicinchoninic acid (BCA) method (#23225, Pierce) according to manufacturer's instructions. The rest of the sample was treated with formic acid to a final concentration of 0.5%, and stored immediately

at -80º C. Prior to analysis, C2C12 myotubes were thawed on ice and then centrifuged at 12,000 rpm for 5 min at 5º C using an Avanti 30 Centrifuge (Beckman Coulter, New South Wales, Australia) to remove precipitated proteins and cellular debris. For GSH determination, 50 µL of the supernatant was diluted into 450 µL of 5% aqueous formic acid, filtered through a 0.45 µm nylon membrane and analysed. For GSSG determination, the supernatant (100 µL) was combined with Tris-HCl buffer (0.675 M; 20 µL; pH 8.0) and *N*-ethylmaleimide (NEM, 6.3×10^{-3} M; 20 µL) and left for one minute. Subsequently, 2-mercaptoethanol (8×10^{-3} M; 20 µL) was added and the sample left for another minute. Then tris(2-carboxyethyl)phosphine (TCEP, 7.8×10^{-4} M; 20 µL) was added and the solution was left for 60 min at 50° C to allow complete disulfide reduction. Finally, 5% aqueous formic acid (20 µL) was added, and the sample filtered through a 0.45 µm nylon membrane and analysed. GSH and GSSG data are presented normalised to protein content.

2.6 Determination of cell viability - mitochondrial function (MTT assay) and membrane integrity (ethidium uptake assay)

Mitochondrial function and membrane integrity were used as markers of cell viability, as both are compromised in stressed cells undergoing apoptosis or necrosis. For the MTT assay, C2C12 myotubes were incubated with 0.5 mg ml^{-1} thiazolyl blue tetrazolium bromide for 15 min at 37° C and 5% CO_2 to allow for the conversion of thiazolyl blue tetrazolium bromide to dark blue MTT-formation by mitochondrial dehydrogenases. The cells were then solubilised with isopropanol and the intensity of colour development was measured at 570 nm in a micro-plate reader (Bio-Rad) with 630 nm as the reference wavelength. The MTT results are presented relative to cells in the control media (0 mU mL^{-1} glucose oxidase), which were considered to be 100% viable.

For the membrane integrity assay, myotubes were incubated with 8 μM ethidium (2 mM stock solution in DMSO; Invitrogen) in Hank's Buffered Salt Solution (HBSS, 5.5 mM glucose) plus or minus glucose oxidase for 10 min at 37° C and 5% CO_2. Ethidium uptake is greater in cells with compromised membrane integrity and this increase in fluorescence intensity was measured with a FlexStation II Scanning Fluorometer (Molecular Devices, Sunnyvale, California, U.S.A; λ_{ex} = 590 nm, λ_{em} = 612 nm). Ethidium uptake is presented as fold-change in absolute fluorescence relative to control media (0 mU mL^{-1} glucose oxidase).

2.7 Determination of oxidative stress - H_2O_2 assay

H_2O_2 levels were measured with a commercially available Amplex Red H_2O_2 kit (#A22188, Molecular Probes - Invitrogen), according to the manufacturer's instructions. Briefly, C2C12 myotubes were incubated with 50 μM of Amplex Red reagent dissolved in DMSO and 0.1 U mL^{-1} horseradish peroxidase in HBSS (5.5 mM glucose) for 10 min at 37° C and 5% CO_2. The increase in fluorescence intensity was measured with a FlexStation II Scanning Fluorometer (Molecular Devices; λ_{ex} = 590 nm, λ_{em} = 612 nm). To confirm the efficacy of the glucose oxidase treatment, H_2O_2 levels were determined with glucose oxidase present in the assay media. All doses of glucose oxidase increased Amplex Red oxidation. Results are presented relative to control media (0 mU mL^{-1} glucose oxidase). Note: statistically analysed data were not normalised to protein content.

2.8 Statistical analysis

All data are presented as mean ± SEM. One-way ANOVA with Tukey post-hoc analysis, when applicable, was used to assess the effect of glucose oxidase treatment on cellular redox state, markers of oxidative stress and cell viability.

3. Results and Discussion

3.1 Preliminary chemiluminescence investigations

Li and co-workers reported a weak emission of light from the oxidation of GSH with acidic potassium permanganate, which was significantly enhanced by the addition of quinine [220]. It has been previously shown that this chemiluminescence reaction involves two interdependent light-producing pathways [113, 151]; the analyte is oxidised to an intermediate capable of transferring energy to the efficient fluorophore (λ_{max} = 458 nm), and the permanganate is reduced to an electronically excited manganese(II) species [113, 151]. Considering that the manganese(II) emission from other reactions with acidic potassium permanganate has been significantly enhanced by the addition of sodium polyphosphates to the reagent solution [113], I sought to use this enhancer to promote the manganese(II) pathway. Removing the need for the quinine would eliminate the background emission from reaction between the sensitiser and oxidant [127, 220] and enable post-column chemiluminescence detection of GSH using a single reagent solution.

Preliminary experiments were conducted using FIA as it provided similar conditions to HPLC, but without the relatively time-consuming separation. The reaction of GSH (1×10^{-5} M) with potassium permanganate (1×10^{-3} M in 1% (w/v) sodium polyphosphate solution, adjusted to pH 2 with sulfuric acid) produced a large chemiluminescence response, but no signal was recorded for the disulfide, GSSG (1×10^{-5} M). To find the parameters that would afford the greatest chemiluminescence response for GSH, a series of univariate searchers were performed with the results shown in Figure 27. Based upon these experiments, a 2.5×10^{-4} M potassium permanganate solution containing 1% (w/v) sodium polyphosphates adjusted to pH 3 with sulfuric acid, delivered at a flow rate of

2.5 mL min^{-1} per line, was found to be optimal and therefore utilised in all further experiments.

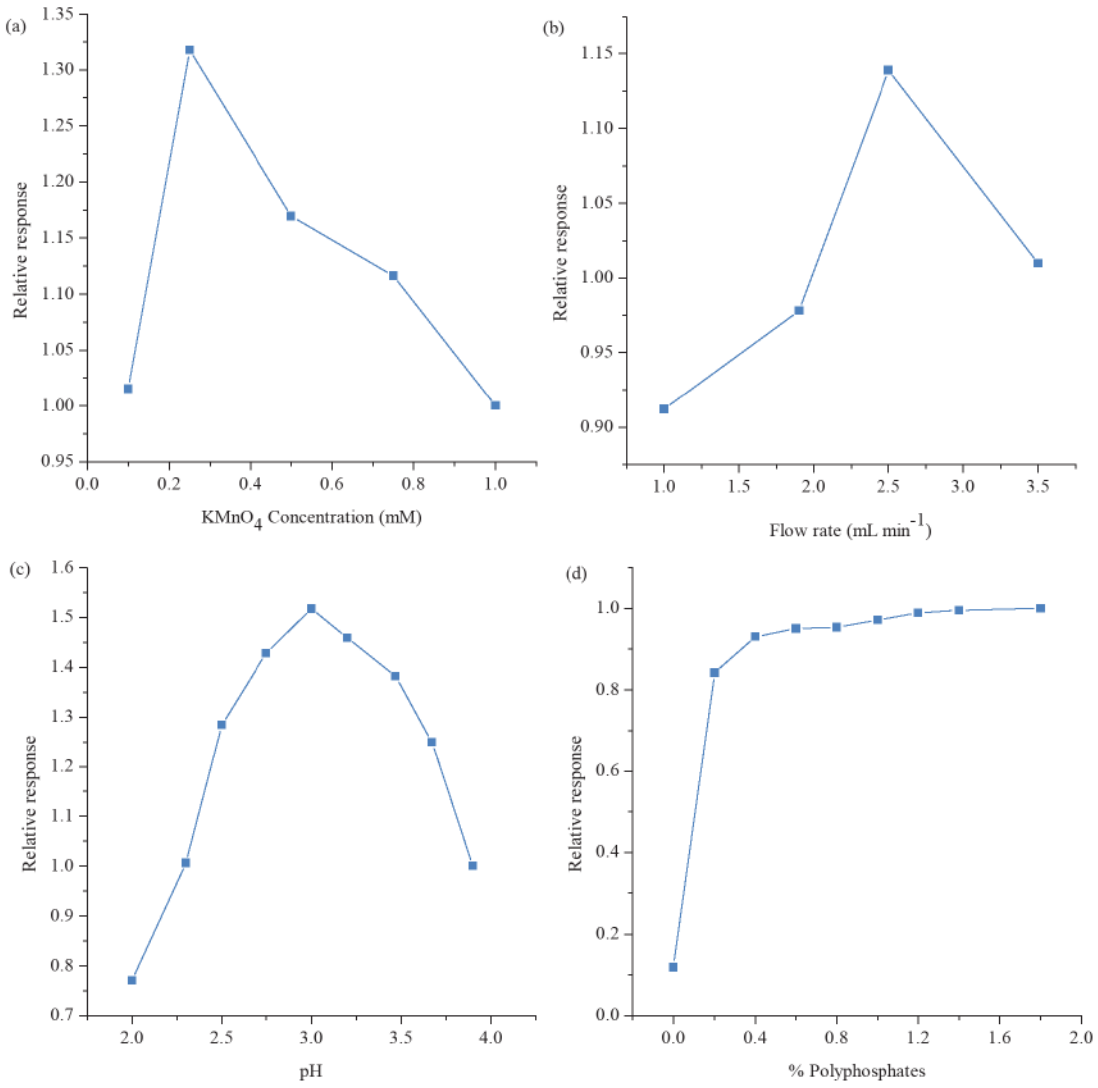

Figure 27. Effect of (a) potassium permanganate concentration, (b) flow rate through FIA manifold, (c), reagent pH and (d) percentage sodium polyphosphates added to reagent on the chemiluminescence signal of GSH.

3.2 High performance liquid chromatography

Reverse-phase HPLC has been incorporated into many methods for the determination of GSH, but they often employ pre-column derivatisation and as a consequence there are very few reports of separations for non-derivatised GSH [41, 42, 46-48]. In a recent review of chromatographic and mass spectrometric

analysis of biological samples for GSH, Iwasaki *et al.* [46] suggested that either highly polar HPLC stationary phases (such as amino, diol) or hydrophobic interaction chromatography is required. However, Zhang *et al.* [211] reported adequate GSH retention using a more conventional non-polar C18 column. Therefore, to resolve GSH from other sample components, an optimisation of HPLC conditions (injection volume, mobile phase composition and pH, temperature and flow rate) using a particle-packed column with either an amino or C18 stationary phase was performed. Conditions found to provide sufficient GSH retention in combination with maximum acidic potassium permanganate chemiluminescence signal are shown in Table 6. These chromatographic parameters allowed for the complete separation of GSH from sample components in less than 6 minutes (Figure 28).

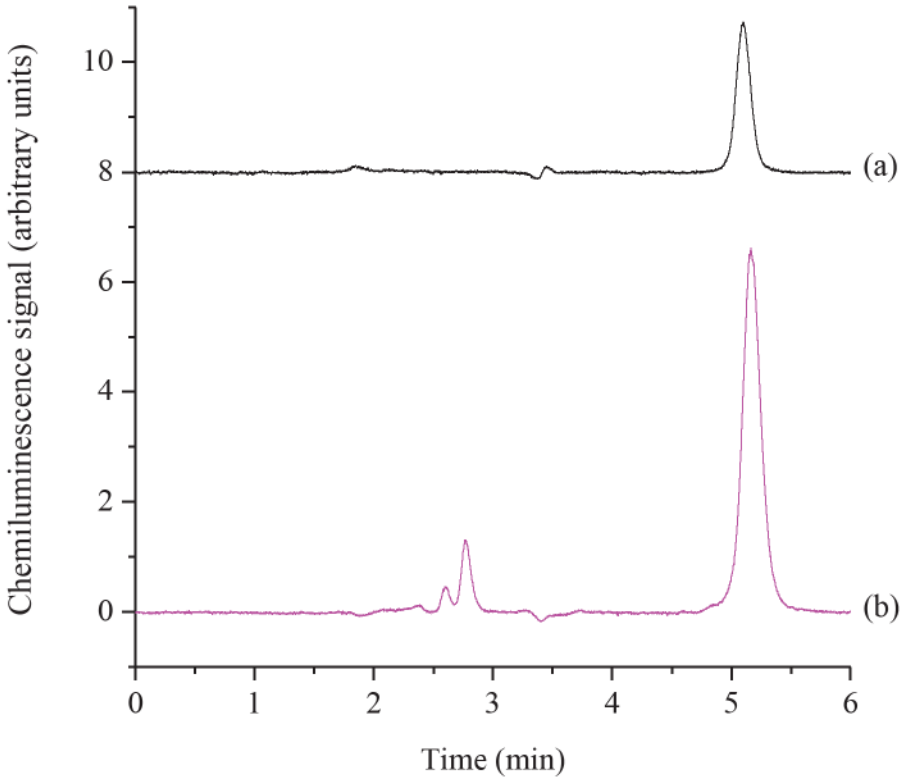

Figure 28. Typical acidic potassium permanganate chemiluminescence traces from the analysis of: (a) GSH standard (1×10^{-5} M) and (b) mouse C2C12 myotubes (sample diluted 1 : 5 into 5% aqueous formic acid) Chromatographic conditions described in Table 6.

3.3 Sample collection and preparation

Glutathione auto-oxidation in alkaline solutions and enzymatic conversion under neutral conditions are major sources of error in GSH measurement [33, 41, 42, 45, 47, 198, 201-204, 206-210]. Therefore, it is has been suggested by numerous authors that the pH of most matrices to be analysed be kept in an acidic range [41, 42, 45, 46, 226]. Rossi *et al.* [209] however, caution against acidification of blood samples as they found it can lead to significant GSH oxidation by unidentified reaction(s) with oxyhemoglobin. Alternatively they suggest blocking the free thiol moiety of GSH using an alkylating agent such as NEM prior to acidification of blood [209]. Furthermore, acidification is one approach to denature and precipitate proteins; an important requirement for analysis [33, 41-43, 45, 46, 48]. Although many methods involve acidification of the sample during collection, neutral or alkaline conditions are often employed for derivatisation reactions or to improve ionisation when mass spectroscopy is used [33, 41, 42, 46, 48, 199]. However, since a low pH improved both the chromatographic retention of GSH and the intensity of the chemiluminescence emission with permanganate, the standards and samples (C2C12 myoblasts) were prepared/collected, stored and analysed in an acidic environment (formic acid, pH 2.8). Additionally, using a commercially available BCA protein assay kit, the amount of protein precipitated when using formic acid was found to be similar to the levels removed when acidifying with the more traditional methanesulfonic acid.

3.4 Disulfide bond reduction

As previously noted, no measurable quantity of light was recorded from the reaction between GSSG and acidic potassium permanganate, preventing direct detection of this species. The same issue is encountered in methodologies that utilise

pre-column derivatisation, as appropriate chromophores or fluorophores are introduced by reaction with the free thiol moiety of GSH, which is absent in GSSG [33, 41, 42, 44-48]. This has been overcome by GSSG disulfide bond reduction, which produces two GSH compounds [33, 41, 42, 45-48]. In this approach, an initial analysis is performed to determine GSH (Figure 29a). The sample is then subjected to a disulfide bond reduction step before analysis (Figure 29b), where the signal is now a combination of endogenous and liberated GSH (often referred to as 'total GSH'). The GSSG concentration is therefore the difference between the two aforementioned measurements.

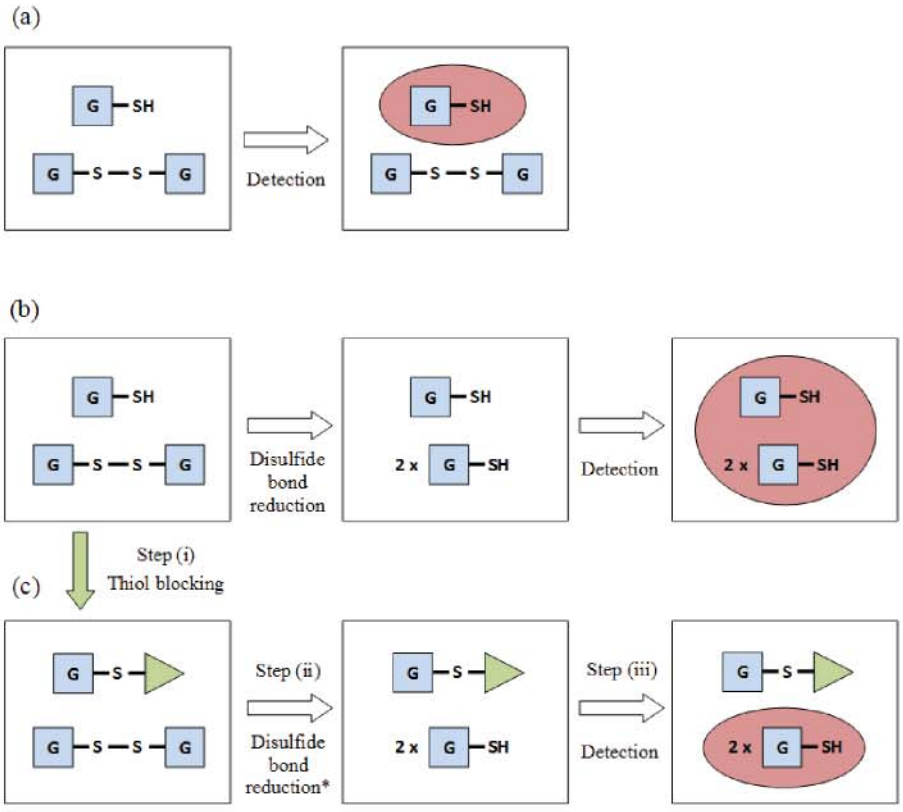

Figure 29. Strategies employed for determination of (a) GSH, (b) 'total GSH' (GSSG + GSH), (c) GSSG (indirect detection). *This step includes initial removal of excess NEM.

Traditionally, GSSG reduction has been achieved using dithiothreitol (DTT) or 2-mercaptoethanol [33, 41, 42, 45-48]. However as both of these reagents themselves

possess a free thiol, cross reactivity with derivatising agents is reportedly an issue [33, 41, 42, 45-48]. This has led researchers to explore alternative reducing agents such as TCEP [33, 41, 42, 45-48, 227-232]. Although eliminating the reaction between reducing and derivatising reagents was of little consequence for this study, TCEP was selected for use as unlike DTT and 2-mercaptoethanol it is highly water soluble, odourless, non-volatile, non-flammable, non-corrosive and is less sensitive to air and humidity [227-232]. Therefore, disulfide bond reduction employing TCEP was explored for the indirect determination of GSSG, where the influence of time, temperature and pH on the reaction was considered. It has been reported that a high excess of reagent results in decreased reaction times [230, 232]. However, as preliminary experiments showed that TCEP also elicited chemiluminescence with permanganate, I was limited to a final concentration no higher than 8.75×10^{-5} M to avoid interference from the closely eluting peak. Initially, GSSG (1×10^{-5} M in aqueous formic acid, pH 2.8) was combined (1:1) with TCEP (1.75×10^{-4} M in deionised water) and the resulting solution was repeatedly injected into the HPLC over time to monitor disulfide bond reduction through the corresponding formation of GSH. Although this reagent reportedly reduces disulfide bonds at low pH [227], only ~50% of GSSG was reduced in 60 min. Considering the rate-limiting step in this reaction is the attack of the disulfide bond by the phosphine nucleophile (pKa 7.66 [233]), deprotonation of TCEP was postulated to greatly enhance GSSG reduction. Therefore, GSSG (1×10^{-5} M in aqueous formic acid, pH 2.8) was combined with TCEP (3.5×10^{-4} M in deionised water) and a Tris-HCl buffer (0.3 M; pH 8.0) in a 2:1:1 ratio. Aliquots of the resulting solution were taken, re-acidified, and injected into the HPLC over time. In this case, ~80% of GSSG was reduced over 60 min. Finally, increasing the reaction temperature to 50°C resulted in complete disulfide reduction within 50 min (Figure 30).

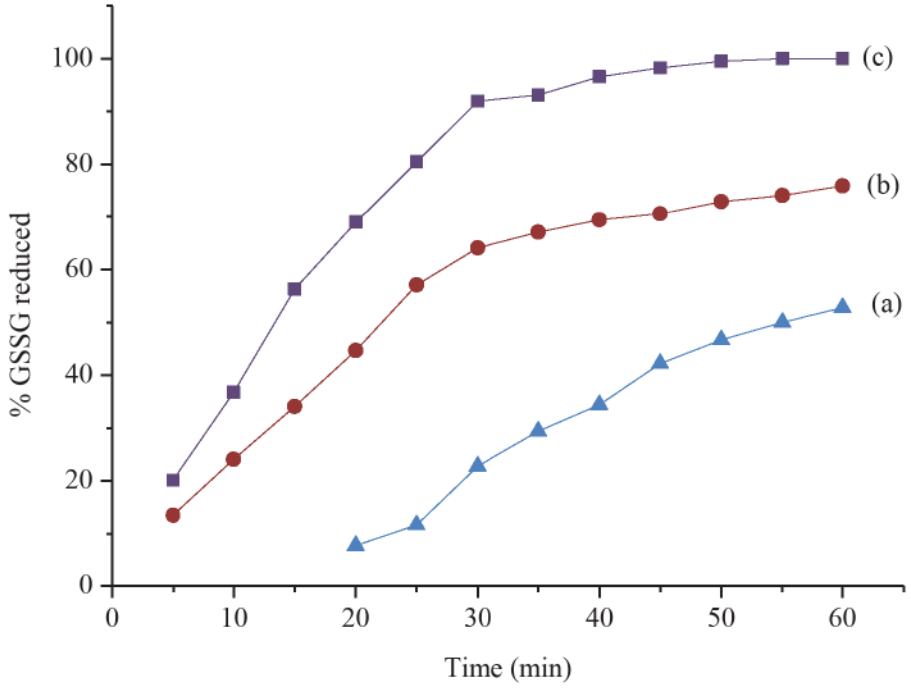

Figure 30. Optimisation of GSSG reduction using TCEP. The components were mixed together and aliquots taken over time for injection into the HPLC to determine resulting GSH concentration by peak area. The curves represent reactions between GSSG (in formic acid, pH 2.8) and TCEP in: (a) deionised water; (b) Tris-HCl buffer; and (c) Tris-HCl buffer, heated to 50° C using a hot-plate. Experimental parameters are described in the text above and chromatographic conditions outlined in Table 6.

3.5 Reaction (blocking) of thiol with *N*-ethylmaleimide

Although conditions were found that afforded complete disulfide bond reduction, the ratio of GSH to GSSG under certain physiological conditions may be as high as 1000:1, making it analytically challenging to accurately measure small GSSG values by subtracting one large GSH concentration from another. Consequently, I examined an alternative approach to the determination of GSSG, based on the methodology of Østergaard and co-workers [234]. The sample was again split into two, with one part analysed immediately for GSH (Figure 31). To the remaining fraction, the thiol alkylating reagent NEM was added to form a thioether derivative of GSH that does not elicit any measurable chemiluminescence with permanganate. GSSG is then reduced by the addition of TCEP and the liberated GSH is detected (Figure 31). Not

only does this approach negate the need to examine the difference between two similar large values, but the addition of NEM also aids in preventing unintended oxidation of GSH. The reaction was initially examined by combining equal volumes of GSH (1×10^{-5} M in aqueous formic acid, pH 2.8) and NEM (1.8×10^{-3} M in deionised water), and injecting the mixture into the HPLC over time to monitor the decrease in GSH. As can be seen in Figure 31, only ~80% of the GSH was blocked by NEM over 25 min. Considering the reaction rate is dependent on thiol deprotonation [45], the GSH alkylation was re-examined by combining GSH (1×10^{-5} M in aqueous formic acid, pH 2.8) with NEM (3.6×10^{-3} M in deionised water) and a Tris-HCl buffer (0.1 M; pH 8.0) in a 2:1:1 ratio. Aliquots of the resulting solution were re-acidified and injected into the HPLC over time. Although increasing solution pH can promote auto-oxidation and unwanted side reactions [33, 41, 42, 45, 46, 198, 201-204, 206-210], when employing a Tris-HCl buffer, alkylation of the GSH at the thiol was practically instantaneous (Figure 31).

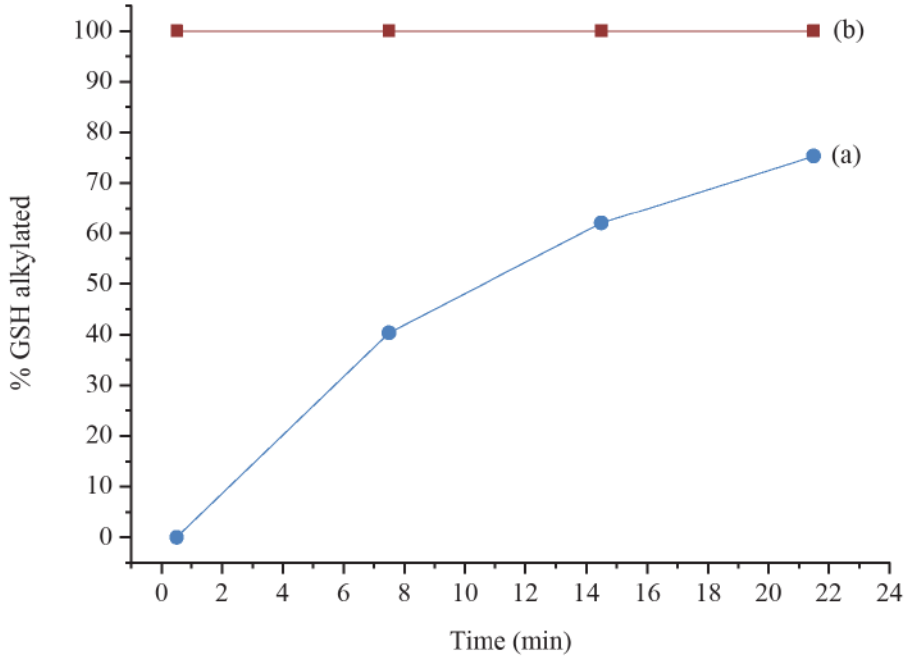

Figure 31. Optimisation of GSH alkylation using NEM. The components were mixed together and aliquots taken over time for injection onto the HPLC to determine resulting GSH concentration by peak area. The curves represent reactions between GSH (in formic acid, pH 2.8) and NEM in: (a) deionised water; and (b) Tris-HCl buffer. Experimental parameters are described in the text above and chromatographic conditions outlined in Table 6.

3.6 Removal of excess *N*-ethylmaleimide

Since NEM is added in excess compared to the level of free thiols, it must be removed prior to disulfide bond reduction, to prevent reaction with the liberated GSH. To achieve this, Østergaard *et al.* [234] added 2-mercaptoethanol because this thiol readily reacts with NEM in an analogous manner to GSH. I evaluated this approach using a mixture of GSH (1×10^{-5} M) and GSSG (1×10^{-5} M) in aqueous formic acid (pH 2.8), which was subjected to the protocols outlined in Figure 29 (parts a and c). Firstly, an aliquot of the mixture was simply filtered and analysed for GSH (Figure 29a). Secondly, to demonstrate the GSH thiol blocking with NEM (Figure 29c, step (i) only), the mixture (100 µL) was combined with Tris-HCl buffer (0.675 M; 20 µL; pH 8.0) and NEM (6.3×10^{-3} M; 20 µL), left for 20 s, filtered and analysed (Figure 29). The disappearance of the peak at 5.1 min in this chromatogram

indicated complete reaction of GSH with NEM. Thirdly, to quantify GSSG, the GSH thiol blocking was followed by removal of excess NEM and disulfide bond reduction prior to analysis (Figure 29, steps (i), (ii) and (iii)). In this procedure, 2-mercaptoethanol (8×10^{-3} M; 20 µL) was added to the mixture containing Tris-HCl buffer and NEM and left for 20 s. Next, TCEP (7.8×10^{-4} M; 20 µL) was added and the mixture was left for 60 min at 50° C to allow complete disulfide reduction (Figure 29c, step (ii)). Aqueous formic acid (5%, 20 µL) was then introduced to re-acidify the sample before filtration and analysis. The absence of a peak corresponding to GSH in Figure 32b, and its appearance in Figure 32c (equivalent to 99.7% of the predicted GSH liberated from GSSG), confirms both the successful removal of excess NEM and the complete reduction of GSSG.

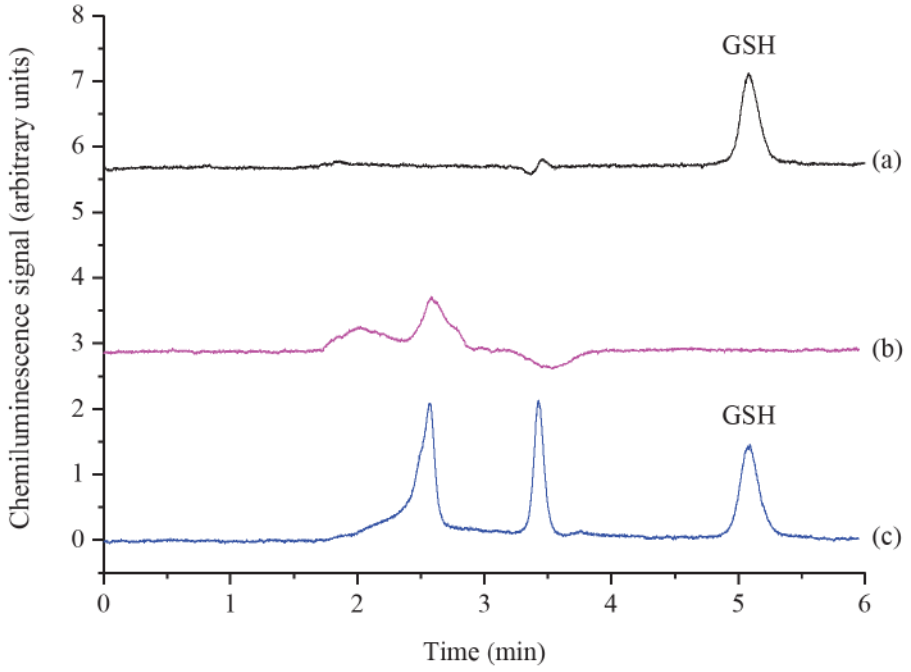

Figure 32. Typical acidic potassium permanganate chemiluminescence traces from the analysis of a mixture of GSH (1×10^{-5} M) and GSSG (1×10^{-5} M) in aqueous formic acid (pH 2.8). (a) Detection of GSH. (b) Signal after the addition of NEM and Tris-HCl buffer to sample. (c) Detection of GSSG after addition of 2-mercaptoethanol and TCEP to the sample already containing NEM and Tris-HCl buffer. Experimental parameters are described in the text above and chromatographic conditions outlined in Table 6.

3.7 Analytical figures of merit

The procedure was evaluated in terms of linearity, sensitivity and precision (Table 7). A calibration curve for GSH prepared using 30 standard solutions over the range of 1×10^{-7} M to 1×10^{-4} M showed an approximate linear relationship from 7.5×10^{-7} M to 1×10^{-4} M (correlation co-efficient, $R^2 = 0.997$). However, within the range of 7.5×10^{-7} M to 1×10^{-5} M the calibration was highly linear with $R^2 = 0.9999$. The limit of detection, defined as the lowest signal detected with a signal-to-noise ratio of 3 was determined to be 5×10^{-7} M GSH. The precision of repeated injections (n = 6) of GSH at low (1×10^{-6} M), medium (2.5×10^{-6} M) and high (5×10^{-5} M) concentration was good (R.S.D. of less than 1.5%). Similar figures of merit (Table 7) were obtained for the determination of GSSG.

Table 7. Analytical figures of merit.

	GSH	GSSG
Calibration function	y = 3304000x-0.71	y = 3291515x-0.90
R^2	0.9999	0.9997
Linear range	7.5×10^{-7} M to 1×10^{-5} M	7.5×10^{-7} M to 1×10^{-5} M
Limit of detection	5×10^{-7} M	5×10^{-7} M
Precision (%RSD)*	0.9	1.3

*Concentration of 2.5×10^{-6} M (n = 6).

3.8 Determination of GSH and GSSG in a biological system

The procedure developed in this chapter was employed for the determination of GSH and GSSG in C2C12 myotubes that had been treated for 24 hr with various quantities of glucose oxidase. This chronically exposed the myotubes to a continuous, biologically relevant source of ROS [224, 225]. Hydrogen peroxide produced by the glucose oxidase in the cell culture medium can diffuse into myotubes through the cell membrane, where in order to maintain redox state, it is quenched by various intracellular antioxidants [224, 225]. However, if there is an

imbalance between H_2O_2 influx and antioxidant capacity, then intracellular ROS levels (including H_2O_2) will increase, cell viability will decrease, and the GSH/GSSG ratio will decrease.

Intracellular H_2O_2 levels were assessed using the commercially available Amplex Red assay, which showed that there was no significant increase in H_2O_2 when the cells were treated with 15 or 30 mU mL^{-1} of glucose oxidase compared to untreated controls (Figure 33a). However, when myotubes were treated with 100, 250 and 500 mU mL^{-1} glucose oxidase, cellular antioxidant defences were overwhelmed and a dose-dependent increase in H_2O_2 was observed ($p<0.05$). C2C12 myotube viability was assessed by measuring mitochondrial function (assessed using the MTT assay; Figure 33b) and cell membrane integrity (based on ethidium uptake; Figure 33c). Both mitochondrial function and cell membrane integrity were compromised in cells treated with 100, 250 and 500 mU mL^{-1} glucose oxidase ($p<0.05$), signifying dead or dying cells undergoing apoptosis or necrosis. Membrane integrity was also reduced in myotubes treated with lower quantities of glucose oxidase (15 and 30 mU mL^{-1}; $p<0.05$). This attribute is sensitive to oxidative stress because it is exposed to increased H_2O_2, both intracellular and extracellular (where there are essentially no antioxidant compounds).

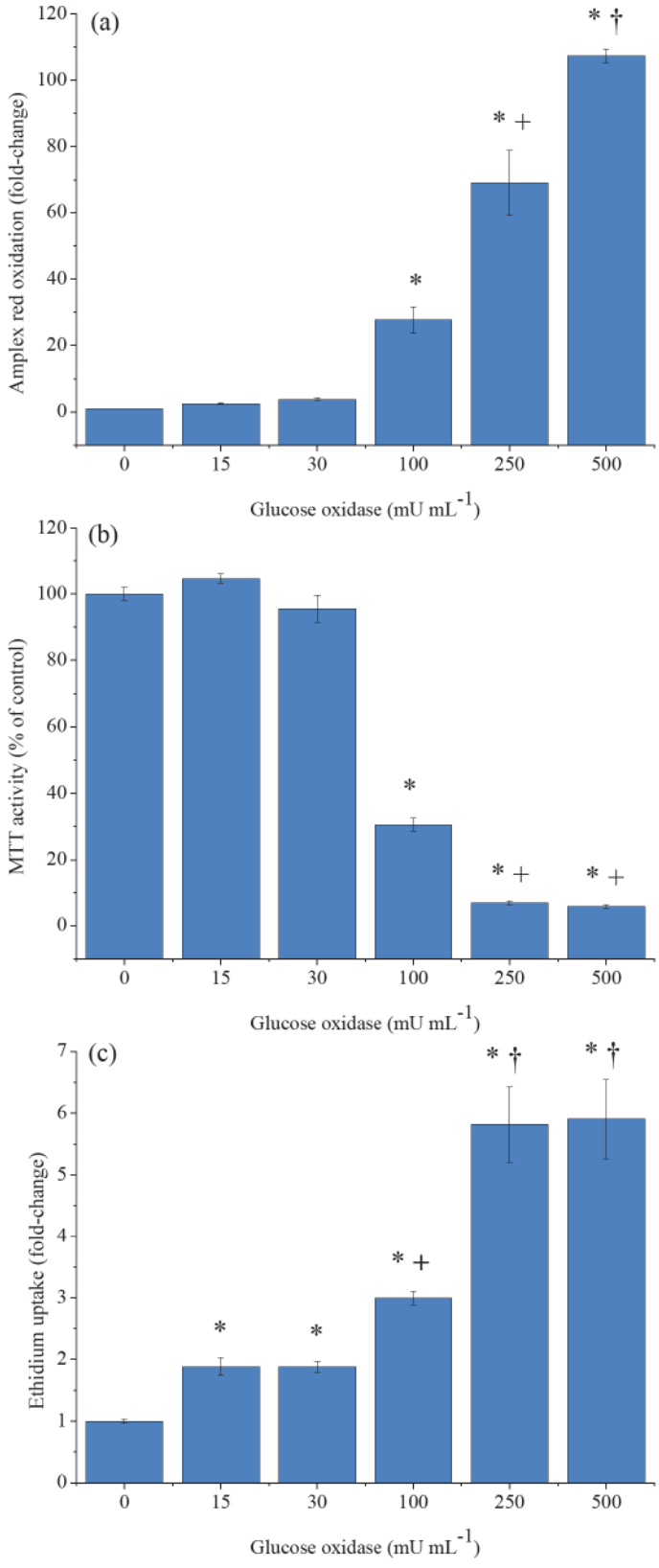

Figure 33. The effects of a 24 h glucose oxidase treatment on intracellular H_2O_2 levels and cell viability in C2C12 myotubes. (a) Amplex Red assay for intracellular H_2O_2 levels (N = 1 experiment with 7 replicates); (b) MTT activity assay to assess mitochondrial function (N = 1 experiment with 8 replicates); (c) Cellular ethidium uptake to assess membrane integrity (N = 2 experiments with 7 replicates). Symbols show significant differences at $p<0.05$ (one-way ANOVA).

Having established that glucose oxidase treatment causes enough oxidative stress to disrupt myotube homeostasis, the intracellular redox environment was assessed by quantifying GSH, GSSG and their respective ratio using the method described in this chapter. The concentrations of GSH and GSSG in the supernatant of the cell lysates (corrected for protein content) are shown in Table 8. In myotubes treated with 15 mU mL^{-1} or 30 mU mL^{-1} glucose oxidase, for which there was no significant increase in H_2O_2 or loss of mitochondrial function, the concentrations of GSH and GSSG were similar to the untreated cells. In myotubes treated with 100 mU mL^{-1} or 250 mU mL^{-1} glucose oxidase, much greater concentrations of GSH and GSSG were found ($p<0.05$), indicating an adaptive response to the oxidative stress stimulus. However, when treated with 500 mU mL^{-1} glucose oxidase, the myotubes had lower GSH and GSSG levels than all other treatments (Table 8; $p<0.05$), presumably mediated by greater membrane damage (Figure 33c).

Table 8. GSH and GSSG in mice C2C12 myotubes.

GO dose (mU mL^{-1})	GSH (µM 100 µg $protein^{-1}$)	GSSG (µM 100 µg $protein^{-1}$)
0	8.5 (1.2)*	0.70 (0.1) *
15	6.0 (0.3)*	0.40 (0.03) *
30	6.7 (0.3)*	0.47 (0.05) *
100	14.6 (1.1)†	2.1 (0.2) †
250	13.3 (0.6) †	2.2 (0.1) †
500	1.4 (0.4)‡	0.40 (0.1) *

These values are reported as means of six determinations (± SEM). For each analyte symbols show significant differences at $p<0.05$ (one-way ANOVA).

The molar ratio of GSH/GSSG in myotubes treated with 15 or 30 mU mL^{-1} glucose oxidase was not significantly different to that in the untreated sample (Figure 34). Therefore, although membrane integrity was reduced (Figure 33c), the myotubes maintained their cellular redox state under this level of oxidative stress. However, when the concentration of glucose oxidase was increased, a dose dependent decrease

in the GSH/GSSG ratio was observed (Figure 34; $p<0.05$), which reflected the increase in ROS (Figure 33a).

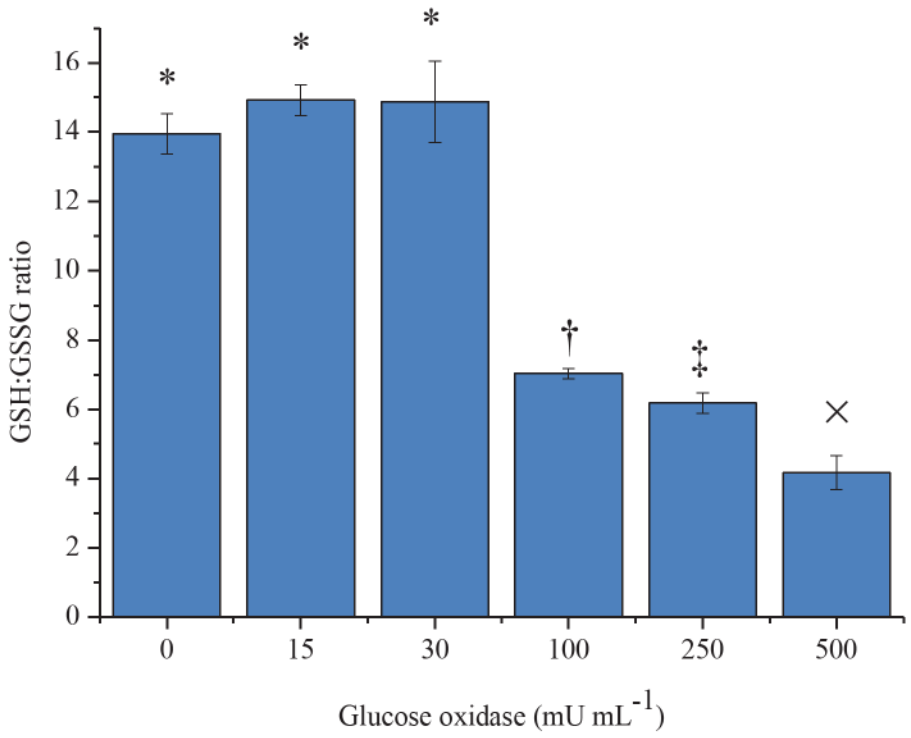

Figure 34. GSH/GSSG ratio in myotubes treated with different quantities of glucose oxidase (N = 2 experiments in triplicate). Symbols show significant differences at $p<0.05$ (one-way ANOVA).

4. Conclusions

Rapid HPLC separation coupled with direct acidic potassium permanganate chemiluminescence detection provided a simple and accurate approach to determine GSH, which was extended to GSSG by incorporating thiol blocking and disulfide bond reduction. Unlike conventional approaches with absorbance or fluorescence detection, this procedure did not require derivatisation of GSH (thus minimising error associated with auto-oxidation) and overcomes problems encountered when deriving the concentration of GSSG from 'total GSH'. The linear range and limit of detection for both analytes were 7.5×10^{-7} to 1×10^{-5} M, and 5×10^{-7} M, respectively. The procedure was applied to the determination of GSH and GSSG in cultured muscle cells treated for 24 h with glucose oxidase (0, 15, 30, 100, 250 and 500 mU mL^{-1}), which exposed them to a continuous source of reactive oxygen species (ROS). Both analyte concentrations were greater in myotubes treated with 100 or 250 mU mL^{-1} glucose oxidase (compared to untreated controls), but were significantly lower in myotubes treated with 500 mU mL^{-1} ($p < 0.05$). Trends in the absolute concentrations of these analytes were rationalised by considering intracellular ROS in conjunction with measures of cell viability. However, the GSH/GSSG ratio in myotubes treated with 100, 250 and 500 mU mL^{-1} glucose oxidase exhibited a dose-dependent decrease that reflected the increase in intracellular ROS. The results of this study also highlight the importance of the GSH/GSSG ratio to assess the overall intracellular redox environment. The work presented in this chapter resulted in a recent publication [235].

CHAPTER FIVE

Production of a stable tris(2,2′ bipyridine)ruthenium(III) reagent for chemiluminescence detection of glutathione and glutathione disulfide

- **Introduction**
- **Experimental**
- **Results and discussion**
- **Conclusion**

1. Introduction

Over the past four decades, tris(2,2′-bipyridine)ruthenium(III) has emerged as one of the most widely used chemiluminescence reagents, particularly for the detection of alkaloids, biomolecules, pharmaceuticals and controlled drugs possessing an amine functionality [109, 133-137]. Although the applications vary significantly, the detection chemistry is essentially based on an initial chemical or electrochemical oxidation of the stable $[Ru(bipy)_3]^{2+}$ complex to form $[Ru(bipy)_3]^{3+}$, and subsequent reaction with a suitable analyte (or analyte oxidation product) to generate $[Ru(bipy)_3]^{2+*}$, which returns to the ground state by emission of a photon (detailed in scheme 1, chapter 1).

Whilst simple, the major limitation of this redox cycle is the inherently poor stability of the $[Ru(bipy)_3]^{3+}$ species in aqueous solution due to its ability to oxidise water [138]. This problem can be overcome by on-line generation of $[Ru(bipy)_3]^{3+}$ at (or immediately prior to) the point of detection, either on an electrode surface, or by merging a stream of oxidant solution [109, 134-138]. These approaches have been extensively used in flow analysis [136], but have several drawbacks. Electrochemical oxidation requires extra instrumentation and suffers from electrode fouling, particularly under the continuous and widely variable conditions of liquid chromatography. Moreover, on-line chemical or electrochemical oxidation results in incomplete generation of $[Ru(bipy)_3]^{3+}$, and possible side reactions between oxidant and analyte, both of which can affect the sensitivity [136, 236]. However, in some cases, reaction between analyte and oxidant or electrode surface (rather than with $[Ru(bipy)_3]^{3+}$) is the dominant pathway to generate intermediates that reduce $[Ru(bipy)_3]^{3+}$ to the electronically excited emitting species [135, 136]. This includes co-reactant ECL systems with relatively low concentrations of $[Ru(bipy)_3]^{2+}$

[135, 237], and the chemiluminescence reaction of certain organic acids with $[Ru(bipy)_3]^{2+}$ and Ce(IV) [238].

Alternatively, $[Ru(bipy)_3]^{3+}$ has been generated off-line in acidic solution immediately prior to analysis using solid lead dioxide, which is removed from solution by filtration [136]. This approach has been successfully utilised for highly sensitive detection in flow-injection analysis and rapid HPLC separations, but it is labour intensive and not appropriate for extended periods of use. So the challenge to-date lies in producing $[Ru(bipy)_3]^{3+}$ reagent with long term stability that is suitable for chemiluminescence detection.

A previous attempt to address this issue involved increasing the concentration of sulfuric acid to 2.0 M, which lowered the extent of reaction between the reagent and water [138]. Although this reagent afforded analytically useful chemiluminescence (with codeine) over 280 h of continuous use, there was significant variation in signal intensity, and high concentrations of buffer were required in the analyte solution. A second approach involved a re-circulating system, in which the reagent was repeatedly passed over lead dioxide immobilised in a filter device and an FIA injection port loop [138]. This eliminated the need to buffer the chemiluminescence reaction and the response with codeine varied by only 14% over 90 h. However, this approach is not suitable for post-column detection, where a constant stream of reagent is required. A subsequent attempt involved the synthesis of a tris(2,2′-bipyridine)ruthenium(III) perchlorate salt that was then dissolved in anhydrous acetonitrile. Spectrophotometric experiments showed a decrease in reagent concentration of less than 6% over a 50 h period. Despite being a significant improvement on previous attempts, this approach has not gained widespread

acceptance, presumably due to the relatively complicated reagent synthesis involving chlorine gas, and problems with batch-to-batch variation.

As previously discussed, of the analytes reported to evoke a chemiluminescence response from $[Ru(bipy)_3]^{3+}$, the majority contain an amine functionality. Investigations by Noffsinger and Danielson [140] showed that as a general rule, the emission intensity from the reactions of amines is in the order: tertiary > secondary > primary. Nevertheless, several studies have shown that under certain conditions secondary amines can react with $[Ru(bipy)_3]^{3+}$ to elicit an analytically useful signal [139, 140, 239, 240]. Although the previous chapter describes the detection of GSH using acidic potassium permanganate chemiluminescence, some sample pre-treatment was still necessary for GSSG detection. However, as these biologically important analytes possess primary and secondary amine functionalities (Figure 26), $[Ru(bipy)_3]^{3+}$ chemiluminescence holds the potential for direct detection of both GSH and GSSG.

This chapter describes two new, conveniently prepared, stable $[Ru(bipy)_3]^{3+}$ reagents (one in an aprotic solvent and the other in a protic non-aqueous solution) for chemiluminescence detection in flow analytical techniques. The reagents were evaluated in terms of temporal stability and capacity to elicit analytically useful chemiluminescence in comparison with conventional $[Ru(bipy)_3]^{3+}$ solutions. The use of HPLC combined with post-column $[Ru(bipy)_3]^{3+}$ chemiluminescence was then explored for the direct detection of GSH and GSSG.

2. Experimental

2.1 Chemicals and reagents

Deionised water (Continental Water Systems, Victoria, Australia) and analytical grade reagents were used unless otherwise stated, obtained from the following sources: $[Ru(bipy)_3]Cl_2 \cdot 6H_2O$ from Strem Chemicals (Minnesota, USA); glacial acetic acid, hydrochloric acid (32%) and perchloric acid (70%) from Univar (New South Wales, Australia); lead dioxide, sodium perchlorate and sodium thiosulfate from Ajax (New South Wales, Australia); acetonitrile from Burdick & Jackson (Michigan, USA); sulfuric acid from Merck (Victoria, Australia); acetic anhydride from Scharlau (Barcelona, Spain); calcium hypochlorite from Hy-Clor (New South Wales, Australia); and dextromethorphan, disodium phosphate enrofloxacin, furosemide, L-glutathione, L-glutathione disulfide, hydrochlorothiazide, monosodium phosphate, ofloxacin, potassium oxalate, phosphorus pentoxide, trifluoroacetic acid from Sigma-Aldrich (New South Wales, Australia) and formic acid from Hopkin and Williams (Essex, England). Codeine, ethylmorphine and thebaine were provided by GlaxoSmithKline (Victoria, Australia).

2.2 Preparation of Reagent A

This well-documented approach [132, 136] involved the addition of PbO_2 (0.2 g per 100 mL) to an aqueous solution of $[Ru(bipy)_3]Cl_2.6H_2O$ in 0.05 M H_2SO_4, followed by stirring for 5 min, after which it became emerald green in colour. This reagent has been commonly used in FIA, where small quantities of solution can be oxidised immediately prior to use and the procedure can be completed before significant degradation of the reagent [136], but it is not ideal for extended periods of use (e.g. those required for HPLC with post-column chemiluminescence detection).

2.3 Preparation of Reagent B

This reagent was prepared using a previously described method [241], in which 400 mg of $[Ru(bipy)_3]Cl_2.6H_2O$ was dissolved in a minimum amount of water (~6 mL) at room temperature. Chlorine gas (generated by drop wise addition of HCl (32%) to $Ca(ClO)_2$ (70% w/w)) was then bubbled through the solution until it turned from orange to dark green. Next, 200 mg of $NaClO_4$ was added directly to the solution which was thoroughly mixed and then placed in an ice bath for 5 min. The resultant green $[Ru^{III}(bipy)_3](ClO_4)_3$ precipitate was vacuum filtered, washed twice with ice water (~2 mL) and dried over phosphorus pentoxide for 24 h. The reagent solution was prepared by dissolving the crystals in dry acetonitrile.

2.4 Preparation of Reagent C

Initially, $[Ru^{II}(bipy)_3](ClO_4)_2$ was prepared by aqueous metathesis reaction between $[Ru(bipy)_3]Cl_2$ and $NaClO_4$. In this approach, 400 mg of $[Ru(bipy)_3]Cl_2.6H_2O$ was dissolved in a minimum amount of water (~6 mL) at room temperature. Then 200 mg of solid $NaClO_4$ was added to the solution which was thoroughly mixed and placed on an ice bath for 5 min. The $[Ru^{II}(bipy)_3](ClO_4)_2$ precipitate was filtered, washed twice with ice water (~2 mL) and dried over phosphorus pentoxide for 24 h. The reagent solution was prepared by dissolving the crystals in acetonitrile containing 0.05 M $HClO_4$. Lead dioxide (0.2 g per 100 mL) was then added, followed by stirring for 1 min to allow formation of $[Ru(bipy)_3]^{3+}$. It is noteworthy that this oxidation occurs more rapidly and the solution colour is more blue-green than when preparing any of the other reagents described in this chapter.

2.5 Preparation of Reagent D

The $[Ru(bipy)_3]Cl_2.6H_2O$ was dissolved in 95:5 glacial acetic acid:acetic anhydride containing 0.05 M H_2SO_4. In this reagent, any water present is eliminated by reaction with acetic anhydride. Lead dioxide (0.2 g per 100 mL) was added and the solution was stirred for 5 min until it changed to blue-green, signifying the formation of $[Ru(bipy)_3]^{3+}$.

2.6 UV-Visible Absorption

Spectra were obtained using a Cary 300 Bio UV-visible spectrophotometer (Varian, Mulgrave, Australia) with 10 mm path length, sealable quartz cuvettes (Starna, Baulkham Hills BC, NSW, Australia). The stability of the reagents (1×10^{-3} M) was assessed by monitoring the peak corresponding to the ruthenium(III) state over time. In the case of reagents A, C and D, the oxidised complex was filtered (0.45 μm, Millipore MillexHN Nylon) to remove PbO_2, immediately prior to placing the solution into a cuvette within the spectrophotometer.

2.7 Sequential Injection Analysis

Changes in chemiluminescence intensity for the reaction of each $[Ru(bipy)_3]^{3+}$ reagent (1×10^{-3} M) with codeine (1×10^{-7} M) over time was established using an automated sequential injection analysis system [242]. Reagent, analyte and carrier solutions were aspirated with a milliGAT pump (Global FIA) through a multiposition valve (model C25Z, Valco) and chemiluminescence detector with a flow-cell comprising of a coil of transparent PTFE tubing and red-sensitive photomultiplier tube (Electron Tubes Model 9828SB; ETP, Ermington, NSW, Australia). The pump and valve were controlled *via* a LabJack U12 data acquisition board, using software written in LabVIEW 8 [242], which was also used to record the output from the

photomultiplier tube. The system was programmed to repeatedly aspirate 50 μL of reagent (valve position 1; 167 μL s^{-1}), 1500 μL of codeine solution (position 2; 167 μL s^{-1}), and 1000 μL of deionised water (position 3; 100 μL s^{-1}), with a 60 min pause after every fifth cycle.

2.7 Flow injection analysis

A conventional FIA manifold with a chemiluminescence detector was constructed in our laboratory. A peristaltic pump (Gilson Minipuls 3, John Morris Scientific, Balwyn, Victoria, Australia) with bridged PVC tubing (DKSH, Caboolture, Queensland, Australia) was used to propel solutions through 0.8 mm i.d. PTFE tubing (DKSH). Standards (1×10^{-5} M) were injected (70 μL) with an automated six-port valve (Valco Instruments, Houston, Texas, USA) into a carrier stream, which merged with a $[Ru(bipy)_3]^{3+}$ reagent (1×10^{-3} M) at a T-piece, and the light emitted from the reacting mixture was detected with a custom built flow-through chemiluminometer, as described in chapter 3, section 2.3. The output from the photomultiplier was documented with a chart recorder (YEW type3066, Yokogawa Hokushin Electric, Tokyo, Japan).

2.8 High performance liquid chromatography

Chromatographic analysis was carried out on an Agilent Technologies 1200 series liquid chromatography system, equipped with a quaternary pump, solvent degasser system, autosampler and diode array detector (Agilent Technologies, Victoria, Australia). Hewlett-Packard Chemstation software (Agilent Technologies) was used to control the HPLC pump and acquire data from the chemiluminescence detector. Before use in the HPLC system, all sample solutions and solvents were filtered through a 0.45 μm nylon membrane. Hewlett-Packard Chemstation software

(Agilent Technologies) was used to control the HPLC and acquire data from the chemiluminescence detector.

Opiate standards were separated using a Chromolith Performance RP-18e monolithic column (100 mm × 3 mm i.d.; Merck, Germany) operating at room temperature with an injection volume of 20 µL. The separation conditions were based on a previous study in our laboratory [243]. Gradient elution was performed at a flow rate of 1 mL min^{-1} with acetonitrile (solvent A) and 0.01% aqueous trifluoroacetic acid (solvent B) as follows: 0-1 min: 7% A, 93% B; 1-7 min: 25 % A, 75% B. Post-column $[Ru(bipy)_3]^{3+}$ chemiluminescence detection of opiate standards was generated using the manifold outlined in Figure 17. The reagent, propelled at a flow rate of 2.5 mL min^{-1} using a Gilson Minipuls 3 peristaltic pump (John Morris Scientific, Victoria, Australia) with bridged PVC tubing (DKSH), merged with the HPLC eluate at a T-piece, and the light emitted from the reacting mixture was detected with a custom built flow-through chemiluminometer as described in chapter 3, section 2.6.

Glutathione and glutathione disulfide were separated using the chromatographic conditions described in chapter 4. Post-column $[Ru(bipy)_3]^{3+}$ chemiluminescence detection of GSH and GSSG standards was generated using a three-line flow-through manifold. The HPLC eluate and a stream of phosphate buffer (40 mM; pH 8; 1 mL min^{-1}) merged at a T-piece located 15 cm from the entrance of the detector. This stream was then combined with a line of Reagent C (1×10^{-3} M; 2 mL min^{-1}) and the light emitted from the reacting mixture was detected with a custom built flow-through chemiluminometer as described in chapter 3, section 2.6.

3. Results and discussion

3.1 Reagent stability

The relative stability of each $[Ru(bipy)_3]^{3+}$ reagent was assessed by monitoring its visible absorbance over time. As shown in Figure 35, the absorption for Reagent A was reduced to 50% of the initial value after only 5 h, with the profile nearly horizontal by 24 h. In contrast, reagents B-D exhibited much greater stability over the 48 h period of investigation. Reagent B decreased by approximately 3%, which is similar to previous observations from my research group [241], where $[Ru(bipy)_3](ClO4)_3$ prepared in acetonitrile showed a less than 6% decrease in absorbance over 50 h Reagents C and D decreased by only 2% and 5%, respectively.

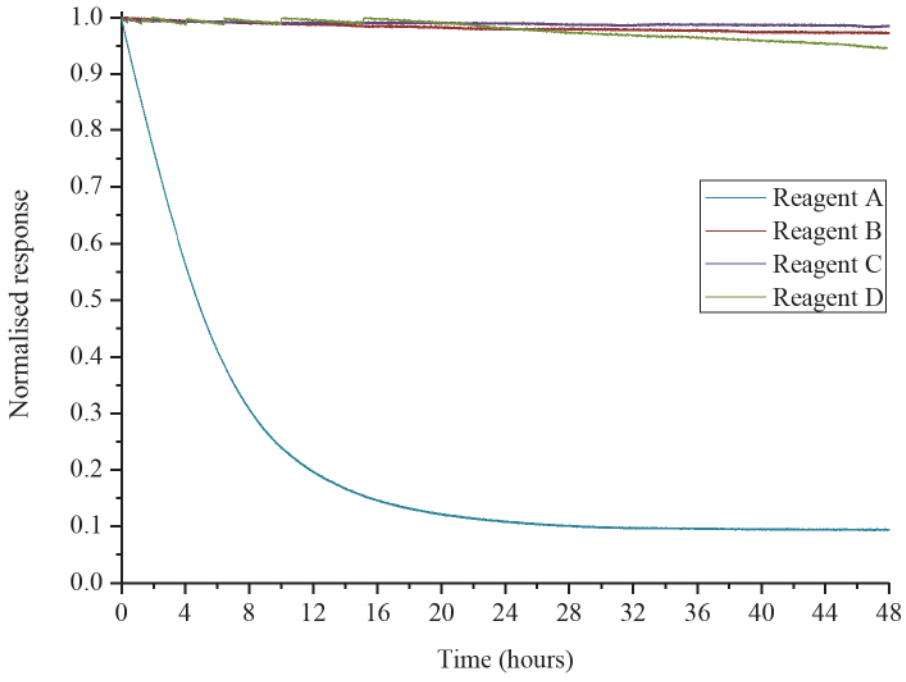

Figure 35. Absorbance versus time measurements for $[Ru(bipy)_3]^{3+}$ (1×10^{-3} M): Reagent A (694 nm); B (674 nm); C (674 nm); and D (705 nm).

The stability of the reagents was also assessed in terms of their chemiluminescence intensity upon reaction with a codeine standard using sequential injection analysis (SIA). The reagent, analyte and carrier solutions were sequentially aspirated through

a chemiluminescence detector, with a 60 min pause after every fifth cycle. This approach is well-suited to fast chemiluminescence reactions, as it minimises the mixing of solutions prior to entering the flow-cell, enabling detection of a greater proportion of the emitted light [242]. Initially, these experiments were conducted after filtering the lead dioxide from reagents A, C and D, but this resulted in a decrease in chemiluminescence intensity for those reagents over time. A corresponding change in the colour of the reagents from blue-green to yellow-green was also observed. The most probable cause of this was the presence of slow reacting organic impurities in the reagents and on the surfaces of glassware, not present in the quartz cuvettes used in the previous spectrophotometric experiments. To overcome this problem, the PbO_2 was left in the reagents. Because of its high density, the PbO_2 settles to a compact layer, particularly in the non-aqueous solvents of C and D. However, to ensure no particulates were carried over, a 0.45 μM filter was placed in-line to remove any traces of the solid oxidant that might be present as the reagent was aspirated. For Reagents C and D, this approach resulted in solutions that visibly remained the same blue-green colour for more than six months. As can be seen in Figure 36, all reagents produced response profiles similar to the previously described absorption measurements (Figure 35). Reagent A again exhibited an exponential decay in signal, with only 50% of the original chemiluminescence intensity upon reaction with codeine observed after 5 h, which further decreased to only 10% after 24 h. Reagent B exhibited reasonable stability, with a 12% decrease in response over 48 h and a corresponding change in the appearance of the reagent solution to yellow-green. This highlights one of the major problems associated with Reagent B – the slow reaction of $[Ru(bipy)_3]^{3+}$ with trace amounts of water present in the acetonitrile. Reagents C and D showed excellent stability over the 48 h. For

these reagents, of course, reduction of the complex by traces of water and organic impurities is prevented by the layer of PbO_2.

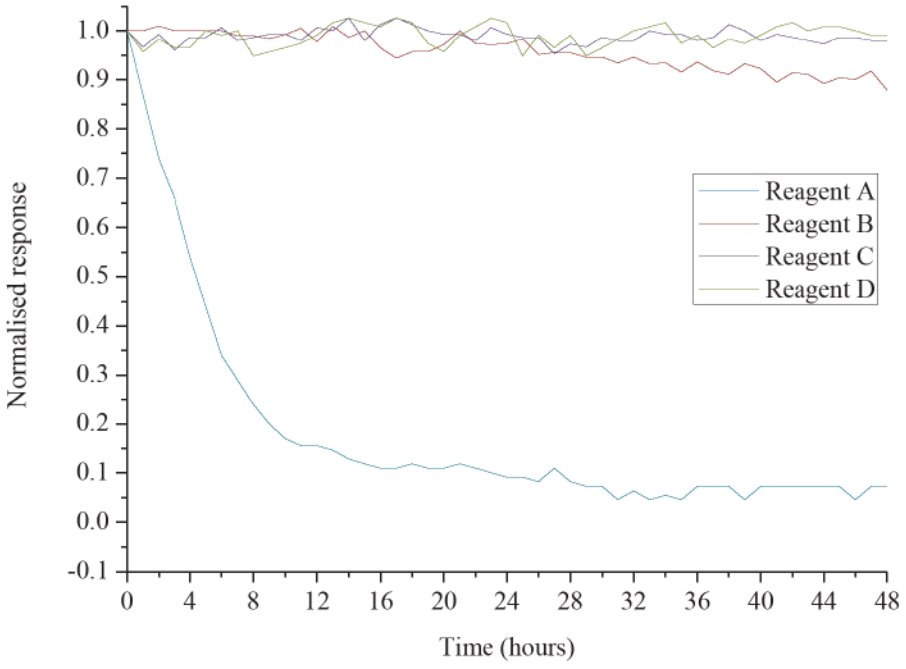

Figure 36. Chemiluminescence response versus time for the reaction of each $[Ru(bipy)_3]^{3+}$ reagent (1×10^{-3} M) with codeine (1×10^{-7} M), generated using SIA.

3.2 Analytical performance

The ability of Reagents B, C and D to provide analytically useful chemiluminescence in comparison to the more traditional Reagent A was investigated using both FIA and HPLC methodology. In the case of FIA, a range of previously studied analytes [236, 244-248] were injected into a deionised water carrier stream that merged with the reagent. When considering the chemiluminescence intensities normalised to Reagent A (Figure 37), some differences in selectivity between each reagent were evident. Reagent D produced the lowest responses across all analytes. Reagents B and C (both prepared in acetonitrile) gave responses between 1.5- and 3.5-fold those obtained using Reagent A, for the analytes codeine, dextromorphan, enrofloxacin, furosemide, but a diminished response with ofloxacin and hydrochlorothiazide.

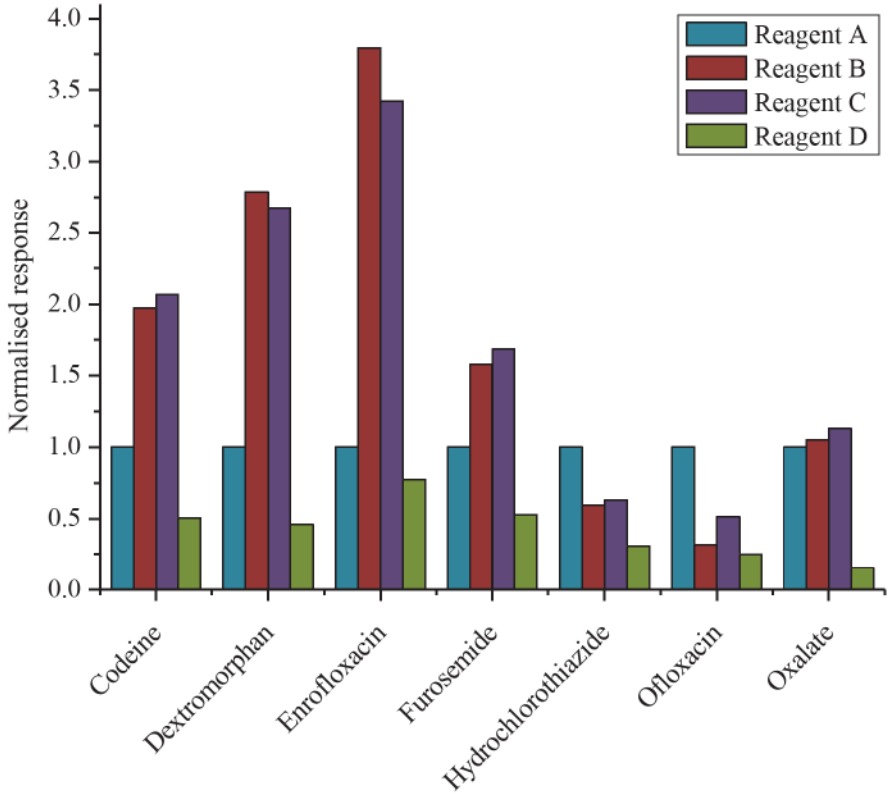

Figure 37. Normalised chemiluminescence intensities for the reaction of selected analytes (5×10^{-6} M) with $[Ru(bipy)_3]^{3+}$ reagents (1×10^{-3} M), generated using FIA.

Calibration functions were prepared for ofloxacin, furosemide and enrofloxacin. As the reaction environment can have a significant influence on $[Ru(bipy)_3]^{3+}$ chemiluminescence response [109, 133-137], a series of univariate searches was performed on reagent and acid concentrations along with flow rate for each reagent/analyte pair, prior to establishing analytical figures of merit. Based on these experiments, a 1×10^{-3} M reagent solution containing 0.05 M of either H_2SO_4 or $HClO_4$ delivered at a flow rate of 2.5 mL min^{-1} per line was found to provide the optimal signal for each reagent. The limits of detection, summarised in Table 9, show that no one reagent has superior sensitivity with all analytes. Mirroring the relative intensities shown in Figure 37, Reagent D gave the poorest limits of detection.

Table 9. Limits of chemiluminescence detection (3σ) for three analytes using FIA methodology.

	Limit of detection (M)		
Reagent	**Enrofloxacin**	**Furosemide**	**Ofloxacin**
A	7×10^{-8}	1×10^{-7}	1×10^{-8}
B	3×10^{-8}	3×10^{-7}	4×10^{-8}
C	3×10^{-8}	3×10^{-7}	3×10^{-8}
D	8×10^{-8}	4×10^{-7}	7×10^{-8}

The utility of the four reagents for post-column chemiluminescence detection over extended periods of analysis was explored using a reversed-phase HPLC separation of four opiate-based analytes (codeine, ethylmorphine, thebaine and dextromorphan), which was repeated 12 times over 48 h. When using the conventional Reagent A (Figure 38a) all peaks were noticeably reduced in size after only 3 h. with a decay to approximately 17% of the original peak area over 10 h. Alternatively, chromatograms obtained using Reagents B, C and D exhibited no loss in peak size over 48 h. Differences in intensity and selectivity were again observed. The chromatograms obtained using Reagent D were similar to the chromatogram using reagent A (prior to significant reagent degradation), but lower in intensity. Not surprisingly, the chromatograms obtained using the two reagents prepared in acetonitrile (B and C) exhibited similar relative peak heights. Reagent B provided the greatest absolute signal intensities, but the chromatograms for this reagent showed significant baseline drift with the solvent gradient.

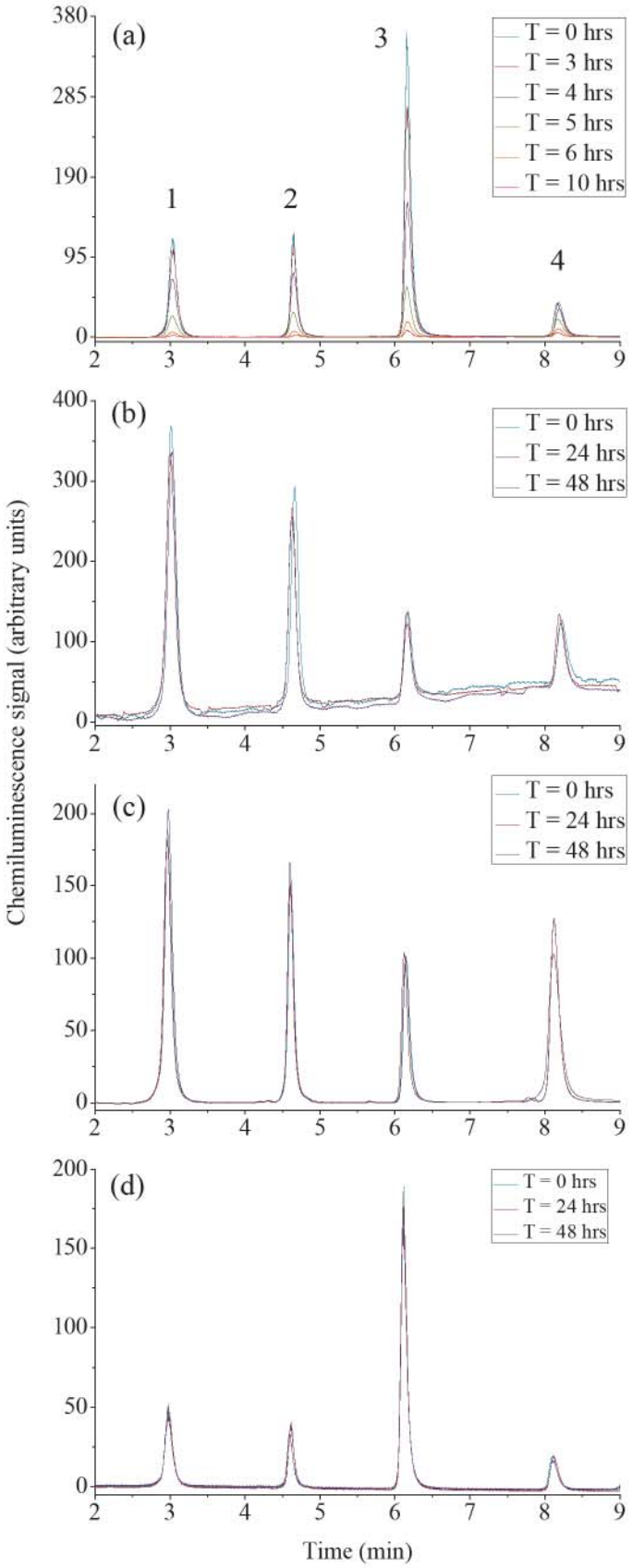

Figure 38. Chromatograms of opiate-based compounds generated over time using HPLC with post-column chemiluminescence detection employing a 1×10^{-3} M solution of: (a) Reagent A; (b) Reagent B; (c) Reagent C; (d) Reagent D. (Peaks: 1, codeine; 2, ethylmorphine; 3, thebaine; 4, dextromethorphan).

3.3 Post-column $[Ru(bipy)_3]^{3+}$ chemiluminescence detection of glutathione and glutathione disulfide using Reagent C

Initial screening experiments were conducted with a two line FIA manifold as it provided similar conditions to HPLC, but without the relatively time-consuming separation. In this approach, standard solutions (1×10^{-5} M) of GSH or GSSG were injected into a carrier stream of aqueous formic acid (pH 2.5; 1 mL min^{-1}; representing the HPLC mobile phase) which then merged with a flowing line of Reagent C (1×10^{-3} M; 2 mL min^{-1}) within the flow-through chemiluminometer immediately prior to entering the detection cell. As can be seen in Figure 39, these conditions afforded a large signal for GSH but a relatively small response for GSSG. This difference was attributed to the free thiol moiety of GSH (not present in the structure of GSSG), which under acidic conditions could be easily oxidised by $Ru(bipy)_3^{3+}$ to result in a strong chemiluminescence emission.

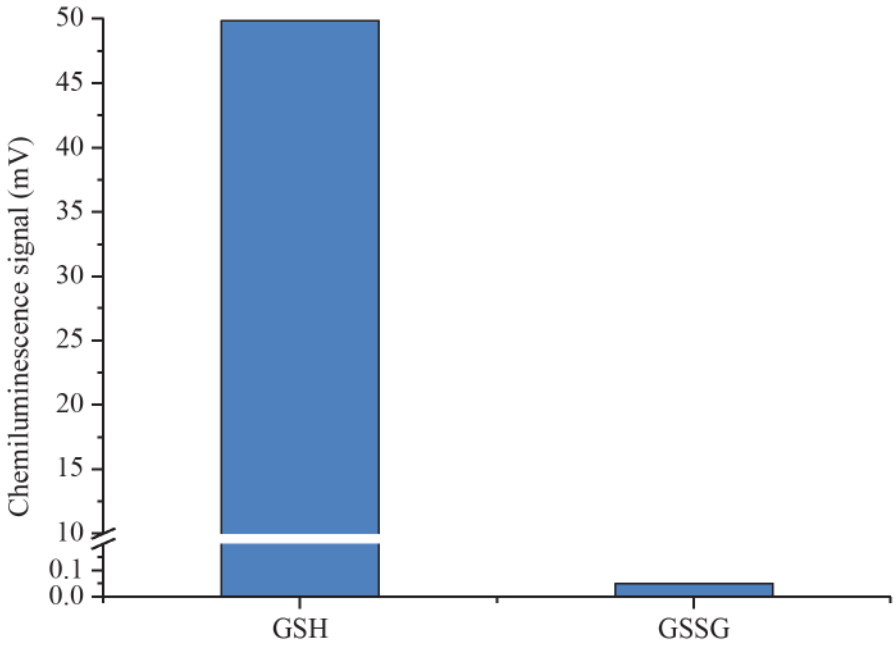

Figure 39. Chemiluminescence intensities for the reactions of GSH or GSSG (1×10^{-5} M) with $[Ru(bipy)_3]^{3+}$ (Reagent C; 1×10^{-3} M), generated using FIA.

Previous research has shown that chemiluminescence emission upon reaction of $Ru(bipy)_3^{3+}$ with secondary amines is largely dependent on pH, with alkaline conditions resulting in optimum responses [139, 140, 239, 240]. Therefore, the ability of GSH and GSSG to provide analytically useful signals upon reaction with $[Ru(bipy)_3]^{3+}$ was re-examined between the pH range 5 – 9.5. Using a three-line FIA manifold, standard solutions (1×10^{-5} M) of the analytes were once again injected into a stream of aqueous formic acid (pH 2.5; 1 mL min^{-1}), but this time merged with a phosphate buffer (40 mM; 1 mL min^{-1}) at a T-piece located 15 cm prior to the entrance of the flow-through chemiluminometer and then combined with a line of Reagent C (1×10^{-3} M; 2 mL min^{-1}) immediately before entering the detection cell. In accordance with other reports [133, 136, 239, 240], the background signal significantly increased as the chemical environment became more alkaline. In spite of this, the best chemiluminescence response for both GSH and GSSG was recorded at pH 8. However, under these conditions the signal for GSH was 8-fold smaller than that obtained for GSSG.

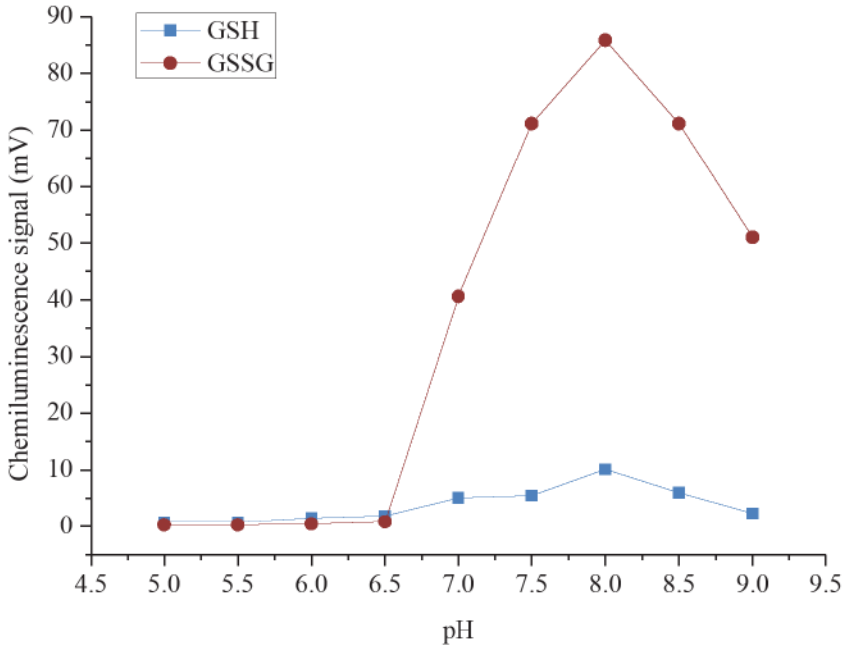

Figure 40. The effect of pH on the $[Ru(bipy)_3]^{3+}$ chemiluminescence signal of GSH and GSSG generated using FIA.

Employing the same chromatographic conditions described in chapter 4, HPLC with post-column $[Ru(bipy)_3]^{3+}$ chemiluminescence was then explored for the separation and detection of GSH and GSSG. Since alkaline conditions were found to afford analytically useful signals for both of these analytes, the HPLC eluate was merged with a phosphate buffer (40 mM; pH 8; 1 mL min^{-1}) 15 cm prior to entering a flow-through chemiluminometer and combining with a line of Reagent C (1×10^{-3} M; 2 mL min^{-1}). Although the chromatographic conditions employed provided adequate baseline separation of both analytes within 14 min, they resulted in a significantly broad GSSG peak that eluted between 8-12 min (Figure 41). The relative size of each signal obtained was reflective of the results displayed in Figure 40, where GSSG exhibited a peak 10-fold larger in area than that of GSH at the same concentration (5×10^{-5} M).

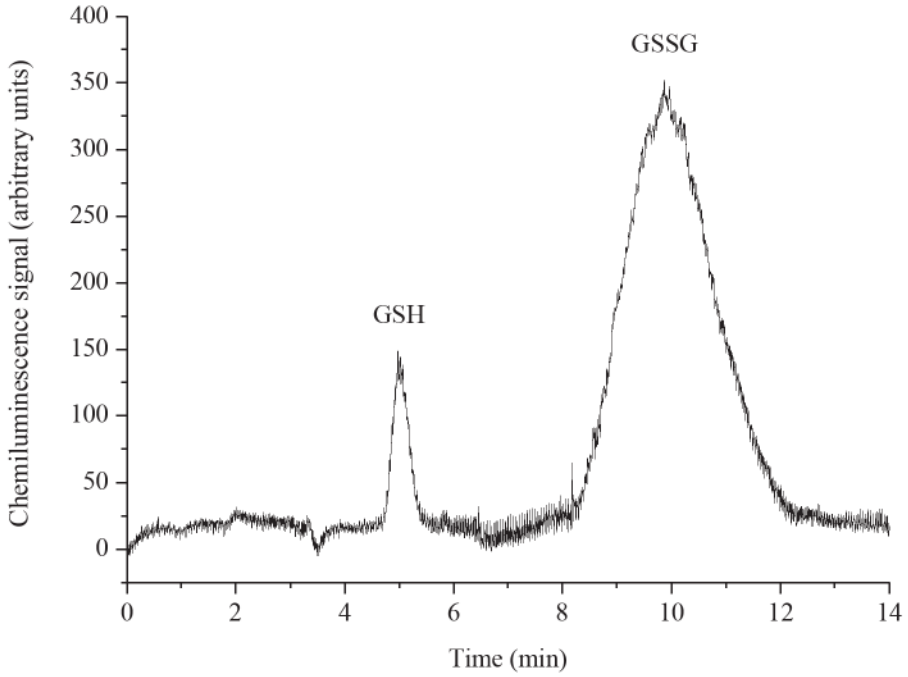

Figure 41. Typical $[Ru(bipy)_3]^{3+}$ chemiluminescence trace from the analysis of a mixture containing GSH (5×10^{-5} M) and GSSG (5×10^{-5} M). Detailed chromatographic conditions are described in the experimental section.

Using HPLC $[Ru(bipy)_3]^{3+}$ chemiluminescence detection analytical figures of merit were obtained for both GSH and GSSG (Table 10). Highly linear calibration plots were obtained for GSH and GSSG along with reasonable precision. However, limits of detection for GSH and GSSG were poor in comparison to those achieved using the chemiluminescence approach described in chapter 4 and reported values obtained using other techniques i.e. derivatisation [33, 41-48]. This was attributed to the alkaline post-column reaction environment necessary for GSSG detection. Under these conditions a large background response was observed (see Figure 41), owing to the reaction of $[Ru(bipy)_3]^{3+}$ with hydroxide ions [138]. Although there are very few methodologies capable of directly detecting both GSH and GSSG within one chromatographic run, the sensitivity achieved using $[Ru(bipy)_3]^{3+}$ chemiluminescence was insufficient for measurement of these analytes in physiological fluids as they can be present in only nM to μM concentrations.

Table 10. Analytical figures of merit.

	GSH	**GSSG**
Calibration function	$y = 8.2\times10^{9}x-168$	$y = 4.1\times10^{9}x -3297$
R^2	0.9998	0.9989
Linear range	7×10^{-6} M to 1×10^{-4} M	1×10^{-6} M to 1×10^{-5} M
Limit of detection	7×10^{-6} M	1×10^{-6} M
Precision (%RSD)*	5.2	3.1

*Concentration of 5×10^{-5} M (n = 6).

4. Conclusion

Two new $[Ru(bipy)_3]^{3+}$ reagents (C and D) for chemiluminescence detection were prepared by dissolving either $[Ru(bipy)_3](ClO4)_2$ in acetonitrile (containing 0.05 M $HClO_4$) or $[Ru(bipy)_3]Cl_2.6H_2O$ in 95:5 glacial acetic acid:acetic anhydride (containing 0.05 M H_2SO_4), followed by oxidation with PbO_2. Unlike the conventional aqueous reagent, the new reagents were exceedingly stable, and allowed extended periods of analysis without the need for constant re-calibration or preparation of fresh reagent, thus overcoming a significant limitation of $[Ru(bipy)_3]^{3+}$ chemiluminescence detection. Reagent D, however, produced lower signal intensities than the other reagents, presumably due to its high acid content. Of all reagents, C was found to be most suitable for HPLC with post-column chemiluminescence detection. Its preparation is more convenient, safe and reproducible than the previously described acetonitrile $[Ru(bipy)_3]^{3+}$ reagent B. Furthermore, it is far less susceptible to degradation due to organic impurities or traces of water in the reagent solution. Reagent C was explored for the direct chemiluminescence detection of GSH and GSSG. Preliminary FIA based experiments revealed that alkaline reaction conditions were necessary to evoke an analytically useful response with these analytes. However, this translated to unworkable limits of detection for GSH and GSSG when using post-column chemiluminescence detection. Some of the work presented in this chapter has been recently accepted for publication [249].

CHAPTER SIX

Detection of biologically significant thiols and disulfides using high performance liquid chromatography with post-column manganese(IV) chemiluminescence

- **Introduction**
- **Experimental**
- **Results and discussion**
- **Conclusion**

1. Introduction

Over the past two decades there has been a growing interest in the quantification of low-molecular-mass thiols and disulfides as researchers gain new insight into their role in significant cellular processes [14, 32-35, 55-58]. From the numerous methods previously developed for the detection of thiols and disulfides, several key analytical challenges have emerged [33, 41-45, 47, 48, 56, 57, 60]. Most commonly used modes of detection require analyte derivatisation, which is time consuming and can add a significant degree of error [33, 41-45, 47, 48, 56, 57, 60]. Furthermore, the determination of disulfides requires a reduction step before subjecting the sample to the same derivatisation, separation and detection processes used for the free thiols [33, 41-45, 47, 48, 56, 57, 60]. The disulfide concentration is then calculated from the difference between the measurements obtained in the two separate analytical steps. Disulfides are normally present in the sample at much lower concentrations than thiols, and even a small degree of auto-oxidation during these extensive sample preparation procedures leads to their considerable overestimation [33, 41-45, 47, 48, 56, 57]. Therefore, measurements of biologically significant thiols and disulfides should ideally combine minimal sample handling (under conditions that prevent auto-oxidation) with direct detection of all target analytes in a single chromatographic separation. Direct detection of thiols and disulfides has previously been achieved with electrochemistry, mass spectrometry or fluorescence quenching [42, 43, 46, 48, 56, 57, 60, 61], and whilst these modes of detection offer advantages over more popular derivatisation techniques in terms of procedural simplicity, their application is limited by equipment complexity, cost, electrode stability and/or analysis time [42, 44, 60, 61].

Several procedures coupling a separation with chemiluminescence detection have been developed for the direct determination of thiols [219, 222]. Li *et al.* [219] exploited the chemiluminescence oxidation of thiols with cerium(IV) (sensitised by Rhodamine B) to detect GSH and cysteine after reversed-phase chromatographic separation, but the two analyte peaks were barely resolved. Zhao *et al.* [222] described the use of microchip electrophoresis and luminol chemiluminescence to determine GSH, cysteine and haemoglobin in red blood cells. Chapter 4 details the use of HPLC with acidic potassium permanganate chemiluminescence for direct detection of GSH. However, like the aforementioned chemiluminescence-based detection systems for thiols [219, 222], the reagent was not suitable to detect disulfides in biological systems, and therefore the quantification of GSSG required thiol blocking and disulfide bond reduction steps prior to a second chromatographic run. Building on this approach, the method described in chapter 5 employed HPLC with post-column $[Ru(bipy)_3]^{3+}$ chemiluminescence for the direct detection of both a thiol (GSH) and disulfide (GSSG) species. However, alkaline reaction conditions were required, which had a detrimental effect on background signal resulting in poor limits of detection for the analytes investigated.

Soluble manganese(IV) is a relatively new chemiluminescence reagent [143, 144]. It is typically prepared by reducing potassium permanganate with sodium formate to furnish solid manganese dioxide which can then be dissolved in 3 M orthophosphoric acid [143, 144]. Manganese(IV) has been shown to display significantly different relationship between analyte structure and chemiluminescence intensity in comparison to what has previously been reported with either acidic potassium permanganate or $[Ru(bipy)_3]^{3+}$ [143-145]. For example, opiate alkaloids that do not possess phenolic functionality such as codeine, papaverine and thebaine, evoke far greater response with $[Ru(bipy)_3]^{3+}$ [133, 136, 250]. In contrast, using potassium

permanganate, an intense emission is elicited by the phenolic alkaloids morphine, pseudomorphine and oripavine [113, 119, 250]. However, studies have shown that manganese(IV) reacts with all of the aforementioned opiate alkaloids (morphine, pseudomorphine, codeine, oripavine, thebaine and papaverine) to provide analytically useful chemiluminescence signals [143-145]. Therefore, this chapter describes the use of a manganese(IV) reagent for the direct detection of biologically significant thiols and disulfides (Figure 42) in a single analysis following separation using HPLC. This approach was applied to the determination of GSH and GSSG in whole blood.

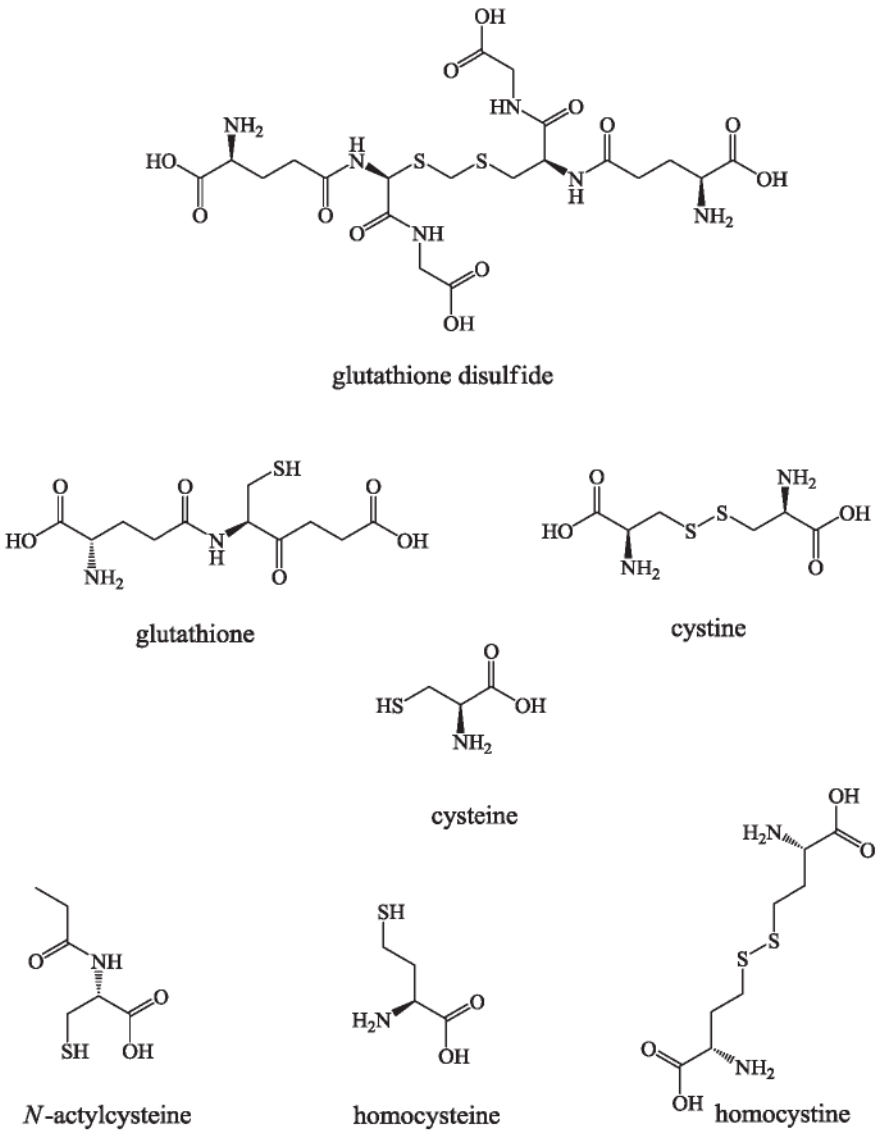

Figure 42. Structures of biologically significant thiols and disulfides.

2. Experimental

2.1 Chemicals and reagents

Deionised water (Continental Water Systems, Victoria, Australia) and analytical grade reagents were used unless otherwise stated. Chemicals were obtained from the following sources: N-acetylcysteine, L-cysteine, L-cystine L-cysteinylglycine, *N*-ethylmaleimide, γ-glutamyl-cysteine, L-glutathione, L-glutathione disulfide, homocysteine, homocystine, L-methionine, sodium polyphosphate (+80 mesh) trichloroacetic acid, trifluoroacetic acid and tris(2-carboxyethyl)phosphine hydrochloride from Sigma-Aldrich (New South Wales, Australia); sodium chloride, potassium permanganate and formaldehyde (37%) from Chem-Supply (South Australia, Australia); sodium formate from BDH (Poole, England); ethylenediaminetetraacetic acid, analytical grade methanol, sulfuric acid and tris(hydroxymethyl)methylamine from Merck (Victoria, Australia); formic acid from Hopkin and Williams (Essex, England); perchloric acid (70% w/v) from Univar (New South Wales, Australia); aqueous soluble starch from Ajax Finechem (New South Wales, Australia); and potassium iodide from Fisons Scientific Equipment (Loughborough, England).

Stock solutions (1×10^{-3} M) of *N*-acetylcysteine, cysteine, cystine, cysteinylglycine, γ-glutamyl-cysteine, GSH, GSSG, homocysteine, homocystine and methionine were prepared daily in deionized water that had been adjusted to pH 2.57 with trifluoroacetic acid, and diluted into the mobile phase (98% Solvent A: deionized water adjusted to pH 2.57 with trifluoroacetic acid; 2% Solvent B: methanol) as required. Formaldehyde was filtered and diluted to the required concentration with deionised water.

Soluble manganese(IV) was prepared as previously described [145], based on the method of Jáky and Zrinyi [147]. Briefly, this involved the reduction of potassium permanganate using excess sodium formate to yield the characteristic dark brown manganese dioxide precipitate which was collected by vacuum filtration (GF/A Whatman, England). After rinsing with deionised water, the freshly precipitated wet manganese dioxide (1.2 g) was added to 1 L of orthophosphoric acid (3 M) and ultrasonicated for 30 min. The colloid was then heated for 1 h (80° C) with stirring, and then cooled to room temperature. The concentration was determined by iodometric titration as described by Vogel [251]. The stock manganese(IV) reagent was diluted daily to the required concentration (5×10^{-4} M) using orthophosphoric acid (3 M). The acidic potassium permanganate reagent (2.5×10^{-4} M) was prepared by dissolution of potassium permanganate in a 1% (m/v) sodium polyphosphate solution and adjusted to pH 3 with sulfuric acid.

2.2 Flow injection analysis

The instrument was constructed from a Gilson Minipuls 3 peristaltic pump (John Morris Scientific, New South Wales, Australia) with bridged PVC pump tubing (1.02 mm i.d., DKSH, Queensland, Australia), a 6-port injection valve (Vici 04W-0192L, Valco Instruments, Texas, USA) and GloCel chemiluminescence detector (Global FIA, Washington, USA) with a dual-inlet serpentine flow-cell [242] and extended range photomultiplier module (Electron Tubes model P30A-05, ETP, New South Wales, Australia). All tubing entering and exiting the detector was black PTFE (0.76 mm i.d., Global FIA). The output signal obtained from the photomultiplier module was recorded using 'e-corder 410' data acquisition (eDAQ, New South Wales, Australia).

2.3 Chemiluminescence spectra

A Cary Eclipse fluorescence spectrophotometer (Varian, Mulgrave, Victoria, Australia) with R928 photomultiplier tube (Hamamatsu, Japan) was operated in Bio/Chemiluminescence mode. A three-line continuous flow manifold was used to merge the GSH or GSSG solution (1×10^{-4} M; 1 mL min^{-1}) with formaldehyde (2 M; 1 mL min^{-1}), and then with the manganese(IV) reagent (5×10^{-4} M in 3 M orthophosphoric acid; 1 mL min^{-1}), and propel the reacting mixture through a coiled PTFE flow-cell (200 µL, 0.8 mm i.d.) that was mounted against the emission window of the spectrophotometer. Final spectra were an average of 20 scans (1000 ms gate time, 1 nm data interval, 20 nm band pass, PMT voltage of 800 V) and corrected as previously described [252].

2.4 High performance liquid chromatography

Chromatographic analysis was carried out on an Agilent Technologies 1200 series liquid chromatography system, equipped with a quaternary pump, solvent degasser system and autosampler (Agilent Technologies, Forest Hill, Victoria, Australia), using an Alltech Alltima C18 column (250 mm × 4.6 mm i.d., 5 µm) at room temperature, with an injection volume of 100 µL and a flow rate of 1 mL min^{-1}. Isocratic elution was performed with 98% Solvent A: deionized water adjusted to pH 2.57 with trifluoroacetic acid and 2% Solvent B: methanol. A Hewlett-Packard analogue to digital interface box (Agilent Technologies) was used to convert the signal from the chemiluminescence detector. Before use in the HPLC system, all sample solutions and solvents were filtered through a 0.45 µm nylon membrane.

For manganese(IV) chemiluminescence measurements, the column eluate and a formaldehyde carrier (2 M) were merged at a T-piece located 22 cm from the entrance of the detector. This stream was then combined with the manganese(IV)

reagent (5×10^{-4} M in 3 M orthophosphoric acid) in the detector employed for flow injection analysis as described above. A peristaltic pump was used to deliver the formaldehyde solution and manganese(IV) reagent at a flow rate of 1 mL min^{-1} per line (Figure 43). For acidic potassium permanganate chemiluminescence measurements, the column eluate and reagent (propelled at a flow rate of 2.5 mL min^{-1} using a peristaltic pump) merged at a T-piece and the light emitted from the reacting mixture was detected with a custom built flow-through luminometer as previously described in chapter 4.

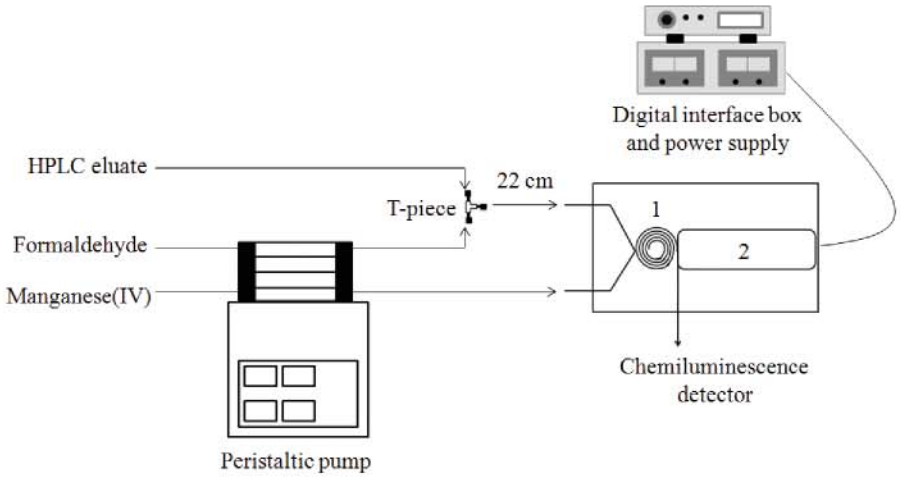

Figure 43. Instrument setup for HPLC with post-column manganese(IV) chemiluminescence detection. 1: GloCel detector with dual-inlet serpentine flow-cell; 2: PMT.

2.5 Sample collection and analysis

The method of Stempak *et al.* [253] was followed when collecting and processing blood samples. Venous blood samples (5 mL) were drawn from twelve healthy, non-fasting adult volunteers into ethylenediaminetetraacetic acid (EDTA) lined blood tubes (Becton and Dixon, UK) and immediately placed on ice. Aliquots (500 µL) of ice-cold perchloric acid (15% v/v containing 2 mM EDTA) were pipetted into 1.5 mL eppendorf tubes, followed by 500 µL of whole blood. The samples were then vortexed and incubated on ice for 10 minutes to completely precipitate blood

proteins. The acidic suspensions were then centrifuged at 13000 rpm for 15 min at 4° C, and immediately analysed or stored at -80° C. For analysis, 10 µL of the acidic supernatant was mixed with 990 µL of mobile phase (98% Solvent A: deionized water adjusted to pH 2.57 with trifluoroacetic acid; 2% Solvent B: methanol), vortexed and filtered with a 0.2 µM cellulose acetate filter, before injection onto the HPLC column.

3. Results and discussion

3.1 Preliminary chemiluminescence investigations

As outlined in the review by Brown *et al.* [143] only a small number of analytical applications of manganese(IV) chemiluminescence have been reported to date. Of these, only one manuscript describes the use of manganese(IV) for post-column chemiluminescence detection, where a mixture of six opiate alkaloid standards were determined following HPLC separation with a monolithic column [145]. Owing to the limited number of studies, little is known regarding the relationship between analyte structure and the chemiluminescence response with this reagent [143]. Moreover, there have been no published reports of manganese(IV) chemiluminescence emission upon reaction with thiols or disulfides.

The thiols cysteine and GSH along with their disulfides cystine and GSSG were initially screened with manganese(IV) using a three-line flow injection analysis (FIA) manifold, which provided similar conditions to HPLC, but without the relatively time-consuming separation. The analytes (1×10^{-5} M) were each injected (70 μL) into a 100% aqueous carrier stream (simulating a HPLC eluate; 3.5 mL min^{-1}) that merged with a flowing stream of 1 M formaldehyde (used as an enhancer to significantly improve the emission intensity [143]; 3.5 mL min^{-1}) at a T-piece located 22 cm prior to the flow-through detector inlet. The manganese(IV) reagent (3.5 mL min^{-1}) was pumped into the second inlet and merged with the analyte/formaldehyde solution within the serpentine reaction channel [242] of the detector. Strong signals were recorded for thiols (cysteine and GSH) as well as disulfides (cystine and GSSG). Therefore, conditions known to affect manganese(IV) chemiluminescence [143] were optimised. Using the aforementioned analytes, a series of univariate searches were performed on flow rate and the concentration of

formaldehyde. A 2 M formaldehyde solution and flow rates of 1 mL min^{-1} per line were found to afford the greatest chemiluminescence response and were used for all further experiments. Using the optimised parameters, a wider range of biologically important thiols and disulfides (cystine, cysteine, homocystine, homocysteine, GSH, GSSG, *N*-acetylcysteine, cysteinylglycine, γ-glutamyl-cysteine, and methionine) were screened with the manganese(IV) reagent. As shown in Figure 44, all analytes elicited a response, demonstrating the potential of manganese(IV) chemiluminescence for the detection of both thiols and disulfides.

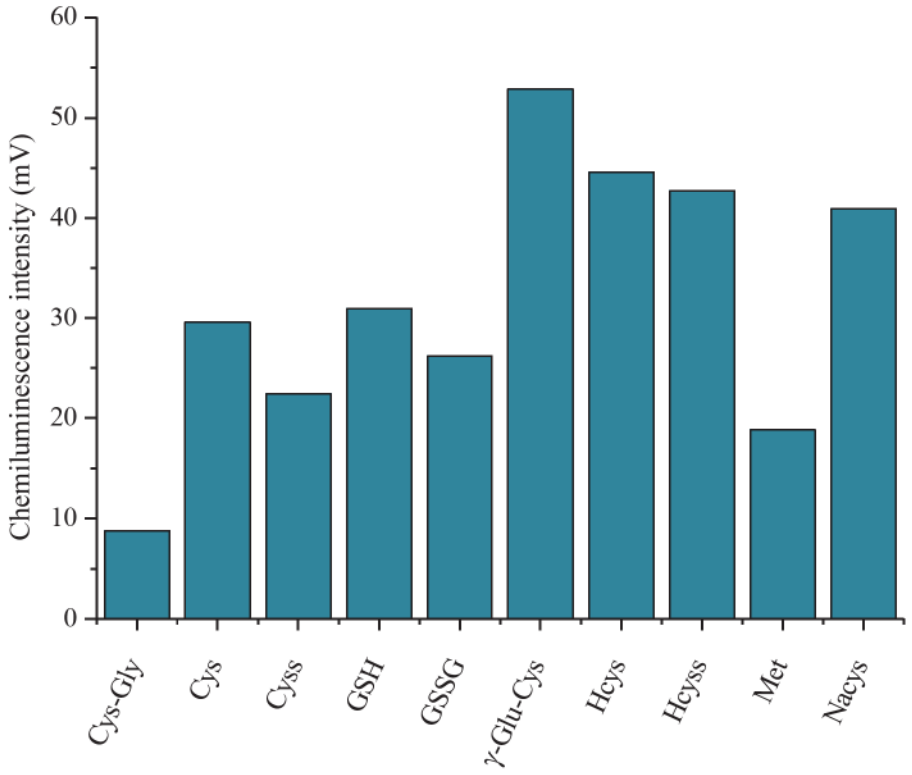

Figure 44. Chemiluminescence signal (peak height) for reactions between various thiols and disulfides (5×10^{-6} M) and manganese(IV) using flow injection analysis methodology (See experimental for conditions). Analytes: cysteinylglycine (Cys-Gly), cystine (Cyss), cysteine (Cys), glutathione (GSH), glutathione disulfide (GSSG), γ-glutamylcysteine (γ-Glu-Cys), homocysteine (Hcys), homocystine (Hcyss), methionine (Met) and *N*-acetylcysteine (Nacys).

Chemiluminescence emission spectra (corrected for the detector response and monochromator transmission [252]) for the oxidation of a thiol (GSH) and a

disulfide (GSSG) were collected (Figure 45). Both spectra contained a single broad band with a maximum at 734 ± 5 nm, which matched the characteristic emission observed from other reactions with manganese-based reagents, attributed to an electronically excited manganese(II) species [113, 120, 121, 143-145, 151].

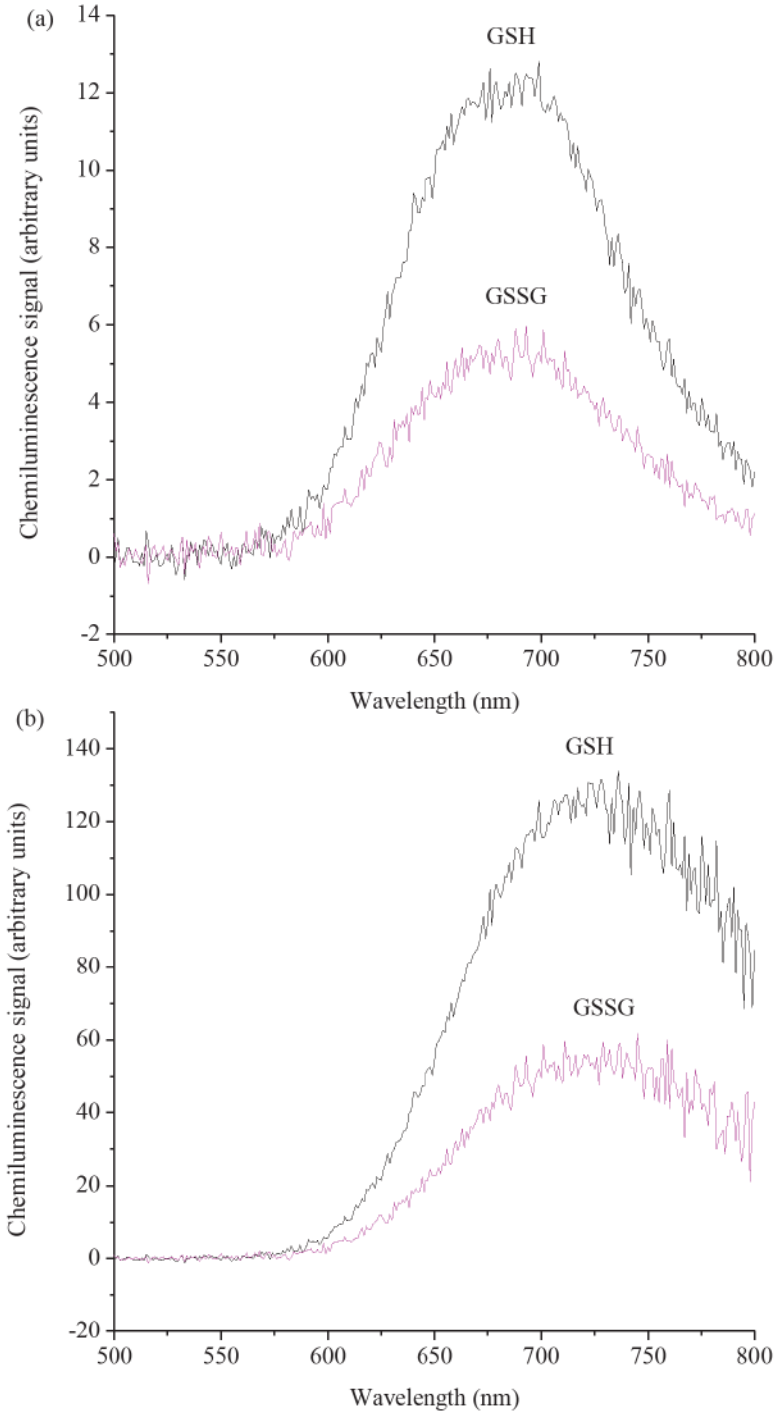

Figure 45. (a) Uncorrected and (b) corrected chemiluminescence spectra for the reactions between manganese(IV) (5×10^{-4} M) and glutathione (GSH, 1×10^{-4} M) or glutathione disulfide (GSSG, 1×10^{-4} M), using formaldehyde (2 M) as an enhancer.

3.2 Separation conditions and analytical figures of merit

As the vast majority of techniques for the detection of biological thiols and disulfides employ pre-column derivatisation, very few involve separation of these molecules in their native forms [33, 41, 44-48, 55-57]. However, from these accounts, satisfactory separation has been achieved using reverse phase HPLC with an almost 100% aqueous isocratic solvent system. A mobile phase consisting of 98% aqueous trifluoroacetic acid (pH 2.57) and 2% methanol was examined for the separation of a mixture containing seven routinely measured thiols and disulfides. These conditions were found to provide a resolution of 1.3 between cysteine and cystine and baseline separation for all other analytes within 20 min (Figure 46a). Furthermore, to highlight the advantage of this procedure in comparison to that reported in chapter 4, the same mixture was subjected to an identical separation but detected using acidic potassium permanganate (Figure 46b). As can be seen in Figure 46, both reagents can be used to detect thiols, but the markedly different selectivity of manganese(IV) also allows for the direct detection of disulfides as well.

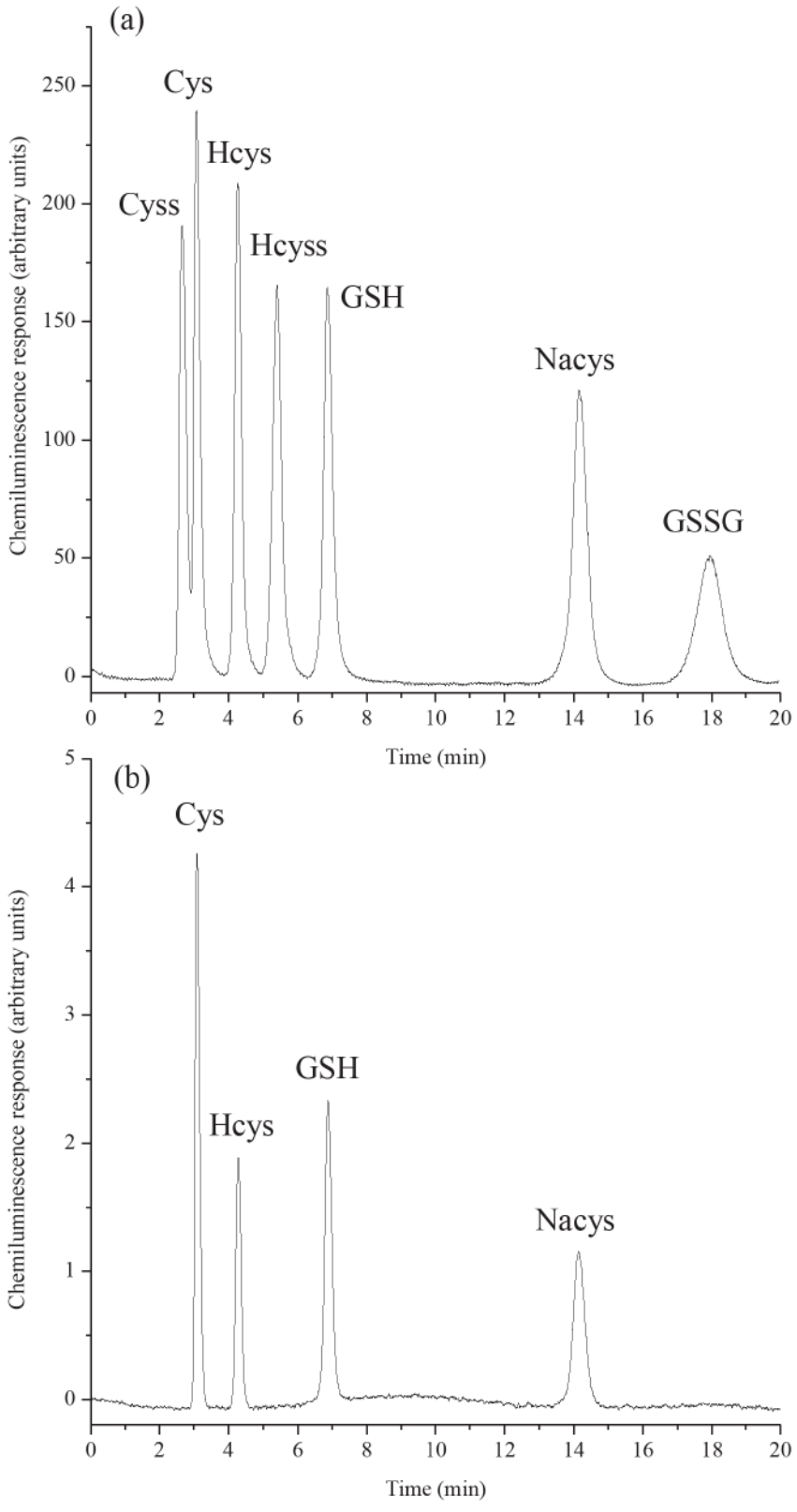

Figure 46. Separation of a mixture containing thiols and disulfides (1×10^{-5} M) using either (a) manganese(IV) or (b) acidic potassium permanganate chemiluminescence detection. Separation and post-column chemiluminescence conditions are described in the Experimental section. Peaks: cystine (Cyss), cysteine (Cys), homocysteine (Hcys), homocystine (Hcyss), glutathione (GSH), *N*-acetylcysteine (Nacys), and glutathione disulfide (GSSG).

The procedure was evaluated in terms of linearity, sensitivity and precision (Table 11). Calibration curves were constructed for each analyte using twelve standards prepared over the range of 3×10^{-8} M to 5×10^{-5} M. As can be seen from the correlation co-efficients (R^2) in Table 11, all thiols and disulfides exhibited a highly linear relationship between signal (peak area) and concentration over their respective dynamic range. The detection limits, defined as a signal-to-noise ratio of 3, were in the range of 5×10^{-8} M to 1×10^{-7} M for all analytes, which is comparable to those reported using other techniques capable of direct thiol and disulfide quantification [33, 41, 42, 44-48, 55-57]. The precision of repeated injections (n = 10) was excellent for all analytes; relative standard deviations were less than 0.3% for retention times and less than 2% for peak areas.

Table 11. Analytical figures of merit.

Analyte	Retention		R^2	Linear range (µM)	R.S.D. (%)*	LOD (M)
	Time (min)	R.S.D. (%)*				
cystine	2.6	0.1	0.988	0.05 - 10	1.3	5×10^{-8}
cysteine	3.2	0.1	0.996	0.05 - 10	1.1	5×10^{-8}
homocysteine	4.3	0.1	0.998	0.05 - 7	0.8	5×10^{-8}
homocystine	5.5	0.2	0.998	0.05 - 7	1.4	5×10^{-8}
GSH	7.0	0.1	0.998	0.07 - 10	1.4	7×10^{-8}
N-acetylcysteine	14.1	0.1	0.999	0.07 - 10	1.1	7×10^{-8}
GSSG	18.2	0.3	0.998	0.1 - 10	2.0	1×10^{-7}

*n = 4

3.3 Determination of GSH and GSSG in whole blood

As previously noted, quantifying the molar ratio of GSH to its dimer, GSSG, is one of the most important indicators of cellular health [14, 32-35]. Although these biomarkers are ubiquitous in all human organs, it has been suggested that their concentrations in blood may reflect the redox status of other less accessible tissues and hence provide a useful indicator of a whole subject's oxidative status

[201, 209, 254, 255]. However, the sample processing required in most procedures for the determination of GSH and GSSG in blood (i.e. thiol blocking and/or derivatisation, disulfide bond reduction, sample pH neutralisation, etc.) can lead to erroneous measurements [201, 203, 204, 255]. Therefore, the use of HPLC with manganese(IV) chemiluminescence detection for the determination of GSH and GSSG in whole blood was explored, where samples were simply deproteinised, centrifuged and diluted prior to analysis.

The deproteinisation of physiological fluids prior to GSH and GSSG determination is an indispensable step [33, 41-43, 46-48]. Stempak *et al.* [253] examined a range of commonly employed acids for the deproteinisation of blood and found that combining samples (1:1) with perchloric acid (15% v/v containing 2 mM ETDA) prior to storage at -80° C afforded the greatest GSH and GSSG stability. However, Rossi *et al.* [255] noted that deproteinisation with perchloric acid or trichloroacetic acid significantly altered the GSH/GSSG ratio in blood. Therefore the methods of sample preparation described by both Stempak *et al.* [253] and Rossi *et al.* [255] were examined, using two blood samples, run in triplicate, with and without the initial introduction of *N*-ethylmaleimide (NEM), which reacts with the free thiol of GSH to prevent unwanted oxidation.

Following the deproteinisation procedure described by Rossi *et al.* [255], we divided a whole blood sample into two aliquots. The first aliquot (370 µL) was combined with a solution of 1.5 g L^{-1} EDTA and 250 mM sodium chloride (40 µL) and then trichloroacetic acid (600 g L^{-1}; 77 µL), centrifuged and diluted 38-fold into the mobile phase, immediately prior to analysis using HPLC with manganese(IV) chemiluminescence detection (Figure 47a; black trace). The second aliquot was mixed with a solution of 1.5 g L^{-1} EDTA and 0.5 M NEM (40 µL) and trichloroacetic

acid (600 g L^{-1}; 77 μL) [255], centrifuged, diluted 38-fold into the mobile phase, and analysed (Figure 47a; red trace). The disappearance of the peak at 7.0 min confirmed the complete reaction of GSH with NEM. A difference (55%-62%) in the GSSG peak (18.2 min) was observed for samples with and without NEM, suggesting that significant oxidation of GSH had occurred during the deproteinisation procedure. However, the change was much lower than that reported by Rossi *et al.* [255], possibly arising from additional error introduced during their subsequent liquid-liquid extraction, analyte derivatisation (pH 10.8, room temperature, 2 h) and re-acidification, prior to analysis.

To replicate the sample preparation conditions of Stempak *et al.* [253], we divided a whole blood sample into two aliquots, one of which was combined (1:1) with perchloric acid (15% v/v containing 2 mM EDTA), centrifuged and diluted 25-fold into the mobile phase, immediately prior to analysis (Figure 4b; black trace). The second aliquot was mixed with NEM (3.6×10^{-3} M) and a Tris-HCl buffer (0.1 M; pH 8.0) in a 2:1:1 ratio. It was demonstrated in chapter 4 (Figure 31) that under these conditions, NEM reacts immediately and completely with GSH to form a thioether derivative. This solution was then acidified by combining with an equal volume of perchloric acid (15% v/v containing 2 mM EDTA), centrifuged, and diluted 12.5-fold into the mobile phase and analysed (Figure 47b (red trace)). The disappearance of the GSH peak again confirmed complete reaction with NEM. In contrast to the results shown in Figure 47a, only a small change (less than 6%) in the peak area for GSSG was observed, indicating that this procedure does not result in significant oxidation of GSH to GSSG in whole blood samples.

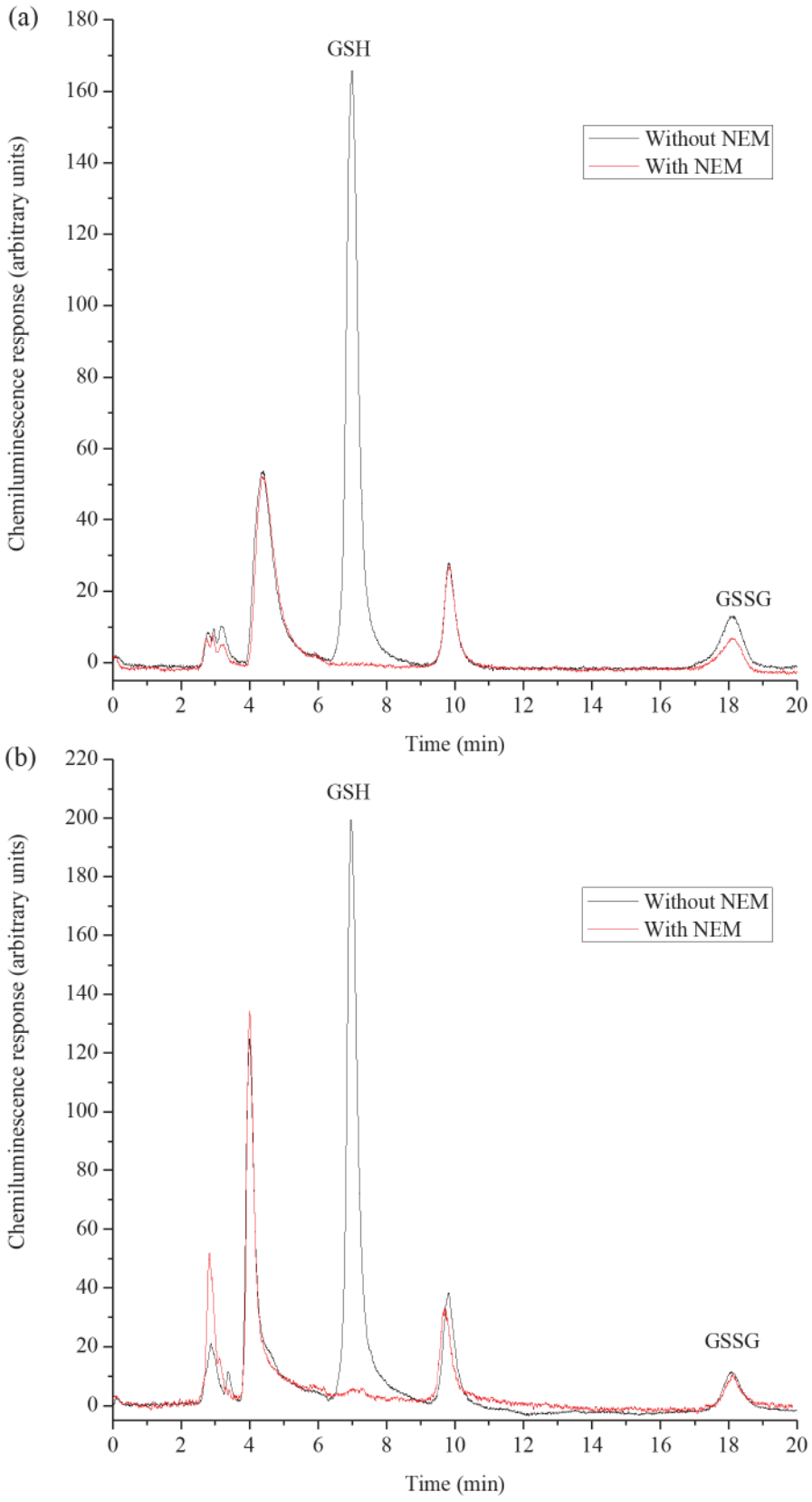

Figure 47. Typical manganese(IV) chemiluminescence chromatograms obtained for the analysis of whole blood, using the deproteinisation procedures of (a) Rossi and co-workers [255] and (b) Stempak and co-workers [253]. Red and black and traces show sample preparation with and without the addition of NEM, as described in the text. Chromatographic conditions as outlined in the Experimental section.

The method described in this chapter was used to determine GSH and GSSG in whole blood from twelve healthy volunteers (six men and six women, 21-30 years old). The results of the study are presented in Table 12, with values obtained for GSH (723–1260 μM) and GSSG (120–191 μM) within the range previously reported by other researchers for healthy subjects of similar age **(add range)**[201, 206, 254, 256-259].

Table 12. Concentrations of GSH and GSSG measured in whole blood.

Sex	Age (years)	GSH (mmol L^{-1})		GSSG (mmol L^{-1})		GSH/GSSG
		Mean	R.S.D. (%)*	Mean	R.S.D. (%)*	
M	25	0.91	5.6	0.167	1.0	5.5
M	25	0.99	3.2	0.158	2.0	6.3
F	24	0.72	2.8	0.134	4.7	5.4
F	24	1.25	1.2	0.180	3.8	6.9
F	22	0.85	2.9	0.182	4.7	4.7
M	31	1.26	1.8	0.163	1.0	7.7
M	30	1.12	4.7	0.129	1.8	8.6
F	24	1.08	5.4	0.191	2.5	5.6
F	24	0.84	3.1	0.120	7.1	7.0
F	24	0.88	4.8	0.134	3.9	6.6
M	21	1.18	2.1	0.137	3.5	8.6
M	23	0.88	3.2	0.146	3.2	6.0

*n = 3

4. Conclusions

HPLC with post-column manganese(IV) chemiluminescence provided a simple and rapid approach for the direct detection of biologically significant thiols and their disulfides. A mixture of seven thiols and disulfides (cysteine, N-acetylcysteine, homocysteine, glutathione (GSH), glutathione disulfide (GSSG), cystine and homocystine) in their native forms were separated within twenty minutes. Detection limits for these analytes ranged from 5×10^{-8} M to 1×10^{-7} M, and the precision for retention times and peak areas was excellent, with relative standard deviations of less than 0.3% and 2%, respectively. This approach was employed to determine two key biomarkers of oxidative stress, GSH and GSSG, in whole blood taken from twelve healthy volunteers. Preliminary experiments showed that deproteinisation of blood using perchloric acid (15% v/v containing 2 M EDTA) during sample preparation did not result in significant GSH oxidation. Samples were simply deproteinised, centrifuged and diluted prior to analysis. Concentrations of GSH and GSSG in the blood samples were within a comparable range to multiple other reports. The findings of this chapter resulted in a recent publication [260].

REFERENCES

1. B. Halliwell, *Plant Physiol.* **2006** 141 312.
2. M. Valko, D. Leibfritz, J. Moncol, M.T.D. Cronin, M. Mazur, and J. Telser, *Int. J. Biochem. Cell Biol.* **2007** 39 44-84.
3. B. Halliwell and J.M.C. Gutteridge, *Free radicals in biology and medicine*, Clarendon Press, Oxford, 1989.
4. R. Olinescu and T.L. Smith, *Free radicals in medicine*, Nova Science Publishers, Huntington, 2002.
5. H. Bayr, *Crit. Care Med.* **2005** 33 S498-S501.
6. M. Valko, C.J. Rhodes, J. Moncol, M. Izakovic, and M. Mazur, *Chem-Biol. Interact.* **2006** 160 1-40.
7. B.P. Yu, *Physiol. Rev.* **1994** 74 139-162.
8. E.H. Sarsour, M.G. Kumar, L. Chaudhuri, A.L. Kalen, and P.C. Goswami, *Antioxid. Redox Signal.* **2009** 11 2985-3011.
9. K. Apel and H. Hirt, *Annu. Rev. Plant Biol.* **2004** 55 373-399.
10. W. Dröge, *Physiol. Rev.* **2002** 82 47-95.
11. K.K. Griendling and D.G. Harrison, *Circ. Res.* **1999** 85 562-563.
12. J. Hancock, R. Desikan, and S. Neill, *Biochem. Soc. Trans.* **2001** 29 345-349.
13. E. Cadenas, *Biofactors* **1997** 6 391-397.
14. D. Giustarini, I. Dalle-Donne, D. Tsikas, and R. Rossi, *Crit. Rev. Clin. Lab. Sci.* **2009** 46 241-281.
15. B. Halliwell, *J. Sci. Food Agric.* **2006** 86 1992-1995.
16. H. Jaeschke, *Antioxidant Defense Mechanisms*, in *Comprehensive Toxicology*, H. Jaeschke, *Antioxidant Defense Mechanisms*, Elsevier, Oxford, 2010.

17. G. Vendemiale, I. Grattagliano, and E. Altomare, *Int. J. Clin. Lab. Res.* **1999** 29 49-55.

18. L.A. Ridnour, J.S. Isenberg, M.G. Espey, D.D. Thomas, D.D. Roberts, and D.A. Wink, *Proc. Natl. Acad. Sci. U. S. A.* **2005** 102 13147-13152.

19. P. Kovacic and J.D. Jacintho, *Curr. Med. Chem.* **2001** 8 773-796.

20. H. Sies, *Antioxidants in disease mechanisms and therapy*, Academic Press, San Diego, 1996.

21. H. Sies, *Oxidative Stress and Vascular Disease*, Kluwer Academic Publishers Group, Dordrecht, 2000.

22. P. Jenner, *Ann. Neurol.* **2003** 53 S26-S38.

23. B.S. Berlett and E.R. Stadtman, *J. Biol. Chem.* **1997** 272 20313-20316.

24. L. Flohe, W.A. Gunzler, and H.H. Schock, *FEBS Lett.* **1973** 32 132-4.

25. C. Michiels, M. Raes, O. Toussaint, and J. Remacle, *Free Radic. Biol. Med.* **1994** 17 235-248.

26. A. Wendel, *Methods Enzymol.* **1981** 77 325.

27. P. Chelikani, I. Fita, and P.C. Loewen, *Cell. Mol. Life Sci.* **2004** 61 192-208.

28. I. Fridovich, *Annu. Rev. Biochem.* **1975** 44 147-159.

29. I. Fridovich, *Annu. Rev. Biochem.* **1995** 64 97-112.

30. T. Grune, P. Schröder, and H. Biesalski, *Low Molecular Weight Antioxidants*, in *Reactions, Processes*, T. Grune, P. Schröder, and H. Biesalski, *Low Molecular Weight Antioxidants*, Springer Berlin 2005.

31. R.H. Burdon, *Free Radic. Biol. Med.* **1995** 18 775-794.

32. J.M. Estrela, A. Ortega, and E. Obrador, *Crit. Rev. Clin. Lab. Sci.* **2006** 43 143-181.

33. A. Pastore, G. Federici, E. Bertini, and F. Piemonte, *Clin. Chim. Acta* **2003** 333 19-39.

34. C. Perricone, C. De Carolis, and R. Perricone, *Autoimmun. Rev.* **2009** 8 697-701.

35. D.M. Townsend, K.D. Tew, and H. Tapiero, *Biomed. Pharmacother.* **2003** 57 145-155.

36. I.A. Cotgreave and R.G. Gerdes, *Biochem. Biophys. Res. Commun.* **1998** 242 1-9.

37. A. Meister, *J. Biol. Chem.* **1988** 263 17205-17208.

38. E. Mosharov, M.R. Cranford, and R. Banerjee, *Biochemistry* **2000** 39 13005-13011.

39. S.C. Lu, *FASEB J.* **1999** 13 1169-1183.

40. O.W. Griffith, *Free Radic. Biol. Med.* **1999** 27 922-935.

41. E. Camera and M. Picardo, *J. Chromatogr. B* **2002** 781 181-206.

42. P. Monostori, G. Wittmann, E. Karg, and S. Túri, *J. Chromatogr. B* **2009** 877 3331-3346.

43. F. Carlucci and A. Tabucchi, *J. Chromatogr. B* **2009** 877 3347-3357.

44. X. Chen, Y. Zhou, X. Peng, and J. Yoon, *Chem. Soc. Rev.* **2010** 39 2120-2135.

45. R.E. Hansen and J.R. Winther, *Anal. Biochem.* **2009** 394 147-158.

46. Y. Iwasaki, Y. Saito, Y. Nakano, K. Mochizuki, O. Sakata, R. Ito, K. Saito, and H. Nakazawa, *J. Chromatogr. B* **2009** 877 3309-3317.

47. K. Kusmierek, G. Chwatko, R. Glowacki, and E. Bald, *J. Chromatogr. B* **2009** 877 3300-3308.

48. T. Toyo'oka, *J. Chromatogr. B* **2009** 877 3318-3330.

49. D. Barford, *Curr. Opin. Struct. Biol.* **2004** 14 679-686.

50. L.K. Moran, J.M.C. Gutteridge, and G.J.Q. . *Curr. Med. Chem.* **2001** 8 763-772.

51. M.S.B. Paget and M.J. Buttner, *Annu. Rev. Genet.* **2003** 37 91-121.

52. P.G. Richman and A. Meister, *J. Biol. Chem.* **1975** 250 1422-1426.

53. J.D. Finkelstein and S.H. Mudd, *J. Biol. Chem.* **1967** 242 873-880.

54. S.H. Mudd, J.D. Finkelstein, F. Irreverre, and L. Laster, *J. Biol. Chem.* **1965** 240 4382-4392.

55. V. Ducros, K. Demuth, M.-P. Sauvant, M. Quillard, E. Caussé, M. Candito, M.-H. Read, J. Drai, I. Garcia, and M.-F. Gerhardt, *J. Chromatogr. B* **2002** 781 207-226.

56. J. Lock and J. Davis, *TrAC, Trends Anal. Chem.* **2002** 21 807-815.

57. O. Nekrassova, N.S. Lawrence, and R.G. Compton, *Talanta* **2003** 60 1085-1095.

58. J.S. Stamler and A. Slivka, *Nutr. Rev.* **1996** 54 1-30.

59. D. Toroser and R.S. Sohal, *Biochem. J.* **2007** 405 583-589.

60. P.C. White, N.S. Lawrence, J. Davis, and R.G. Compton, *Electroanalysis* **2002** 14 89-98.

61. N.S. Lawrence, J. Davis, and R.G. Compton, *Talanta* **2001** 53 1089-1094.

62. B. Frei, *Natural antioxidants in human health and disease*, Academic Press, London, 1994.

63. C.M. Andre, Y. Larondelle, and D. Evers, *Curr. Nutr. Food Sci.* **2010** 6 2-12.

64. J. Bouayed and T. Bohn, *Oxid. Med. Cell. Longev.* **2010** 3 228-237.

65. F. Shahidi, *Natural antioxidants: an overview*, AOCS press, 1997.

66. W. Willett, F. Sacks, A. Trichopoulou, G. Drescher, A. Ferro-Luzzi, E. Helsing, and D. Trichopoulos, *Am. J. Clin. Nutr.* **1995** 61 1402S-1406S.

67. J.G. Bieri and R.P. Evarts, *Am. J. Clin. Nutr.* **1974** 27 980-986.

68. J.E. Packer, T.F. Slater, and R.L. Willson, *Nature* **1979** 278 737-738.

69. R. Brigelius-Flohe and M.G. Traber, *FASEB J.* **1999** 13 1145-1155.

70. A. Meister, *J. Biol. Chem.* **1994** 269 9397-9397.

71. S.J. Padayatty, A. Katz, Y. Wang, P. Eck, O. Kwon, J.-H. Lee, S. Chen, C. Corpe, A. Dutta, S.K. Dutta, and M. Levine, *J. Am. Coll. Nutr.* **2003** 22 18-35.

72. W.C. Willett, *Science* **1994** 264 532.

73. F. Visioli and C. Galli, *Nutr. Metab. Cardiovasc. Dis.* **1995** 5 306-306.

74. K.M. Yoo, I.-K. Hwang, and B. Moon, *J. Food Sci.* **2009** 74 C419-C425.

75. R.H. Liu, *Am. J. Clin. Nutr.* **2003** 78 517S-520S.

76. N.V. Yanishlieva and E.M. Marinova, *Eur. J. Lipid Sci. Technol.* **2001** 103 752-767.

77. R. Kahl and A.G. Hildebrandt, *Food Chem. Toxicol.* **1986** 24 1007-1014.

78. J.O. Ragnarsson and T.P. Labuza, *Food Chem.* **1977** 2 291-308.

79. R. Acheson and D.R.R. Williams, *The Lancet* **1983** 321 1191-1193.

80. D. Huang, B. Ou, and R.L. Prior, *J. Agric. Food Chem.* **2005** 53 1841-1856.

81. A. Karadag, B. Ozcelik, and S. Saner, *Food Analytical Methods* **2009** 2 41-60.

82. L.M. Magalhães, M.A. Segundo, S. Reis, and J.L.F.C. Lima, *Anal. Chim. Acta* **2008** 613 1-19.

83. J.-K. Moon and T. Shibamoto, *J. Agric. Food Chem.* **2009** 57 1655-1666.

84. W. Brand-Williams, M.E. Cuvelier, and C. Berset, *Lebensmittel-Wissenschaft und Technologie/Food Science and Technology* **1995** 28 25-30.

85. C. Sánchez-Moreno, J.A. Larrauri, and F. Saura-Calixto, *J. Sci. Food Agric.* **1998** 76 270-276.

86. N. Miller, C. Rice-Evans, M. Davies, V. Gopinathan, and A. Milner, *Clin. Sci.* **1993** 84 407-412.

87. R. van den Berg, G.R.M.M. Haenen, H. van den Berg, and A. Bast, *Food Chem.* **1999** 66 511-517.

88. N.J. Miller and C.A. Rice-Evans, *Free Radic. Res.* **1997** 26 195.

89. H.A.G. Niederländer, T.A. van Beek, A. Bartasiute, and I.I. Koleva, *J. Chromatogr. A* **2008** 1210 121-134.

90. S.-Y. Shi, Y.-P. Zhang, X.-Y. Jiang, X.-Q. Chen, K.-L. Huang, and H.-H. Zhou, *TrAC Trends in Analytical Chemistry* **2009** 28 865-877.

91. K. Robards, *J. Chromatogr. A* **2003** 1000 657-691.

92. K. Hostettmann, J.L. Wolfender, and C. Terreaux, *Pharm. Biol.* **2001** 39 18-32.

93. D.J. Hook, E.J. Pack, J.J. Yacobucci, and J. Guss, *J. Biomol. Screen.* **1997** 2 145.

94. M.A. Strege, *Journal of Chromatography B: Biomedical Sciences and Applications* **1999** 725 67-78.

95. A. Dapkevicius, T.A. van Beek, H.A.G. Niederländer, and A. de Groot, *Anal. Chem.* **1998** 71 736-740.

96. A. Ogawa, H. Arai, H. Tanizawa, T. Miyahara, and T. Toyo'oka, *Anal. Chim. Acta* **1999** 383 221-230.

97. T. Toyo'oka, T. Kashiwazaki, and M. Kato, *Talanta* **2003** 60 467-475.

98. P.S. Francis, J.W. Costin, X.A. Conlan, S.A. Bellomarino, J.A. Barnett, and N.W. Barnett, *Food Chem.* **2010** 122 926-929.

99. A. Dapkevicius, T.A. van Beek, G.P. Lelyveld, A. van Veldhuizen, A. de Groot, J.P.H. Linssen, and R.P. Venskutonis, *J. Nat. Prod.* **2002** 65 892-896.

100. A. Dapkevicius, T.A. van Beek, and H.A.G. Niederländer, *J. Chromatogr. A* **2001** 912 73-82.

101. I.I. Koleva, H.A.G. Niederländer, and T.A. van Beek, *Anal. Chem.* **2000** 72 2323-2328.

102. T. Oki, M. Kobayashi, T. Nakamura, A. Okuyama, M. Masuda, H. Shiratsuchi, and I. Suda, *J. Food Sci.* **2006** 71 C18-C22.

103. M. Pérez-Bonilla, S. Salido, T.A. van Beek, P.J. Linares-Palomino, J. Altarejos, M. Nogueras, and A. Sánchez, *J. Chromatogr. A* **2006** 1112 311-318.

104. A. Pukalskas, T.A. van Beek, R.P. Venskutonis, J.P.H. Linssen, A. van Veldhuizen, and A. de Groot, *J. Agric. Food Chem.* **2002** 50 2914-2919.

105. Q. Zhang, E.J.C. van der Klift, H.-G. Janssen, and T.A. van Beek, *J. Chromatogr. A* **2009** 1216 7268-7274.

106. A.M. García-Campaña and W.R.G. Baeyens, *Chemiluminescence in analytical chemistry*, Marcel Dekker, New York, 2001.

107. F.J. Lara, A.M. García-Campaña, and A.I. Velasco, *Electrophoresis* **2010** 31 1998-2027.

108. A. García-Campaña and F. Lara, *Anal. Bioanal. Chem.* **2007** 387 165-169.

109. L. Gámiz-Gracia, A.M. García-Campaña, J.F. Huertas-Pérez, and F.J. Lara, *Anal. Chim. Acta* **2009** 640 7-28.

110. A.M. García-Campaña, F.J. Lara, L. Gámiz-Gracia, and J.F. Huertas-Pérez, *TrAC, Trends Anal. Chem.* **2009** 28 973-986.

111. F. Li, C. Zhang, X. Guo, and W. Feng, *Biomed. Chromatogr.* **2003** 17 96-105.

112. S.W. Lewis, D. Price, and P.J. Worsfold, *J. Biolumin. Chemilumin.* **1993** 8 183-199.

113. J.L. Adcock, P.S. Francis, and N.W. Barnett, *Anal. Chim. Acta* **2007** 601 36-67.

114. P.S. Francis, N.W. Barnett, S.W. Lewis, and K.F. Lim, *Luminescence* **2004** 19 94-115.

115. P. Fletcher, K.N. Andrew, A.C. Calokerinos, S. Forbes, and P.J. Worsfold, *Luminescence* **2001** 16 1-23.

116. F.J. Lara, A.M. García-Campaña, and J.-J. Aaron, *Anal. Chim. Acta* **2010** 679 17-30.

117. E.N. Harvey, *J. Biol. Chem.* **1917** 31 311-336.

118. J. Stauff and W. Jaeschke, *Atmos. Environ.* **1975** 9 1038-1039.

119. B.J. Hindson and N.W. Barnett, *Anal. Chim. Acta* **2001** 445 1-19.

120. J.L. Adcock, P.S. Francis, T.A. Smith, and N.W. Barnett, *Analyst* **2008** 133 49-51.

121. N.W. Barnett, B.J. Hindson, P. Jones, and T.A. Smith, *Anal. Chim. Acta* **2002** 451 181-188.

122. C.M. Hindson, P.S. Francis, G.R. Hanson, J.L. Adcock, and N.W. Barnett, *Anal. Chem.* **2010** 82 4174-4180.

123. E.N. Frankel and J.B. German, *J. Sci. Food Agric.* **2006** 86 1999-2001.

124. S.B. Lotito and B. Frei, *Free Radic. Biol. Med.* **2006** 41 1727-1746.

125. N. Anastos, N.W. Barnett, B.J. Hindson, C.E. Lenehan, and S.W. Lewis, *Talanta* **2004** 64 130-134.

126. J.W. Costin, N.W. Barnett, S.W. Lewis, and D.J. McGillivery, *Anal. Chim. Acta* **2003** 499 47-56.

127. B. Gómez-Taylor Corominas, M. Catalá Icardo, L. Lahuerta Zamora, J.V. García Mateo, and J. Martínez Calatayud, *Talanta* **2004** 64 618-625.

128. J.L. Adcock, N.W. Barnett, J.W. Costin, P.S. Francis, and S.W. Lewis, *Talanta* **2005** 67 585-589.

129. J.W. Costin, S.W. Lewis, S.D. Purcell, L.R. Waddell, P.S. Francis, and N.W. Barnett, *Anal. Chim. Acta* **2007** 597 19-23.

130. T. Slezak, P.S. Francis, N. Anastos, and N.W. Barnett, *Anal. Chim. Acta* **2007** 593 98-102.

131. F.H. Burstall, *J. Chem. Soc. A.* **1936** 173-175.

132. D.M. Hercules and F.E. Lytle, *J. Am. Chem. Soc.* **1966** 88 4745-4746.

133. R.D. Gerardi, N.W. Barnett, and S.W. Lewis, *Anal. Chim. Acta* **1999** 378 1-41.

134. X.-B. Yin, S. Dong, and E. Wang, *TrAC, Trends Anal. Chem.* **2004** 23 432-441.

135. M.M. Richter, *Chem. Rev.* **2004** 104 3003-3036.

136. B.A. Gorman, P.S. Francis, and N.W. Barnett, *Analyst* **2006** 131 616-639.

137. W. Miao, *Chem. Rev.* **2008** 108 2506-2553.

138. R.D. Gerardi, N.W. Barnett, and P. Jones, *Anal. Chim. Acta* **1999** 388 1-10.

139. W.A. Jackson and D.R. Bobbitt, *Anal. Chim. Acta* **1994** 285 309-320.

140. J.B. Noffsinger and N.D. Danielson, *Anal. Chem.* **1987** 59 865-868.

141. T. Pérez-Ruiz, C. Martínez-Lozano, V. Tomás, and J. Martín, *Talanta* **2002** 58 987-994.

142. C.G. Nana, W. Jian, C. Xi, D.J. Pinga, Z.Z. Feng, and C.H. Qing, *Analyst* **2000** 125 2294-2298.

143. A. Brown, P. Francis, J. Adcock, K. Lim, and N. Barnett, *Anal. Chim. Acta* **2008** 624 175-183.

144. N.W. Barnett, B.J. Hindson, S.W. Lewis, P. Jones, and P.J. Worsfold, *Analyst* **2001** 126 1636-1639.

145. A.J. Brown, C.E. Lenehan, P.S. Francis, D.E. Dunstan, and N.W. Barnett, *Talanta* **2007** 71 1951-1957.

146. M. Jáky, L.I. Simándi, and V.Y. Shafirovich, *Inorg. Chim. Acta* **1984** 90 L39-L41.

147. M. Jáky and M. Zrinyi, *Polyhedron* **1993** 12 1271-1275.

148. J.F. Perez-Benito and C. Arias, *J. Colloid Interface Sci.* **1992** 152 70-84.

149. J.F. Perez-Benito, C. Arias, and E. Amat, *J. Colloid Interface Sci.* **1996** 177 288-297.

150. J.F. Perez-Benito, E. Brillas, and R. Pouplana, *Inorg. Chem.* **1989** 28 390-392.

151. J.L. Adcock, P.S. Francis, and N.W. Barnett, *J. Fluoresc.* **2009** 19 867-874.

152. N. Fei, L. Jiuru, and N. Weifen, *Anal. Chim. Acta* **2005** 545 129-136.

153. F. Nie, J. Lu, Y. He, and J. Du, *Talanta* **2005** 66 728-733.

154. F. Nie, J. Lu, Y. He, and J. Du, *Luminescence* **2005** 20 315-320.

155. E. Nalewajko-Sieliwoniuk, I. Tarasewicz, and A. Kojło, *Anal. Chim. Acta* **2010** 668 19-25.

156. M.S. Blois, *Nature* **1958** 181 1199-1200.

157. D. Bandonienė and M. Murkovic, *J. Agric. Food Chem.* **2002** 50 2482-2487.

158. D. Bandonienė and M. Murkovic, *J. Biochem. Biophys. Methods* **2002** 53 45-49.

159. D. Bandonienė, M. Murkovic, W. Pfannhauser, P.R. Venskutonis, and D. Gruzdienė, *Eur. Food Res. Technol.* **2002** 214 143-147.

160. D. Bandonienė, M. Murkovic, and P.R. Venskutonis, *J. Chromatogr. Sci.* **2005** 43 372-376.

161. M. Koşar, H.J.D. Dorman, O. Bachmayer, K.H. Can Başer, and R. Hiltunen, *Chem. Nat. Compd.* **2003** 39 161-166.

162. M. Koşar, H.J.D. Dorman, K.H. Can Başer, and R. Hiltunen, *Chromatographia* **2004** 60 635-638.

163. M. Koşar, H.J.D. Dorman, K.H. Can Başer, and R. Hiltunen, *J. Agric. Food Chem.* **2004** 52 5004-5010.

164. N. Nuengchamnong, C.F. de Jong, B. Bruyneel, W.M.A. Niessen, H. Irth, and K. Ingkaninan, *Phytochem. Anal.* **2005** 16 422-428.

165. A. Pukalskas, T.A. van Beek, and P. de Waard, *J. Chromatogr. A* **2005** 1074 81-88.

166. V. Exarchou, Y.C. Fiamegos, T.A. van Beek, C. Nanos, and J. Vervoort, *J. Chromatogr. A* **2006** 1112 293-302.

167. A. Bartasiute, B.H.C. Westerink, E. Verpoorte, and H.A.G. Niederländer, *Free Radic. Biol. Med.* **2007** 42 413-423.

168. E.M. Gioti, Y.C. Fiamegos, D.C. Skalkos, and C.D. Stalikas, *Food Chem.* **2009** 117 398-404.

169. M. Mnatsakanyan, T.A. Goodie, X.A. Conlan, P.S. Francis, G.P. McDermott, N.W. Barnett, D. Shock, F. Gritti, G. Guiochon, and R.A. Shalliker, *Talanta* **2010** 81 837-842.

170. Y.-T. Tung, J.-H. Wu, C.-Y. Hsieh, P.-S. Chen, and S.-T. Chang, *Food Chem.* **2009** 115 1019-1024.

171. H. Wang, J.-H. Chen, H.-Q. Zhao, L.-L. Wang, Dao-Lai Zhang, X.-R. Wang, and D.-F. Yang, *Fenxi Huaxue* **2009** 37 795-800.

172. J.-H. Wu, C.-Y. Huang, Y.-T. Tung, and S.-T. Chang, *J. Agric. Food Chem.* **2007** 56 328-332.

173. N. Nuengchamnong and K. Ingkaninan, *Food Chem.* **2010** 118 147-152.

174. I.I. Koleva, H.A.G. Niederländer, and T.A. van Beek, *Anal. Chem.* **2001** 73 3373-3381.

175. B. Ozcelik, J.H. Lee, and D.B. Min, *J. Food Sci.* **2003** 68 487-490.

176. A. Soriano, P.M. Pérez-Juan, A. Vicario, J.M. González, and M.S. Pérez-Coello, *Food Chem.* **2007** 104 1295-1303.

177. G.P. McDermott, L.K. Noonan, M. Mnatsakanyan, R.A. Shalliker, X.A. Conlan, N.W. Barnett, and P.S. Francis, *Anal. Chim. Acta* **2010** 675 76-82.

178. B. Halliwell and M. Whiteman, *Br. J. Pharmacol.* **2004** 142 231-255.

179. J.F. Young, J. Hansen-Møller, and N. Oksbjerg, *J. Agric. Food Chem.* **2004** 52 7158-7163.

180. H. Wang and J.A. Joseph, *Free Radic. Biol. Med.* **1999** 27 612-616.

181. S. Dudonné, X. Vitrac, P. Coutière, M. Woillez, and J.-M. Mérillon, *J. Agric. Food Chem.* **2009** 57 1768-1774.

182. P.S. Francis and C.F. Hogan, *Advances in flow injection analysis and related techniques*, in *Comprehensive analytical chemistry*, P.S. Francis and C.F. Hogan, *Advances in flow injection analysis and related techniques*, Oxford, 2008.

183. S.-Y. Li, Y. Yu, and S.-P. Li, *J. Agric. Food Chem.* **2007** 55 3358-3362.

184. A. Cano, O. Alcaraz, M. Acosta, and M. Arnao, *Redox Rep.* **2002** 7 103-109.

185. A. Stalmach, W. Mullen, C. Nagai, and A. Crozier, *Braz. J. Plant Physiol.* **2006** 18 253-262.

186. A.J. Stewart, W. Mullen, and A. Crozier, *Mol. Nutr. Food Res.* **2005** 49 52-60.

187. G. Guiochon, *J. Chromatogr. A* **2007** 1168 101-168.

188. G.P. McDermott, X.A. Conlan, L.K. Noonan, J.W. Costin, M. Mnatsakanyan, R.A. Shalliker, N.W. Barnett, and P.S. Francis, *Anal. Chim. Acta* **2011** 684 134-141.

189. X.A. Conlan, N. Stupka, G.P. McDermott, N.W. Barnett, and P.S. Francis, *Anal. Methods* **2010** 2 171-173.

190. M. Mnatsakanyan, P.G. Stevenson, X.A. Conlan, P.S. Francis, T.A. Goodie, G.P. McDermott, N.W. Barnett, and R.A. Shalliker, *Talanta* **2010** 82 1358-1363.

191. F.G. Hopkins, *J. Biol. Chem.* **1927** 72 185-187.

192. F.G. Hopkins, *J. Biol. Chem.* **1922** 54 527-563.

193. F.G. Hopkins, *J. Biol. Chem.* **1929** 84 269-320.

194. D. Grill and M. Tausz, *Significance of glutathione to plant adaptation to the environment*, Springer, Dordrecht, 2001.

195. R. Masella and G. Mazza, *Glutathione and sulfur amino acids in human health and disease*, Wiley, New York, 2009.

196. I.K. Abukhalaf, N.A. Silvestrov, J.M. Menter, D.A. von Deutsch, M.A. Bayorh, R.R. Socci, and A.A. Ganafa, *J. Pharm. Biomed. Anal.* **2002** 28 637-643.

197. A.R.T.S. Araujo, M.L.M.F.S. Saraiva, and J.L.F.C. Lima, *Talanta* **2008** 74 1511-1519.

198. M. Asensi, J. Sastre, F.V. Pallardo, J.G. Delaasuncion, J.M. Estrela, and J. Vina, *Anal. Biochem.* **1994** 217 323-328.

199. E. Camera, M. Rinaldi, S. Briganti, M. Picardo, and S. Fanali, *J. Chromatogr. B* **2001** 757 69-78.

200. M. Floreani, M. Petrone, P. Debetto, and P. Palatini, *Free Radic. Res.* **1997** 26 449-455.

201. D. Giustarini, I. Dalle-Donne, R. Colombo, A. Milzani, and R. Rossi, *Free Radic. Biol. Med.* **2003** 35 1365-1372.

202. R. Glowacki and E. Bald, *J. Chromatogr. B* **2009** 877 3400-3404.

203. X. Guan, B. Hoffman, C. Dwivedi, and D.P. Matthees, *J. Pharm. Biomed. Anal.* **2003** 31 251-261.

204. D.P. Jones, J.L. Carlson, P.S. Samiec, P. Sternberg, V.C. Mody, R.L. Reed, and L.A.S. Brown, *Clin. Chim. Acta* **1998** 275 175-184.

205. X.-F. Guo, H. Wang, Y.-H. Guo, Z.-X. Zhang, and H.-S. Zhang, *J. Chromatogr. A* **2009** 1216 3874-3880.

206. R. Kand'ár, P. Záková, H. Lotková, O. Kucera, and Z. Cervinková, *J. Pharm. Biomed. Anal.* **2007** 43 1382-1387.

207. Y. Rao, B. Xiang, E. Bramanti, A. D'Ulivo, and Z. Mester, *J. Agric. Food Chem.* **2010** 58 1462-1468.

208. J.M. Rosenfeld, *TrAC, Trends Anal. Chem.* **2003** 22 785-798.

209. R. Rossi, A. Milzani, I. Dalle-Donne, D. Giustarini, L. Lusini, R. Colombo, and P. Di Simplicio, *Clin. Chem.* **2002** 48 742-753.

210. A.K. Sakhi, K.M. Russnes, S. Smeland, R. Blomhoff, and T.E. Gundersen, *J. Chromatogr. A* **2006** 1104 179-189.

211. F. Zhang, M.J. Bartels, D.R. Geter, Y.-C. Jeong, M.R. Schisler, A.J. Wood, L. Kan, and B.B. Gollapudi, *Rapid Commun. Mass Spectrom.* **2008** 22 3608-3614.

212. S. Pelletier and C.A. Lucy, *Analyst* **2004** 129 710-713.

213. O. Yilmaz, S. Keser, M. Tuzcu, M. Guvenc, B. Cetintas, S. Irtegun, H. Tastan, and K. Sahin, *J. Anim. Vet. Adv.* **2009** 8 343-347.

214. L.A. Allison and R.E. Shoup, *Anal. Chem.* **1983** 55 8-12.

215. J. Du, Y. Li, and J. Lu, *Anal. Chim. Acta* **2001** 448 79-83.

216. A.A. Ensafi, T. Khayamian, and F. Hasanpour, *J. Pharm. Biomed. Anal.* **2008** 48 140-144.

217. H.-Y. Han, Z.-K. He, and Y.-E. Zeng, *Microchim. Acta* **2006** 155 431-434.

218. W.L. Hinze, T.E. Reihl, H.N. Singh, and Y. Baba, *Anal. Chem.* **1984** 56 2180-2191.

219. H.-n. Li, Y.-x. Cl, and L. Huang, *Anal. Sci.* **1997** 13 821-824.

220. Y. Li, A. Zhang, J. Du, and J. Lu, *Anal. Lett.* **2003** 36 871-879.

221. L. Wang, Y. Li, D. Zhao, and C. Zhu, *Microchim. Acta* **2003** 141 41-45.

222. S. Zhao, Y. Huang, F. Ye, M. Shi, and Y.-M. Liu, *J. Chromatogr. A* **2010** 1217 5732-5736.

223. S. Wang, H. Ma, J. Li, X. Chen, Z. Bao, and S. Sun, *Talanta* **2006** 70 518-521.

224. S.B. Bankar, M.V. Bule, R.S. Singhal, and L. Ananthanarayan, *Biotechnol. Adv.* **2009** 27 489-501.

225. J.C. Lee, Y.O. Son, K.C. Choi, and Y.S. Jang, *Mol. Cells* **2006** 22 21-9.

226. J.-L. Luo, F. Hammarqvist, I.A. Cotgreave, C. Lind, K. Andersson, and J. Wernerman, *J. Chromatogr. B* **1995** 670 29-36.

227. J.A. Burns, J.C. Butler, J. Moran, and G.M. Whitesides, *J. Org. Chem.* **1991** 56 2648-2650.

228. E.B. Getz, M. Xiao, T. Chakrabarty, R. Cooke, and P.R. Selvin, *Anal. Biochem.* **1999** 273 73-80.

229. J.C. Han and G.Y. Han, *Anal. Biochem.* **1994** 220 5-10.

230. P. Husek, P. Matucha, A. Vránková, and P. Simek, *J. Chromatogr. B* **2003** 789 311-322.

231. J. Krijt, M. Vackova, and V. Kozich, *Clin. Chem.* **2001** 47 1821-1828.

232. P. Sevcíková, Z. Glatz, and J. Tomandl, *J. Chromatogr. A* **2003** 990 197-204.

233. J. Podlaha and H. Podlahová, *Collect. Czech. Chem. Commun.* **1973** 38 1730-1736.

234. H. Østergaard, C. Tachibana, and J.R. Winther, *J. Cell Biol.* **2004** 166 337.

235. G.P. McDermott, P.S. Francis, K.J. Holt, K.L. Scott, S.D. Martin, N. Stupka, N.W. Barnett, and X.A. Conlan, *Analyst* **2011**

236. M.M. Cooke, E.H. Doeven, C.F. Hogan, J.L. Adcock, G.P. McDermott, X.A. Conlan, N.W. Barnett, F.M. Pfeffer, and P.S. Francis, *Anal. Chim. Acta* **2009** 635 94-101.

237. Y. Zu and A.J. Bard, *Anal. Chem.* **2000** 72 3223-3232.

238. B.A. Gorman, K.F. Lim, C.F. Hogan, and N.W. Barnett, *Talanta* **2007** 72 568-574.

239. J.L. Adcock, N.W. Barnett, R.D. Gerardi, C.E. Lenehan, and S.W. Lewis, *Talanta* **2004** 64 534-537.

240. J.W. Costin, P.S. Francis, and S.W. Lewis, *Anal. Chim. Acta* **2003** 480 67-77.

241. N.W. Barnett, B.J. Hindson, S.W. Lewis, S.D. Purcell, and P. Jones, *Anal. Chim. Acta* **2000** 421 1-6.

242. J.M. Terry, J.L. Adcock, D.C. Olson, D.K. Wolcott, C. Schwanger, L.A. Hill, N.W. Barnett, and P.S. Francis, *Anal. Chem.* **2008** 80 9817-9821.

243. J.L. Adcock, P.S. Francis, K.M. Agg, G.D. Marshall, and N.W. Barnett, *Anal. Chim. Acta* **2007** 600 136-141.

244. P.S. Francis and J.L. Adcock, *Anal. Chim. Acta* **2005** 541 3-12.

245. G.P. McDermott, E.M. Zammit, E.K. Bowen, M.M. Cooke, J.L. Adcock, X.A. Conlan, F.M. Pfeffer, N.W. Barnett, G.A. Dyson, and P.S. Francis, *Anal. Chim. Acta* **2009** 634 222-227.

246. M.S. Burkhead, H. Wang, M. Fallet, and E.M. Gross, *Anal. Chim. Acta* **2008** 613 152-162.

247. X. Zhou, D. Xing, D. Zhu, Y. Tang, and L. Jia, *Talanta* **2008** 75 1300-1306.

248. G.M. Greenway, A.W. Knight, and P.J. Knight, *Analyst* **1995** 120 2549-2552.

249. G.P. McDermott, P. Jones, N.W. Barnett, D.N. Donaldson and P.S. Francis, *Anal. Chem.*, **2011** 83 5453-5457.

250. P.S. Francis, J.L. Adcock, J.W. Costin, S.D. Purcell, F.M. Pfeffer, and N.W. Barnett, *J. Pharm. Biomed. Anal.* **2008** 48 508-518.

251. A.I. Vogel, *A Textbook of Quantitative Inorganic Including Elementary Instrumental Analysis*, Longmans, Green and Co., London, 1957.

252. P.S. Francis, J.L. Adcock, and N.W. Barnett, *Spectrochim. Acta, Part A* **2006** 65 708-710.

253. D. Stempak, S. Dallas, J. Klein, R. Bendayan, G. Koren, and S. Baruchel, *Ther. Drug Monit.* **2001** 23 542.

254. J. Richie, Jr, P. Abraham, and Y. Leutzinger, *Clin. Chem.* **1996** 42 1100-1105.

255. R. Rossi, I. Dalle-Donne, A. Milzani, and D. Giustarini, *Clin. Chem.* **2006** 52 1406-1414.

256. V. Angeli, H. Chen, Z. Mester, Y. Rao, A. D'Ulivo, and E. Bramanti, *Talanta* **2010** 82 815-820.

257. G. Zunic and S. Spasic, *J. Chromatogr. B* **2008** 873 70-76.

258. M.K. Halbert and R.P. Baldwin, *J. Chromatogr. B* **1985** 345 43-49.

259. Q. Weng and W. Jin, *J. Chromatogr. A* **2002** 971 217-223.260.

260. G.P. McDermott, J.M. Terry, X.A. Conlan, N.W. Barnett and P.S. Francis, *Anal. Chem.* **2011** 83 6034-6039.